THESE

Pour l'obtention du Grade de

DOCTEUR DE L'UNIVERSITE DE POITIERS

(Faculté des Sciences Fondamentales et Appliquées)
(Diplôme National - Arrêté du 25 mai 2016)

Ecole Doctorale :
Chimie Ecologie Géosciences Agrosciences « *Théodore Monod* »

Secteur de Recherche : Biologie des populations et écologie

Présentée par :

Simon ROUET

****

Modélisation de la phénologie reproductive du ray-grass anglais (*Lolium perenne* L.) : intégration des effets de l'environnement et de la diversité génétique sur les interactions entre morphogénèse végétative et induction florale.

****

Directeur de Thèse :
Jean-Louis DURAND
Encadrant de Thèse :
Romain BARILLOT

****

Soutenue le 19 mai 2021
devant la Commission d'Examen

****

JURY

Delphine LUQUET	Chargée de recherche, Cirad UMR AGAP	Rapporteure
Christophe GODIN	Directeur de recherche, Inria UMR RDP	Rapporteur
Maryse LALOI	Maître de conférences, Université de Poitiers	Examinatrice
Iñaki GARCIA DE CORTAZAR	Chargé de recherche, INRAE US AGROCLIM	Examinateur
Rossitza ATANASSOVA	Professeure, Université de Poitiers	Examinatrice
Bruno ANDRIEU	Directeur de recherche, INRAE UMR ECOSYS	Examinateur
Jean-Louis DURAND	Directeur de recherche, INRAE UR P3F	Directeur de thèse
Romain BARILLOT	Chargé de recherche, INRAE UR P3F	Co-Directeur

Remerciements

La réalisation de ce travail aura été permise par le cofinancement d'une bourse de thèse par la **Région Nouvelle-Aquitaine** et par l'**INRAE**. Je souhaite ici les remercier pour l'opportunité qui m'a été donnée.

Je tiens à adresser mes remerciements aux membres du jury : **Rossitza Atanassova** qui l'a présidé, **Delphine Luquet** et **Christophe Godin** qui ont accepté d'être rapporteurs de mon travail et **Maryse Laloi, Iñaki Garcia de Cortazar** et **Bruno Andrieu** pour en avoir été examinateurs.

Mes remerciements vont également à tout le personnel de l'**École doctorale Théodore Monod** de l'Université de Poitiers pour le suivi administratif et les formations proposées.

La bonne progression de ce travail de thèse a été permise grâce à un environnement de travail très favorable au sein l'équipe de l'INRAE de Lusignan dont je tiens à remercier en particulier tous les collègues de l'**équipe Ecophy de l'URP3F** pour les bonnes relations à la fois professionnelles et amicales que nous avons construites. Merci à **Abad**, **Abraham**, **Annie**, **Arthur**, **Béa**, **Cédric, Didier**, **Ela**, **Eric, Erick**, **Gaëtan**, **Isabelle**, **Jean-Louis**, **Marianne**, **Nabilla**, **Romain** et **Wagdi**.
Merci également à **Nathalie** et **Liliane**, aux membres de l'**équipe de Génétique** de l'URP3F et de l'Unité SDAR.

En particulier, je remercie **Annie Eprinchard** pour sa bonne humeur, ses conseils pratiques et les nombreuses heures passées ensemble à mesurer des élongations foliaires en chambre climatisée dans le froid et le bruit ; **Cédric Perrot** et **Eric Roy** qui ont tout mis en œuvre pour créer et maintenir un environnement contrôlé sur mesure pour que je puisse réaliser mes expérimentations dans les meilleures conditions ; ainsi que **Franck Gelin** et **Pascal Vernoux** pour la préparation des plants.
Merci également à **Didier Combes** pour tout son travail sur le modèle L-Grass et pour son regard extérieur sur ma thèse.

Des avancées majeures de mes questionnements et le succès des travaux expérimentaux résultent aussi du travail remarquable effectué par les deux stagiaires que j'ai eu la chance d'encadrer **Jade Debourbe** et **Alice Troux** que je remercie pour leur engagement.

Enfin, la concrétisation de ce travail de thèse aurait été beaucoup plus difficile sans l'implication bienveillante de mes deux directeurs de thèse **Jean-Louis Durand** et **Romain Barillot**. Merci Jean-Louis pour ta confiance dans mes choix, ton expérience et tes relectures attentives tout au long de ma thèse. Merci Romain pour ton implication au quotidien, pour ces heures passées à discuter et implémenter le modèle, pour ton soutien jusque dans les derniers instants et pour ta bienveillance exceptionnelle en toutes circonstances. Je suis heureux d'avoir passé ces années à travailler avec vous.

Table des matières

Remerciements 3

Table des matières 5

Introduction générale 9

Chapitre 1 : Comprendre les effets des interactions entre la diversité génétique et la variabilité environnementale : une revue des processus et des modèles existants. 15

1. Introduction 16

2. Botanical structure, vegetative and reproductive cycles in perennial grasses 19

3. Floral induction and reproductive development at tiller scale 22

4. Sexual reproduction versus vegetative reproduction at plant scale and consequences on tiller demography 33

5. Modelling grassland phenology: what is known and what is still to be determined? 38

6. Conclusion 46

Résumé du chapitre 1 48

Chapitre 2 Effet de la durée des phases d'induction florale sur la date d'épiaison et la morphogénèse chez *Lolium perenne*. 49

1. Introduction 50

2. Materials and methods 51

3. Results 59

4. Discussion 66

5. Conclusion 70

6. Supplementary Chapter 2 71

Résumé du chapitre 2 74

Chapitre 3 L-GrassF, un modèle structure-fonction du développement reproducteur des talles de graminées pérennes..... 76

1. Introduction..... 77

2. Model description..... 78

3. Model calibration..... 96

4. Results..... 100

5. Discussion 107

6. Conclusion..... 111

Résumé du chapitre 3 113

Chapitre 4 Simulation des effets des interaction entre la diversité génétique et la variabilité environnementale sur la date d'épiaison de variétés de *Lolium perenne* cultivées sur plusieurs sites et années 115

1. Introduction..... 116

2. Materials and method 117

3. Results..... 126

4. Discussion 133

Résumé du chapitre 4 137

Discussion générale..... 139

1. Atteinte des objectifs de l'étude 140

2. Prendre en compte la diversité génétique dans les modèles..... 143

3. Vers la simulation du développement reproducteur à l'échelle de la plante et des conséquences sur la pérennité..... 145

4. Vers une utilisation du modèle dans des conditions de croissance non-optimales 148

5. Quels usages pour le modèle L-GrassF? 149

6. Conclusion 150

Références 151

Introduction générale

La phénologie est l'étude de l'apparition d'évènements périodiques chez les êtres vivants en relation avec les facteurs climatiques (Schwartz, 2013). La phénologie est soumise à de nombreuses pressions de sélection qui déterminent largement la capacité de reproduction des espèces dans des environnements variables et au cours de périodes favorables (King and Heide, 2009). Chez les plantes, on peut citer comme exemples d'évènements phénologiques : la germination, la reprise printanière de la croissance foliaire, la floraison, la fructification ou la sénescence. En impactant leur *fitness* la phénologie est un acteur majeur de la distribution géographique des espèces (Chuine, 2010).

Chez les graminées pérennes, la phénologie de la reproduction sexuée a un rôle prépondérant dans les pratiques de gestion agricole des prairies. En effet, le développement reproducteur est associé à de nombreuses modifications du développement de la prairie. Le début du développement reproducteur coïncide avec une augmentation de la croissance des organes végétatifs (Davies, 1971; Parsons and Robson, 1980) et au développement des organes reproducteurs (Johnston and Waite, 1965). Ces deux phénomènes amènent à une augmentation de la production de biomasse par la prairie (Corrall and Fenlon, 1978). Toutefois, le bénéfice tiré de l'augmentation de la production de biomasse est balancé par une nette diminution de qualité fourragère, c'est-à-dire une diminution de sa digestibilité pour les ruminants et de sa valeur nutritive (Carrère *et al.*, 2010; Chapman *et al.*, 2014). Ainsi, le choix de la période de récolte du fourrage et la date de mise à l'herbe des ruminants sont directement dépendants de la phénologie des plantes. Le développement reproducteur est également un processus ayant de fortes répercussions sur la pérennité des graminées pérennes (Matthew *et al.*, 2000). En effet, à l'échelle de la talle, le développement reproducteur peut être apparenté à un développement monocarpique. Ainsi, une talle engagée dans le développement reproducteur a un développement fini qui s'achève par la mort de la talle. Les talles reproductrices sont remplacées par des talles nouvellement formées qui participent au renouvellement de la population de talles et permettent la pérennité de l'individu.

Actuellement, les pratiques agricoles s'orientent vers une réduction de leurs impacts négatifs sur l'environnement. L'augmentation de la diversité au sein des agrosystèmes est une des solutions proposées pour répondre à cet enjeu. Dans le cas

des prairies, la complexification peut passer par l'association de différentes espèces et/ou variétés au sein d'un même couvert. De nombreux bénéfices peuvent être attendus même si leur quantification doit encore être investiguée (Sanderson *et al.*, 2011). L'association de graminées (*Poaceae*) et légumineuses (*Fabaceae*) par exemple peut contribuer à une réduction de l'apport d'engrais exogène par la fixation d'azote directement par les plantes de la culture. Dans certaines conditions de stress, les associations plurispécifiques et pluri-variétales ont également montré une meilleure résilience (Prieto *et al.*, 2015). Récemment il a été montré que cette résilience accrue était liée à des rythmes de production différents entre espèces et variétés, la phénologie se révélant ainsi un caractère de premier ordre parmi ceux à considérer pour établir des règles d'assemblage (Prieto *et al.*, 2015; Meilhac *et al.*, 2020).

Dans un futur proche, l'agriculture est menacée par le changement climatique (Le Treut, 2018). Les modélisations actuelles du changement climatique prédisent une augmentation certaine des températures moyennes accompagnée d'une augmentation de la fréquence des évènements climatiques extrêmes (IPCC 5th report, Stocker *et al.*, 2013). En France métropolitaine, il est attendu des hivers plus doux et des étés chauds et secs. En parallèle, certaines variables environnementales indépendantes du climat ne vont pas être modifiés, comme c'est le cas de la photopériode. Or, la phénologie reproductive est fortement sous le contrôle de la température et de la photopériode, elle est ainsi susceptible d'être sensiblement impactée par le changement climatique. Il se pose alors la question de la capacité des plantes à réaliser le développement reproducteur ainsi que du maintien de ce développement pendant une période favorable (*e.g.* hors sécheresse) (Cleland *et al.*, 2007).

Pour répondre à ces enjeux, plusieurs leviers peuvent être actionnés simultanément. Le premier est celui de l'utilisation de la diversité génétique présente chez les espèces fourragères ou naturelles pour améliorer les performances de couverts complexes et leur adaptation aux conditions climatiques futures (Blanco-Pastor *et al.*, 2019; Meilhac *et al.*, 2019). Le second est celui d'une modification des pratiques agricoles telles que la date de semis, récolte ou de pâturage (Gillet and Breisch, 1982).

Concernant le développement reproducteur, il subsiste des lacunes importantes sur la connaissance des interactions entre la diversité génétique et la variabilité environnementale (lieu et année de culture, date de semis). Jusqu'à présent la recherche s'est en effet majoritairement portée sur (i) des aspects agronomiques visant à optimiser la quantité et la qualité du fourrage, indépendamment de la phénologie, (ii) l'établissement de liens entre le génotype et le phénotype par des approches de génétique quantitative, où l'étude de la phénologie consiste principalement en un classement relatif des génotypes, (iii) l'identification de molécules et/ou gènes impliqués dans les processus reproducteurs (approche de biologie moléculaire).

La phénologie reproductive des graminées pérennes est un phénomène difficile à appréhender chez les graminées car les transformations qui lui sont associées sont majoritairement cachées *i.e.* non visibles à l'œil nu car les méristèmes caulinaires apicaux sont situés à la base des talles, entourés des gaines des feuilles matures. La date d'épiaison, c'est-à-dire l'émergence de l'épi hors des gaines de la talle, est donc le stade utilisé comme repère du développement reproducteur car il facile à observer. Toutefois, c'est un évènement tardif qui découle d'une cascade de phénomènes complexes antérieurs qui concernent le développement reproducteur (*e.g.* induction florale, émission d'épillets) mais aussi végétatif. En effet, la dimension des organes végétatifs conditionne en partie le temps nécessaire à l'émergence de l'épi ainsi que l'acquisition des ressources nécessaires à la croissance des organes reproducteurs. Pour prédire la date d'épiaison, il est par conséquent nécessaire d'utiliser des modèles pour prendre en compte ces phénomènes antérieurs, y compris végétatifs, et leur dépendance à l'environnement (climat, pratiques agricoles…).

L'objectif de cette thèse est d'élaborer un modèle informatique qui améliore la prise en compte des effets de l'environnement et de la diversité génétique sur le développement reproducteur des graminées pérennes. L'originalité du modèle repose sur une approche individu-centrée rendant compte des interactions entre morphogénèse végétative et induction florale à l'échelle de la talle. Le défi posé par cet objectif réside en grande partie sur l'identification et la formalisation des processus clés à intégrer dans le modèle malgré les manques de connaissances actuels chez les graminées pérennes fourragères. La cible du modèle, qui a majoritairement servi à son

évaluation au cours de ce rapport, est un stade phénologique important et fréquemment observé dans la littérature : la date d'épiaison. A ce stade, l'objectif de la thèse est de donc de produire un modèle d'écophysiologie intégrant les processus nécessaires à la simulation de la date d'épiaison d'une talle. A plus long terme, une utilisation plus complète sera envisagée afin notamment de prédire les conséquences de la phénologie reproductrice sur le fonctionnement et la production de services par les prairies dans de nouveaux contextes et usages mais aussi de progresser sur la compréhension de la pérennité des plantes prairiales qui est largement dépendante de l'investissement reproducteur des plantes (proportion de talles épiées).

La thèse soutenue est qu'un modèle intégrant une représentation explicite des processus inducteurs et morphogénétiques à l'échelle d'une talle permet d'améliorer la prise en compte de la diversité génétique et de la variabilité environnementale de la phénologie reproductive des graminées pérennes.

Organisation du manuscrit

Le chapitre 1 est consacré à une synthèse des connaissances actuelles sur la phénologie reproductive des graminées pérennes et sa modélisation. A travers une étude à plusieurs échelles allant de la talle à la plante, cette revue permet d'identifier les principaux déterminants environnementaux du développement reproducteur en intégrant la variabilité génétique inter- et intraspécifique. Ce chapitre comporte également une approche comparative de la prise en compte de la phénologie reproductive dans les modèles de graminées pérennes de la littérature.

Le chapitre 2 présente une expérimentation réalisée en conditions contrôlées dont le but était d'acquérir une connaissance plus fine de certains aspects du développement reproducteur et de créer un jeu de données utilisable pour la calibration d'un modèle de développement reproducteur à l'échelle de la talle.

Le chapitre 3 présente le modèle L-GrassF développé au cours de cette thèse. L-GrassF simule le développement végétatif (production de feuilles) et reproducteur (transition florale, épiaison, production épillets) à l'échelle de la talle individuelle. Pour cela, nous avons développé un modèle d'induction florale dépendant des conditions environnementales perçues par l'apex de la talle. Le modèle rend également compte

de l’effet des interactions entre fonctionnement végétatif et progression de l’induction florale.

Le chapitre 4 est consacré à la calibration et à la validation du modèle en conditions naturelles à l’aide d’un jeu de données décrivant les dates d'épiaison de 7 variétés de ray-grass anglais (*Lolium perenne*) cultivées dans des environnements contrastés.

La discussion générale revient sur les objectifs annoncés en début de manuscrit au regard des résultats obtenus au cours de cette thèse. Elle propose également des perspectives d’utilisation du modèle.

Les chapitres du manuscrit sont présentés sous la forme d’articles scientifiques. Le chapitre 1 a été soumis à la revue *Frontiers in Plant Science*. Les chapitres 3 et 4 seront adaptés et fusionnés pour être publiés ultérieurement.

Chapitre 1 :

Comprendre les effets des interactions entre la diversité génétique et la variabilité environnementale : une revue des processus et des modèles existants.

1. Introduction

Grasslands are the most widespread terrestrial ecosystem, covering more than three billion hectares (http://faostat.fao.org/) and constituting the basis of many agrosystems. They provide multiple ecosystem services such as forage production for herbivores, preservation of water quality, erosion control, maintenance of biodiversity and carbon storage (Huyghe *et al.*, 2012; Martin *et al.*, 2020). Despite the importance of grasslands in livestock farming, the quantity and quality of forage is often sub-optimal (Boval *et al.*, 2015; Doole and Romera, 2015). This is partly explained by a mismatch between the dynamics of biomass production and the harvesting dates (by mowing or grazing). Improving our capacity to predict the annual fluctuation of biomass quantity and quality is therefore crucial to increase the efficiency of these major agrosystems.

One of the main components of the annual dynamics in grassland productivity is the reproductive development, which encompasses a set of processes ranging from floral induction to seed production. The floral transition, which characterizes the transition from a vegetative state to a reproductive state, is a major phenological event occurring in spring in temperate climate areas and a crucial episode for grassland management. Firstly, floral transition is often associated with a peak in biomass production due to a concomitant increase of leaf growth rate (Parsons and Robson, 1980). Secondly, following floral transition, internodes of grasses begin to elongate, which decreases the biomass quality for ruminants (Chapman *et al.*, 2014). Finally, the floral transition also affects the perenniality of grasslands as reproductive tillers die after heading (spike emergence from the tiller's pseudostem) and seed dispersal (Barre *et al.*, 2017). Moreover, the reproductive development of perennial grasses allows the genetic evolution of grassland species and affects other ecosystem services provided by grasslands such as the hosting of auxiliaries and pathogens and the rate of leaf turnover, which alters litter quality.

Despite the importance of reproductive development on grassland functioning and management, there is still a significant knowledge gap that prevents the prediction of the occurrence of reproductive stages for a wide range of environments and

genotypes. The prediction of the reproductive development in grasslands faces several challenges, which should be addressed in numerical models. Firstly, the role of environmental factors must be identified and quantified in order to account for various climatic conditions and inter-annual variations. This aspect becomes even more crucial in the context of climate change. Indeed, for a given area, climate change may result in combinations of photoperiod, temperature and water availability never encountered before, which could significantly affect the phenological events of local perennial grass species and cultivars. Over the last 20 years, Vuffray *et al.* (2016) already observed earlier heading dates and a more frequent alternation between very early and very late headings. Such changes would combine with the effects of projected modifications in water balance and atmospheric CO_2 concentration. Secondly, the diversity of phenotypes observed among cultivars and species must be accounted for, as grasslands are usually mixtures. That genetic diversity increases the complexity for the prediction of reproductive development but constitutes an interesting lever for plant adaptation to contrasted environmental conditions. The French Variety and Seed Study and Control Group (GEVES) uses multiannual and multisite experimentations to evaluate cultivar performances (www.geves.fr), enabling the assessment of the relative contributions of the genetic and environmental factors on the phenological diversity within a species (Figure 1.1). The analysis of 50 *Lolium perenne* cultivars from the French forage seed catalog revealed a high genetic diversity in heading date with differences of up to 45 days between the earliest and latest cultivars in all sites and years (Figure 1.2). The range of intraspecific variability in heading date is similar to that observed between sites and years, thus constituting an interesting pool of genetic resources to increase diversity and durability of grasslands (Prieto *et al.*, 2015; Litrico *et al.*, 2016). Lastly, models of reproductive development should lead to better predictions of the dynamics of biomass quantity and quality in order to optimize grassland management.

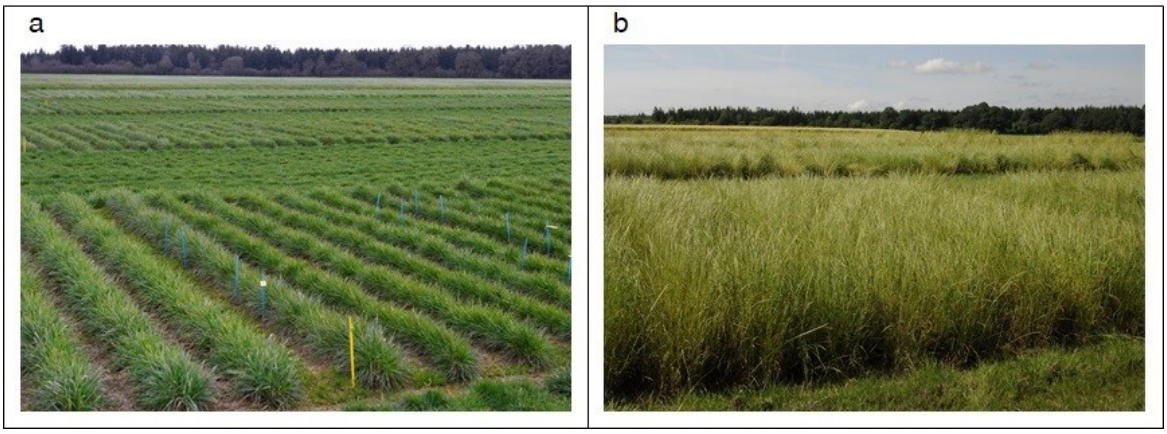


Figure 1.1: Effect of the reproductive development on the above-ground morphology in Lolium perenne.

(a) Cultivars of Lolium perenne at vegetative state on March 20th 2018. (b) Same plants at reproductive state on June 8th 2018. The experiment is conducted by the GEVES in Lusignan (France)

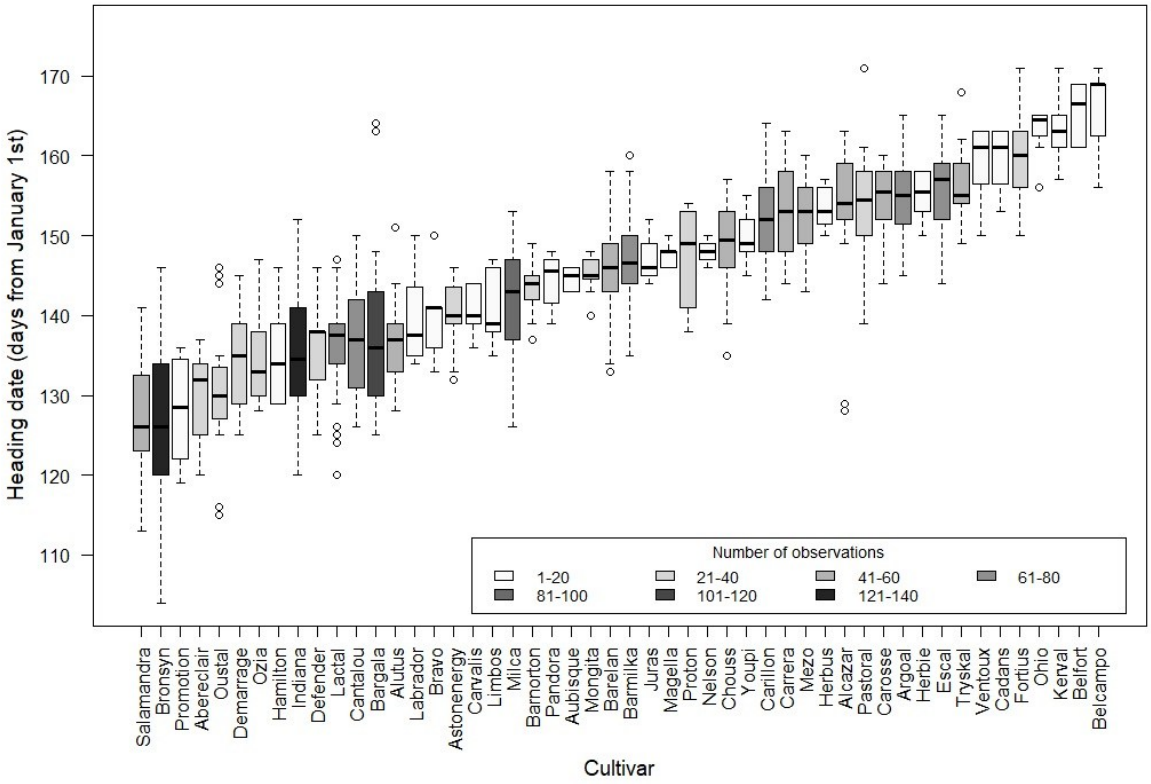


Figure 1.2: Heading dates of 50 commercial cultivars of Lolium perenne grown for 17 years in 7 French locations with contrasted climatic conditions.

*. Heading date is defined as the date when at least 10 tillers reach heading per linear meter of plants sown during the previous spring. Boxplots represent the variability of heading date between year-location combinations for each cultivar (plot in the style of Tuckey: -1.5*IQR, 2nd quartile, median, 3rd quartile, +1.5*IQR). The greyscale represents the number of observations per cultivar.*

The aim of the present paper is to provide a synthesis of the different aspects of the reproductive development that should be accounted for in models to improve the

prediction of grassland functioning and thereby management. First, we reviewed the current knowledge about the effects of the genetic × environment interactions on the transition from a vegetative to a reproductive tiller and the consequences on tiller development and morphogenesis. Then, we focused on the effects of reproductive development at the whole plant scale *i.e.* on the interactions between the different tillers of a plant and the consequences on plant perenniality, defined as the maintenance of a minimum tiller density following cutting. Finally, we gave a critical review of the current simulation models of grasslands, detailing their assumptions related to the reproductive development.

2. Botanical structure, vegetative and reproductive cycles in perennial grasses

In perennial grasses, individual plants consist in a colony of genetically identical cohorts of tillers, originating from the same seed generally sown at the beginning of spring or during autumn in temperate regions. At the tiller level, vegetative and reproductive development are successively realized by the same apex (Figure 1.3). After seed germination (Figure 1.3.1), a first vegetative tiller, called main stem, emerges from the seed and grows (Figure 1.3.2). All vegetative tillers can be represented as a succession of vegetative phytomers, each initiated by the terminal apex and constituted of a leaf (lamina and sheath), an internode and a node which bears an axillary bud (Moore and Moser, 1995). During the vegetative stages, the terminal apex (Figure 1.3.A, Figure 1.3.B) of a tiller is usually located close to the ground, inside the pseudostem made of the superposition of leaf sheaths (Thomas, 1980). The apex bears several vegetative primordia which are emitted periodically (plastochron) and will later develop into a phytomer. New tillers originate from the axillary buds located at the axil of each leaf (Figure 1.3.3) (Davies and Thomas, 1983). The development of axillary buds into tillers, called tillering (Jewiss, 1972; Thomas, 1980), is under control of the environment, in particular the Red/Far-Red ratio (Casal et al. 1986, Gautier et al 1999, 1987; Casal 2013). Depending on the environmental conditions experienced by each tiller, floral induction may be completed (Figure 1.3.3, Figure 1.3.5), thus leading to the floral transition of the apex, which then becomes

reproductive (Figure 1.3.C). This new status modifies the primordia appearance rate and leads to the elongation of non-mature internodes (Figure 1.3.6) and finally the formation of spikelets (Figure 1.3.D) (Gillet, 1980). These reproductive phytomers are the last phytomers and form an inflorescence (Figure 1.3.E). Not all tillers of a plant become reproductive, some remain vegetative *i.e.* their terminal apex keep producing vegetative phytomers (Figure 1.3.5-Figure 1.3.7). For reproductive tillers, internode elongation leads to the progressive increase of apex and tiller height. At the end of flag leaf expansion and due to the elongation of the inflorescence and peduncle, the terminal spikelet appears out of the pseudo-stem. This event is referred to as the heading of the tiller (Figure 1.3.6) (Gillet, 1980; Thomas, 1980). The further development of the inflorescence conducts to anthesis, seed formation and seed maturation (Figure 1.3.7). After seed maturation, the tiller senescence is complete. Tiller death can also occur earlier if the apex is removed by mowing or grazing. Tillers remaining vegetative ensure plant perenniality through leaf production and tillering. Thus, two pathways coexist in perennial grasses to ensure plant survival: the sexual reproduction by seed production (Figure 1.3.8) and the vegetative multiplication by tillering (Figure 1.3.9) (Gillet, 1980).

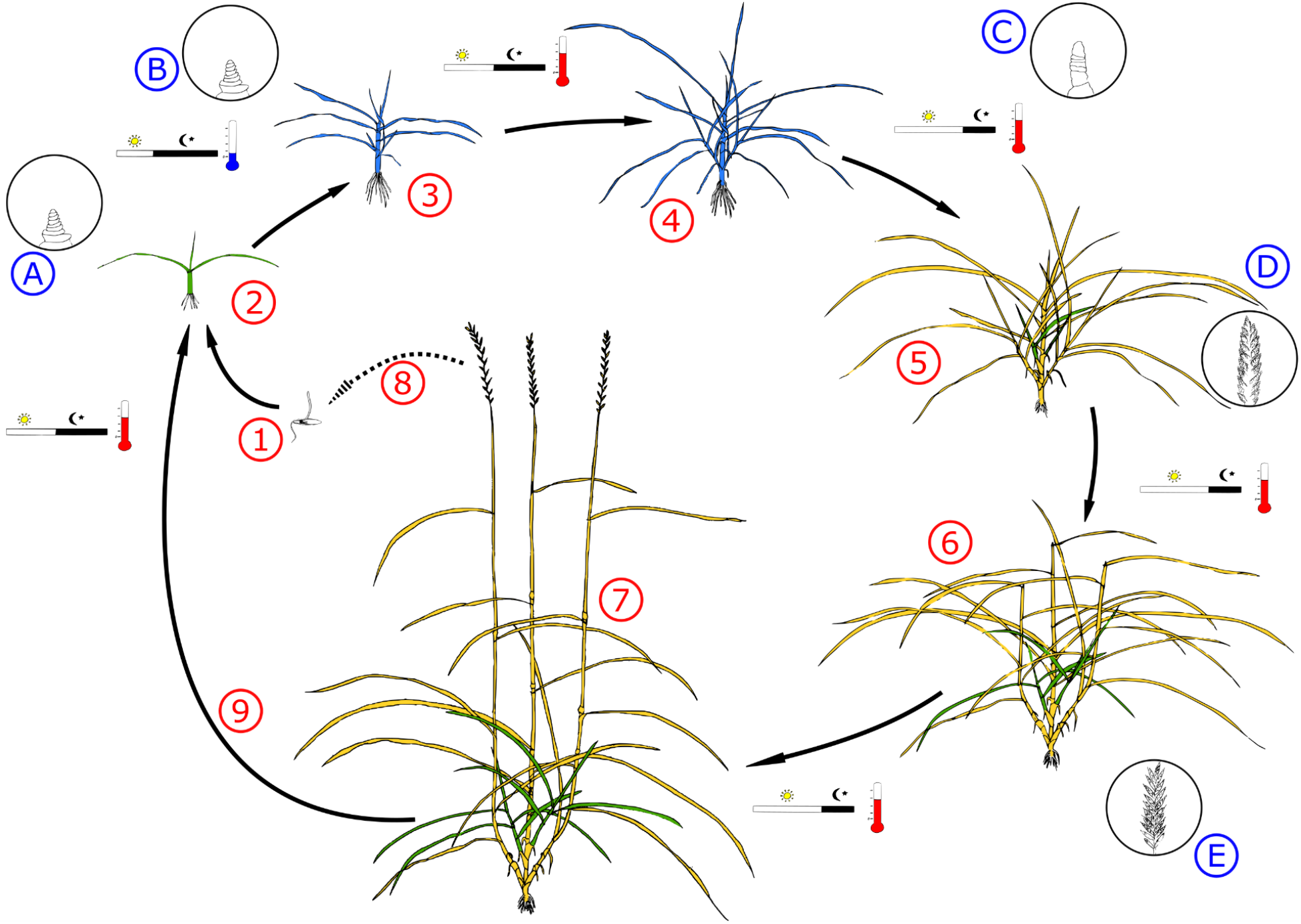

A
B
C
D
E
1
2
3
4
5
6
7
8
9

Figure 1.3: Life cycle of a perennial grass plant and the evolution of apex morphology in relation with climatic conditions.
Variations in photoperiod are represented by horizontal bars indicating the proportion of day and night within 24 hours. Three configurations are represented: day/night ≈ 1 (equivalent to spring and autumn), day/night > 1 (equivalent to summer), day/night <1 (equivalent to winter). Two temperature levels are represented: mean to elevated temperature (red thermometer) and low temperature (blue thermometer). The main steps of the vegetative and reproductive development are represented; 1: Seed germination; 2: Vegetative development of the main tiller; 3: Plant ramification with the emergence of two tillers and primary induction of the three tillers (in blue); 4: Increase of leaf growth rate producing longer leaves; 5: Secondary induction of the first three present tillers (in yellow). Emergence of two supplementary tillers, which did not reach primary induction and remain vegetative (in green); 6: Heading. Emergence of the last leaves of the reproductive tiller, start of internode elongation and emergence of the last spikelet from the pseudo-stem; 7: Anthesis. End of internode elongation, flower development and stamina emergence; 8: Completion of the sexual reproduction by seed production, after fecundation and seed filling; 9: Plant perenniality is ensured by the tillers remaining vegetative; A: Apex of the main stem bearing primordia differentiated in leaves and undifferentiated primordia; B: Permanent regime. The rate of primordia emission by the meristematic area is equivalent to the rate of leaf emergence; C: 'Double-ridges' stage. Differentiation of primordia with the appearance of a second wrinkle; D: Spikelet development; E: Heading. Spike emerges from the last leaf sheath. Spikelet number of the spike is determined but internodes between spikelets are not elongated

3. Floral induction and reproductive development at tiller scale

In grasses, the tiller is a functional unit having its own shoot organs and root system. Also, all stages of reproductive development, from floral induction to seed production, occur at the individual tiller scale. Below, we report the current knowledge on floral induction and its consequences on the tiller development and morphogenesis.

3.1. Inductive conditions

The floral induction of a tiller leads to the transition from a vegetative to a reproductive apex. Without completion of the floral induction, tillers remain vegetative and produce vegetative phytomer indefinitely. Heide (1994) wrote a comprehensive review of the environmental conditions that induce floral induction in diverse perennial grasses. For a large majority of perennial grasses, floral induction can be divided into two successive phases referred to as 'primary induction' and 'secondary induction'

which are mainly dependent on two environmental variables: temperature and photoperiod (Heide, 1994). In a majority of species, the distinction of two phases (dual induction), instead of a single continuous phase is explained by the fact that tiller induction requires an exposure to two different levels of the same environmental variable, *e.g.* low and high temperature or short and long photoperiods.

The primary induction is a progressive phenomenon mainly controlled by low temperatures and short photoperiods, which corresponds to winter conditions in temperate regions. The completion of the primary induction depends on the interaction between temperatures, photoperiod and exposure duration of several weeks. In most perennial grasses, low temperatures (0-6°C) for a period of 4 to 20 weeks is sufficient to complete the primary induction whatever the photoperiod. Under higher temperatures, the influence of the photoperiod becomes significant and primary induction can only occur under short photoperiod conditions (Lindsey and Peterson, 1964; Heide, 1994; Aamlid *et al.*, 2000). However, in some cultivars, low temperature or short photoperiod can be sufficient whatever the value of the other climatic variable (Heide, 1987, 1988). In a majority of cases, the completion of primary induction is definitive, as devernalization has been observed only in a few cases detailed in Heide (1988). Within a given species, primary induction varies between populations in terms of temperature, photoperiod and exposure duration according to their genetic make-up which can depend on their geographical origin. In *Lolium perenne*, which has a large latitudinal extension (from Scandinavia to the Mediterranean area in Europe), the range of conditions for primary induction varies from no-requirement for Mediterranean genotypes to a primary induction with obligatory low temperatures enhanced by short photoperiods for more northern genotypes (6°C/8h for more than 3 weeks) (Aamlid *et al.*, 2000). For various grass species, the apparent absence of primary induction was generally reported in ecotypes originating from regions with low risk of late frost and an early dry season (Cooper, 1960; Aamlid *et al.*, 2000).

The secondary induction starts only once primary induction has been completed and requires the exposure to long photoperiods over a generally short period (>12h for less than one week) (Evans, 1958; Heide, 1987; Aamlid *et al.*, 2000). The effects of long photoperiods can be mimicked by an interruption of the dark period with an exposure to light for less than 2h near the middle of the night (Heide *et al.*, 1985). The

secondary induction is apparently not related to an increase in the incident radiative energy (Cooper, 1958; Aamlid *et al.*, 2000). Furthermore, the induction process itself has been shown to be independent of the carbohydrate status of the apex, in particular to sucrose content (King and Evans, 1991). As for primary induction, the critical photoperiod required varies with the geographical origin of the ecotypes. Genotypes from high latitude areas require the longest photoperiod and the highest number of long photoperiod cycles. Within the species *Lolium perenne*, Aamlid *et al.* (2000) found that the critical photoperiod to obtain 50% of heading plants ranged from 12h for a Mediterranean cultivar to ca. 17h for the northern ecotypes. For most *Lolium perenne* genotypes, elevated temperatures have a positive effect on the completion of the secondary induction, implying that they could increase the completion rate of the secondary induction. For example, 8 days of exposure to long days (24h) at 12°C are required to obtain 50% of heading plants, while the same result is observed with only 4 days at 18°C (Aamlid *et al.*, 2000).

Previous studies on different ecotypes of *Lolium perenne* (Aamlid *et al.*, 2000) and *Festuca* (Bean, 1970) highlighted that both single induction and dual induction could exist within a single species, depending on the genetic make-up which can depend on their geographical origin of the population. What is more, the cross between different ecotypes is genetically possible and can result in a high variability in primary induction requirements, which questions the conceptual frontier between the single and dual induction cases. Similarly, hybrids of close species in the *Lolium* genus (*L. perenne*, *L. multiflorum*, *L. rigidum* and *L. temulentum*) have all intermediary induction requirements without clear distinction between single and dual induction (Cooper, 1960; Evans, 1960a). Another example exists in *Phleum* where the wildtype *Phleum alpinum* has a dual induction while the cultivated hexaploid *Phleum* only requires an induction by long photoperiods without any primary induction (Heide, 1994).

As mentioned by Heide (1994), growing plants in various controlled conditions and observing the floral transition or heading is a convenient methodology to determine the threshold requirements for floral induction. However, these results alone do not allow an exhaustive quantification of floral induction requirements. In particular, they do not allow a discretization of floral induction advancement at a daily time step. Such

information would be useful for the prediction of the floral transition under field conditions where temperature and photoperiod vary from day to day.

3.2. Perception and integration of the inductive signals

If exposure to sufficient inductive conditions is necessary for a plant to become reproductive, the success of the floral induction also requires the plant to be competent to perceive and integrate the inductive signals (Lang, 1965). In many cases, young plants remain unable to complete their floral induction, staying in a so-called juvenile stage (Heide, 1994). The duration of this stage varies considerably between species and genotypes (60 to 110 days) whereas no explicit juvenile stage was reported in *Lolium perenne*, as plants can be primary induced as soon as seed germination (Cooper, 1960; Bommer, 1961). In contrast, in *Dactylis glomerata*, *Festuca pratensis*, *Festuca rubra* and *Poa pratensis*, seed induction was never observed even after a long exposure to low temperatures (2°C for 116 days) in the dark (Bommer, 1961). The perception site of low temperature has not been determined to our knowledge although apices can complete the primary induction without any other organ as shown by Arumuganathan *et al.* (1991) who obtained flowering plants of *Lolium temulentum* from excised shoot meristems exposed to low temperatures (2°C). In seeds, the apex sensitivity to low inductive temperatures depends on carbohydrate supply and could therefore be linked to the size of the caryopses (Heide, 1994). Nevertheless, this dependence disappears after germination, as no relations were observed between the carbohydrate content of the apices in seedlings and their ability to be induced (King and Evans, 1991). The methodologies used to study the primary induction always use long exposure periods to a constant temperature. Therefore, the integration time lapse for the inductive thermal signal by the plant still remains unknown. This review will not consider in details the recent findings at the molecular scale. However, it is worthy to mention here that it has been shown that the expression of a limited number of genes *i.e. VRN1*, *VRN2* and *MADS-box* genes plays a key role in the genetic variations of the primary induction (Colasanti and Coneva, 2009; Seppänen *et al.*, 2010; Ergon *et al.*, 2013; Wang and Forster, 2017).

The photoperiodic signal is perceived by leaves through specific photoreceptors. The use of mutants in the model grass *Brachypodium distachyon*, revealed that the initial perception of long photoperiods occurs through the *phytochrome C* (Woods *et al.*, 2014; Arojju *et al.*, 2016). Similar results concerning the key role of the *phytochrome C* were observed in wheat for which Chen (2014) proposed a theoretical model to explain the effects of the *phytochrome C* in the long-photoperiod induction process, depending on daylength and circadian clock (Chen *et al.*, 2014; Song *et al.*, 2015).

3.3. Apex morphology and functioning following floral transition

The completion of the floral induction constitutes the end of the floral transition and leads to the first morphological changes of the apex (Figure 1.3.C). The earliest changes occur within the meristematic zone, shortly after the completion of the floral induction. In *Lolium perenne*, Gonthier and Francis (1989) observed no modification of the apex length (between 100 and 300 µm) when the primary induction was reached, and the mitotic index was similar to that of non-induced tillers (<4%). Primary-induced apices kept the same morphological appearance if they were maintained under short photoperiods (8h), even under high temperature (18°C). Significant increase of the meristem length (up to 700 µm) and of the mitotic index were observed for tillers exposed to long-photoperiod (20 hours of light for eight days) after the completion of the primary induction (Gonthier and Francis, 1989). Apex length and mitotic index can be related to the initiation rate of primordium. Before the completion of the primary induction, the initiation rate of new primordia by apices usually follows the rate of leaf appearance or is slightly slower (0.45 to 1.09 the rate of leaf appearance, depending on cultivars), meaning that the number of leaf primordia remains approximately constant at the apex (Kemp *et al.*, 1989). When the photoperiod is sufficiently long for the onset of the secondary induction, the number of primordia on the apex quickly increases due to a drastic reduction of the plastochron while the phyllochron remains almost constant (Malvoisin, 1984). During the secondary induction in *Lolium perenne*, the plastochron is divided by 3 to 11 depending on the cultivars (Kemp *et al.*, 1989).

The date of increase in the rate of primordia production shows a high genetic variability among *Lolium perenne* cultivars, but was not correlated with the heading date (Cooper, 1950; Kemp *et al.*, 1989; Hazard *et al.*, 1996). Also in *Lolium perenne*, Gonthier and Francis (1989) observed that the accumulation of primordia was dependent on the number of long photoperiod cycles perceived by the tiller after the completion of the primary induction.

During these phases of apex lengthening and rapid primordium initiation, the first macroscopic marks of the floral transition appear on the apex. First, white stripes appear at the basis of the newly produced primordia. These stripes are characterized by a high cellular density and will later elongate into long internodes. Then, the morphology of the youngest primordia changes: a second ridge appears and will later become a spikelet, while the older primordia will differentiate into leaves. The mechanisms regulating the development of primordia during the floral transition into leaves or spikelets are largely unknown. Finally, the meristematic dome located at the top of the apex differentiates into the terminal spikelet, stopping new spikelet production (Malvoisin, 1984). The cessation of spikelet primordia production appears to be coordinated with the emergence of the flag leaf tip in *Lolium perenne* and wheat (Kemp *et al.*, 1989). The accumulation of primordia during the apex differentiation defines the final number of leaves and the number of spikelets of the tiller. The number of leaves remaining to emerge and the size of the spike determine the heading date of the tiller. Some authors proposed to approximate the heading date from the final number of leaves assuming a constant phyllochron (Cooper, 1960).

3.4. Leaf appearance and growth rates

The number of leaves produced from tiller emergence to flowering varies between tillers. In *Panicum virgatum*, Van Esbroeck *et al.* (1997) found that late summer emerging tillers produced less leaves before heading (about seven) than those emerged earlier during spring (nine to eleven leaves). A similar observation was made in *Phleum pratense*, where the final leaf number of reproductive tillers was clearly related to their initiation date, decreasing from ~ 20 leaves for the main tillers to 7 leaves for tillers initiated later in spring (Langer, 1956). For the genus *Lolium*, Cooper

(1950) considered that the rate of leaf emergence was identical for all tillers during their vegetative development as well as during the primary induction, meaning that the final leaf number of each tiller was determined between the start of the secondary induction and heading. He also showed that the number of leaves produced from the start of the secondary induction was negatively correlated to the number of short photoperiod cycles perceived after the end of the primary induction.

In temperate regions, the beginning of spring is associated with a strong increase of grassland production related to an increase of leaf growth rate (multiplied by 3 at 15°C) (Barre *et al.*, 2015). This event occurs at the same period as the floral induction, which therefore raises the question of a causal relation between the phenological state of the plant and the rate of leaf growth. Parsons and Robson (1980) showed that the phenomenon was due to an increase in potential leaf growth rate, meaning that the intrinsic response of leaf growth to temperature was modified. They also concluded that the acceleration of leaf growth occurred only for plants that had previously experienced winter conditions and that the change in the leaf growth rate was due to the floral transition. In contrast, many authors stated that the photoperiod signal itself has a morphogenetic effect on leaf growth in both vegetative and reproductive development (for a review see Hay (1990)) and this, independently of trophic issues. In studies on *Lolium perenne*, *Dactylis glomerata*, *Festuca*, Ryle (1966) observed that increased photoperiod (from 8h to 16h) caused an increase in the final length of both lamina and sheaths, which resulted from an increase of the leaf elongation rate. The rapid elongation rate was later related to an increase in cell division and elongation by Wu (2004). Davies (1971) managed to experimentally decorrelate flowering and leaf growth rate as she observed an increase of the leaf growth rate in tillers exposed to long photoperiods but which did not further exhibit any reproductive development. These results are in line with the study of Hazard (2006) which observed an increase of leaf growth rate at the same time in two *Lolium perenne* morphotypes with contrasted dates of double ridge stage and heading. Therefore, it can be concluded that the increase in leaf growth rate observed in spring is most certainly a direct response to photoperiod, which simultaneously triggers the floral transition of primary-induced apices. Moreover, the decorrelation between spring growth and reproductive development has been intensively used by breeders to

increase the flexibility of grassland use by selecting plants with an early vegetative growth in association to a late heading (Sampoux *et al.*, 2011).

In grass tillers, the final length of leaves usually increases from the basis of the tiller, and then decreases for the last ranks in reproductive tillers (Borrill, 1959; Van Esbroeck *et al.*, 1997). For *Lolium temulentum* grown under natural conditions, the inflorescence initiation is concomitant with the elongation of the leaf having the longest lamina, while sheaths become progressively longer up to the flag leaf (Borrill, 1959). In *Lolium perenne* and *Dactylis glomerata* the elongation of leaves supported by long internodes, *i.e.* the last leaves of the tiller, ends only a few days before the spike emergence (Davies, 1978).

3.5. Internode elongation

On vegetative tillers, internodes remain very short and generally do not elongate further, except in stoloniferous species. On reproductive tillers, a series of long internodes are produced, the last one before the first flower constituting the peduncle. This leads to an important elevation of the canopy (Figure 1.1). Internode elongation of reproductive tillers has strong impacts on plant functioning and grassland management. First, forage quality in late spring decreases as the proportion of internode increases in the total aerial biomass (Buxton and Marten, 1989; Chapman *et al.*, 2014). Secondly, internode elongation increases the terminal apex height above the ground, thus increasing the exposure to climatic hazards (frost) and herbivores. In addition, internode elongation has strong impacts on the sink-source relations of the whole plant as they constitute the main net importers of carbon assimilates in the tiller. As a consequence, (i) assimilate allocation to roots is significantly decreased (Parsons and Robson, 1981) and (ii) the transfer of assimilates from reproductive to vegetative tillers decreases which could lead to the regression of young vegetative tillers (Gillet and Breisch, 1982; Colvill and Marshall, 1984; Matthew *et al.*, 2000). Later in the tiller development, carbohydrates from internodes will be remobilized towards the seeds (Clemence and Hebblethwaite, 1984; Barillot *et al.*, 2016).

A majority of studies involving plant morphological measurements on perennial grasses do not differentiate the internodes composing the culm. However, as observed

by Gillet (1980), the successive mature internodes have different final length and their elongation is not synchronous (Figure 1.4). The number of long internodes varies between species, cultivars and even between tillers of the same plant (4 to 6 in *Lolium perenne* and *Dactylis glomerata*) (Johnston and Waite, 1965). The total length of the culm was shown to vary with the emergence date of the tiller. In *Lolium perenne*, Aamlid (2000) observed that culms were up to 10% shorter (peduncle included) for tillers emerged during the secondary induction compared to those emerged before or during the primary induction. In contrast, the duration of exposure to low temperatures (primary induction) had no effect on the final culm elongation in that study. These results are in accordance with the observation of shorter internodes in reproductive tillers developed during aftermath heading in comparison to those developed during spring (Aamlid *et al.*, 2000).

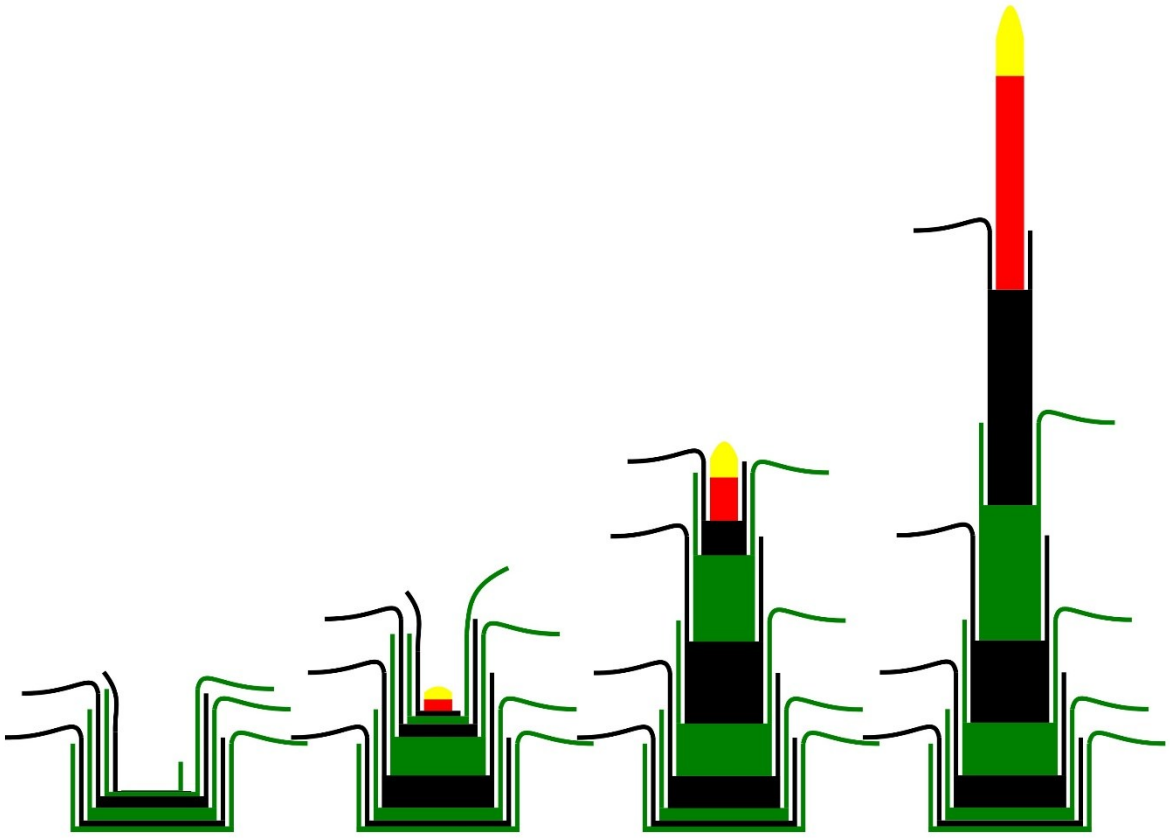


Figure 1.4: Schematic representation of leaf appearance, internode elongation and heading of a reproductive tiller
(adapted from Gillet (1980)). Green and black phytomers represent successive phytomers. Red internode is the peduncle. Yellow structure is the inflorescence.

The timing of successive internodes elongation has not been extensively studied in perennial grasses as it has been for wheat or maize, for which some coordination was established between internode and leaf elongation (Kirby et al., 1994; Fournier and Andrieu, 2000; Vidal and Andrieu, 2009; Zhu et al., 2014; Gauthier et al., 2020).

3.6. Inflorescence development

While the inflorescence of perennial grasses is considered of little interest for forage production, its development and morphology are of great importance for seed production (Scotton, 2018) and grassland ecology. Perennial grass species exhibit a wide diversity of inflorescence morphologies, mainly spikes (*Lolium*, *Festuca*, *Bromus*, *Hilaria*, *Microchloa*), racemes (*Brachypodium*, *Pleuropogon*) and panicles (*Poa*, *Dactylis*, *Andropogon*) (Allred, 1982). These diversified morphologies depend on the branching intensity and duration of terminal and lateral meristems before spikelet formation (Perreta *et al.*, 2009). In addition, the elongation of the inflorescence internodes affects the complete formation of the inflorescence and also determines the grass inflorescence morphology (Perreta *et al.*, 2009).

Within species, inflorescences have the same general pattern but present slight differences between genotypes in terms of length, number of spikelets and number of flowers per spikelet. For instance, Aamlid *et al.* (2000) observed variations in the inflorescence (peduncle not included) among genotypes of *Lolium perenne*, which may be related to their geographical origin as inflorescence length tended to increase with the latitude of origin. Byrne *et al.* (2009) found QTL involved in both inflorescence traits and heading date. Nevertheless, the relation between the heading date and inflorescence morphology remains unclear. Within *Lolium perenne* genotypes, Byrne *et al.* (2009) found a negative correlation between the heading date and inflorescence length, similar to what was observed in wheat (Donmez *et al.*, 2001), whereas McGrath *et al.* (2010) reported a positive correlation.

Environmental conditions are also responsible for differences in inflorescence morphology, which were observed among cultivars and tillers of a plant. In *Lolium perenne*, Colvill and Marshall (1984) found that tillers initiated early in the year preceding heading, *i.e.* during the previous summer, developed slightly longer inflorescences and had one or two supplementary spikelets than tillers produced later during autumn and winter. Early tillers had 35% more florets by spikelet compared to late tillers. Regarding the number of spikelets produced by the apex, Anslow (1963) showed for the *Lolium perenne* cultivar S24 that the number of spikelets was higher for late heading tillers. Under controlled conditions, it was determined for *Lolium*

perenne and *Phleum pratense* that “short long photoperiods” and relatively low temperature (12h/13°C) during secondary induction decreased the final number of spikelets (Ryle and Langer, 1963; Ryle, 1965). Accordingly, Langer (1956) found in *Phleum pratense* that the later the tiller appeared, the shorter the ear length. In *Lolium perenne*, Aamlid *et al*. (2000) reported that tillers which emerged during the secondary induction developed shorter ears with fewer spikelets and florets than tillers which emerged before or during primary induction, and they also headed later. Evans (1960b) observed the production of abnormal inflorescences as the delay between the primary induction and the exposure to long photoperiods increased (secondary induction). Kleinendorst (1974) found a linear relation between the number of primordia at the beginning of the double-ridge stage and the final number of spikelets. The longer the period between primary induction completion and double-ridge stage, the longer was the apex at double ridge stage and the higher the number of spikelets per ear.

4. Sexual reproduction versus vegetative reproduction at plant scale and consequences on tiller demography

4.1. Seasonal evolution of tiller demography

The pattern of tiller demography is usually similar in all temperate grasses (Darwinkel, 1978; Lecarpentier *et al.*, 2019). First, from sowing the number of tillers rapidly increases up to a plateau (7000 tillers/m² in *Lolium perenne* and 6000 tillers/m² in *Lolium multiflorum*), which is usually reached at canopy closure (LAI >3) (Simon and Lemaire, 1987). During spring and early summer, the number of tillers decreases due to the death, also called regression, of vegetative tillers (Figure 1.5). A synchrony between vegetative tiller mortality and the reproductive phenology was regularly observed in *Lolium perenne* (cv. S23) (Ong *et al.*, 1978; Colvill and Marshall, 1984), *Phleum pratense* and *Festuca pratensis* (Langer *et al.*, 1964). Tiller regression usually

occurs during the elongation of reproductive tillers and can decrease tiller population by 50 % (Colvill and Marshall, 1984). Regressing tillers are mainly vegetative young tillers (age < 40 days), which experience an increasing competition for light and assimilates with larger and taller reproductive tillers (Ong, 1978; Colvill and Marshall, 1984; Sachs *et al.*, 1993). After summer, reproductive tillers die after seed dispersion and the remaining vegetative tillers start to produce new leaves and tillers until canopy closure is reached once again during the next growing season (Figure 1.5) (Jewiss, 1972; Matthew *et al.*, 2000). In addition, mowing or grazing can cause tiller death but also decreases the leaf area index (LAI) which in turn enhances tillering. Individual plant perenniality is ensured by a rapid turnover of successive tillers (Colvill and Marshall, 1984). Depending on the growth conditions experienced by individual tillers, part of them reach the floral transition and become reproductive while others remain vegetative (Figure 1.5). On the one hand, reproductive tillers decrease the overall tiller demography but determine the number of seeds produced and therefore the potential size of the next generation. On the other hand, the number of tillers that remain vegetative, *i.e.* that maintain tiller demography, determines the future ability of a plant for resource capture.

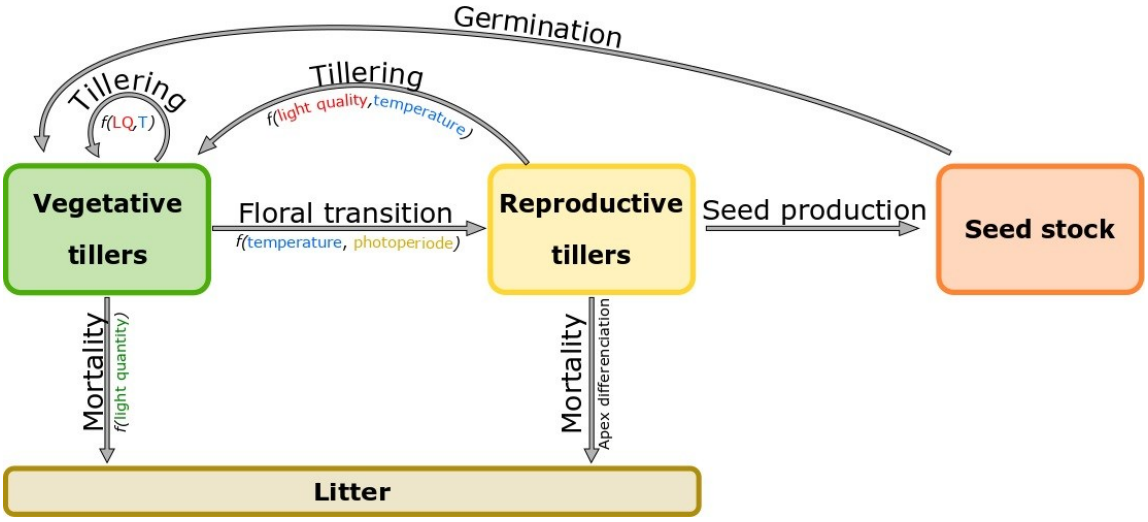


Figure 1.5: Compartmental model of a perennial grass plant.
The plant is divided in three compartments: vegetative tillers (green), reproductive tillers (yellow) and dead tillers composing a litter (brown).

In *Phleum pratense*, almost all tillers initiated before summer, are reproductive, whatever their appearance date. Therefore, new vegetative tillers produced at the basis of reproductive tillers only emerge after the reproductive period. This mode of tiller replacement was qualified by Matthew *et al.* (2000) as a 'reproductive' pathway. In *Festuca pratensis*, Matthew *et al.* (2000) observed a long period of coexistence between reproductive and vegetative tillers, the former being replaced by tillers which emerged during spring and which remained vegetative until the next spring. *Lolium multiflorum* has an important mortality of young tillers in spring in relation with the specificity of the floral induction in this species which does not necessarily require primary induction. In *Lolium perenne*, tiller emergence follows an approximately permanent regime throughout the year (Matthew, 1992). Thus, many age classes of tillers coexist in this species where the youngest ones ensure tiller replacement, following a so-called 'vegetative' pathway.

4.2. Proportion of reproductive tillers in interaction with the environmental conditions

In natural populations of *Lolium perenne* cultivated in a common garden experiment, Barre *et al.* (2017) found that the proportion of reproductive tillers increased for populations originating from low latitudes, which are characterized by a large diurnal temperature range and hot temperatures during the warmest months. In contrast, populations from oceanic climates had the lowest proportion of reproductive tillers. These results suggest that the adaptation of species and populations to their environment led to a higher production of seeds in regions where dry and hot summers alter the vegetative growth. On the contrary, the proportion of reproductive tillers is lower in populations from temperate regions (Poirier *et al.*, 2012), where summer conditions allow some significant vegetative growth. In addition, the proportion of reproductive tillers per plant was found to be highly variable between natural populations of *Lolium perenne*, ranging from 13 to 72% (Barre *et al.*, 2017).

Obviously, the proportion of reproductive tillers is also controlled by the environmental variables responsible for floral induction. For instance, low temperatures during primary induction as well as short photoperiods increased the number of

reproductive tillers in *Lolium perenne* plants cultivated in growth chambers (Aamlid *et al.*, 2000). Similarly, the reproductive tiller proportion was increased by the exposure to long photoperiods during the secondary induction (Aamlid *et al.*, 2000). These observations emphasize that reproductive tiller proportion and floral induction present the same pattern of response to the inductive conditions. Therefore, the earliest cultivars, characterized by lower induction requirements in duration and intensity, produce the highest number of reproductive tillers. While nitrogen fertilization is known to have a positive effect on tillering in grasses, Bahmani *et al.* (2002) showed in *Lolium perenne* that the reproductive tiller proportion was higher in 'Ellett' than in 'Grasslands Ruanui' cultivar at low nitrogen fertilization. However, increasing nitrogen availability increased the reproductive tiller proportion in 'Ellett' but not in 'Grasslands Ruanui'. Conversely, the authors found no effect of water availability on the reproductive tiller proportion. Furthermore, Casal *et al.* (1985) demonstrated that light quality has an impact on reproductive tiller proportion by manipulating the R/FR ratio perceived by tillers. In that experiment, the number of flowering tillers in a reproductive plant of *Lolium multiflorum* increased from 2 to 2.7 under low R/FR. However, an opposite response was observed in the two *Lolium perenne* cultivars 'Ellett' and 'Grasslands Ruanui' (Bahmani, 2000). This may highlight two different aptitudes to maintain vegetative tillers in dense canopies that are characterized by low R/FR (Casal *et al.*, 1986). Bahmani *et al.* (2002) also observed that despite similar heading dates, the two cultivars of *Lolium perenne* 'Ellett' and 'Grasslands Ruanui presented large differences in reproductive tiller proportion.

Defoliation by grazing or cutting also affects the reproductive tiller proportion. First, defoliation changes the light environment perceived by the axillary buds located at the basis of the plant, which can therefore trigger their development into new tillers. When defoliation occurs below the apex of the flowering tillers, which may even occur before heading, the tillers die. After cutting in late spring, a majority of the remaining tillers are vegetative. For some species and cultivars, the cutting of flowering tillers marks the end of the flowering period until the next growing season. However, in some cases a second wave of flowering starts with the development of new reproductive tillers during autumn. Named 'aftermath heading', this behavior is mostly represented in early-heading genotypes (Arojju *et al.*, 2016).

4.3. Inheritance of the reproductive state from mother tillers

Some early researchers assumed that the floral transition occurs independently at the tiller scale *i.e.* each tiller has to experience the whole induction process (primary and secondary induction) to become reproductive (Kleinendorst, 1974). For species and genotypes which primary induction can be completed under the only effect of temperature, no juvenile stage is observed, meaning that each apex is competent to be primary induced whatever its initiation date. However, because the secondary induction requires the presence of leaves to perceive the photoperiodic signal, the floral transition of the primary induced apices will only be effective after the emergence of the first leaf of the tiller. This hypothesis is sufficient to explain the reproductive tiller proportion in some species such as *Lolium perenne*. However, some studies highlighted that the hypothesis of an independent induction process for each apex cannot explain the reproductive tiller proportion of species whose primary induction is partly ensured by the photoperiod. In *Bromus inermis* and *Dactylis glomerata* for instance, the primary induction is mainly controlled by short photoperiods, Havstad *et al.* (2004) observed that many tillers emerging after the end of the short photoperiod treatment were still able to become reproductive, in spite of having no leaf exposed to light during that stage. In another experiment, Havstad *et al.* (2003) exposed only half-plants of *Dactylis glomerata* and *Bromus inermis* to short photoperiods. Although these species have an obligatory short-photoperiod requirement for primary induction, he observed flowering in non-exposed tillers. These observations led to the hypothesis of an inductive signal transferred from the reproductive to the vegetative tillers of the same plant (Havstad *et al.*, 2003, 2004). However, the nature of such an indirect inductive signal remains to be determined to date and raises the question of the conservation of vegetative tillers in the plant if such an inductive signal exists. This would require the involvement of a competing floral inhibitor which may be the gibberellins (Havstad *et al.*, 2004). On the contrary, it was also reported that in some cases, the youngest tillers may experience the floral transition while the oldest ones remain vegetative. For instance, Williamson (2008) observed in *Lolium perenne* that the first primary tiller was flowering in only 28% of plants whereas the second, third and fourth primary tillers were flowering in 94%, 62% and 30% of plants, respectively.

5. Modelling grassland phenology: what is known and what is still to be determined?

Numerical models designed for grassland management seek to account for the reproductive development in order to better predict the seasonality of biomass production as well as grassland perenniality. These models may also constitute research tools for anticipating the effects of climate change on grasslands and identifying plant ideotypes adapted to future growing conditions. One of the difficulties in modelling the phenology of grasslands is related to their perenniality and in particular, to the presence of a large number of tillers of which only a part will undergo the floral transition over a growing season. Below, we present a review of existing models of grassland phenology, highlighting their respective objectives and assumptions (Table 1-1).

Table 1-1: The reproductive phenology in current grassland models.

ID	Name	Reference	Type	Species	Reproductive phenology				
					Primary induction	Secondary induction	Floral transition	Heading	Other
1	-	Fiorelli *et al.* 2001	Mechanist model of tiller population	*Lolium perenne*	-	-	DOY* of first tiller conversion	Emergence of the 1st complete inflorescence (DOY)	-
2	OSYAQ	Hermann and Schachtel 2001	Organ compartments	*Lolium multiflorum* for calibration and validation	-	-	-	-	Change of organ demand is dependent on a sum of daily development rate (*beta* function of temperature) from sowing date
3	CATIMO	Bonesmo and Bélanger 2002	Organ compartments	*Phleum pratense*	-	-	Sum of GDD** basis 0 from May 1st***	Sum of GDD** basis 0 from May 1st***	-
4	OSYAQ	Hermann and Schachtel 2001	Organ compartments	*Lolium multiflorum* for calibration and validation	-	-	-	-	Change of organ demand is dependent on a sum of daily development rate (*beta* function of temperature) from sowing date
5	GrazeGro	Barrett *et al.* 2005	Crop model	*Lolium perenne*	-	-	Mean time of double ridge stage (input value)	Date (input value)	-
6	SISTAL	Mazel *et al.* 2005	Individual based	Perennial grass species but developped on *Festuca arundicea*	Tillers have to be born before the end of winter	-	Probabilistic function of tiller birth date	-	-
7	ModVege	Jouven *et al.* 2006	Crop model	Several species	-	-	Sum of GDD from January 1st***	-	-
8	STICS grasslands	Jégo *et al.* 2013	Crop model	*Phleum pratense*	-	-	Sum of GDD** (provided by CATIMO model)	-	-
10	BASGRA	Höglind *et al.* 2016	Process-based model	Calibrated with *Phleum pratense*	Threshold temperature (low)	-	-	-	-
10	BASGRA_NZ	Woodward *et al.* 2016	Process-based model	*Lolium perenne*	Incremental function of the temperature	-	-	-	-

* DOY: day of year

*** Calendar date fits for the northern hemisphere

** GDD: growing degree-day

ID	Tiller demography				Environmental/Managing factors considered for floral development					
	Proportion of reproductive tillers	Aftermath heading	Tillering	Tiller mortality	Genetics	Water availability	Mineral nutrition	Light radiations	Photoperiod / Latitude	Cutting / Regrowth
1	Linear function of the tiller appearance date during a favorable period	Emergent property	Constant number of live tillers	Death of reproductive tillers when their height is above cutting height	Three cultivars differing in heading date		Effect of nitrogen on leaf growth	-	Latitude. Model validated for 2 latitudes 52°N and 67°N	Yes
2	-	-	-	-	Yes	Change of organ demand	Change of organ demand	Yes	-	Yes
3	-	-	-	-	Yes	Effect of drought on RUE	Effect of nitrogen on RUE	-	-	-
4	Linear function of the tiller appearance date during a favorable period	Emergent property	-	Death of reproductive tillers when their height is above cutting height	Three cultivars differing in heading date	-	Effect of nitrogen on leaf growth	-	Latitude. Model validated for 2 latitudes 52°N and 67°N	Yes
5	All tillers appeared before a given date will become reproductive (March 1st***). Timing of tiller headings follow a normal distribution around the input heading date	-	Affected by flowering	Death of reproductive tillers by decapitation	3 classes of precocity	Yes	Yes	-	-	Impact on leaf growth after flowering tiller decapitation
6	Tiller transition follow a function of tiller birth date. Tillers born after the end of November will remain vegetative. Tillers born before the end of August have the highest chance to become reproductive ***	-	Yes	Vegetative tillers	Yes	Yes	Yes	Canopy closure	-	Yes
7	Reproductive growth is represented by a function of nitrogen nutrition. Start and end- are GDD* sum from January 1st***	-	-	-	4 groups of species	Yes	Nitrogen	-	-	Cutting stops reproductive growth

8	-	-	-	-	-	-	-	-	-	-
9	Tillers become non-elongating reproductive at a daily rate depending on temperature and daylength. Conversion from non-elongating to elongating tiller category follow a constant daily rate if daylength remains above a minimum value	Emergent property	Vegetative tillers are produced proportionally leaf appearance, but site-filling is reduced when LAI is high or C reserves are low	By frost and decapitation	Yes	-	-	Yes	-	Yes
10	Tillers become non-elongating reproductive at a daily rate depending on temperature and daylength. Conversion from non-elongating to elongating tiller category follow a constant daily rate if daylength remains above a minimum value	Emergent property	Vegetative tillers are produced proportionally leaf appearance, but site-filling is reduced when LAI is high or C reserves are low	By frost and decapitation	Yes	-	-	Yes	-	Yes

5.1. Simulation of the floral transition and heading date

In the most empirical implementations of reproductive development, the reproductive events occur at fixed dates expressed either in growing degree-days (GDD) or in calendar time. In the first case, the sum of GDD is initialized at a given date which was empirically determined, January 1st for the model ModVege (Jouven *et al.*, 2006) or May 1st for model CATIMO (Bonesmo and Bélanger, 2002) and STICS (Jégo *et al.*, 2013). Regarding the models based on calendar time, they need to be recalibrated for every location in order to account for the temperature regime and the effect of the latitude on the photoperiod. In addition, these models do not account for the effect of temperature on the growth of reproductive structures (internodes, spikes), which prevents them being used for predicting flowering variability in response to interannual fluctuations of temperature or to climate change.

In models considering the grassland as a population of tillers, the primary induction of each tiller is assumed to occur in tillers emerged before a critical date while others remain vegetative (Fiorelli et al., 2001; Groot and Lantinga, 2004; Barrett et al., 2005; Mazel et al., 2005; Jouven et al., 2006; Höglind et al., 2016). The calibration of these models is based on empirical relationships between tiller emergence date and floral transition as observed in different locations and years. To the best of our knowledge, none of the grassland models accounts for the sequential nature of floral induction *i.e.* the progressive completion of the primary and secondary induction. A recent version of the model BASGRA, named BASGRA_NZ, considers the primary induction with more details (Woodward *et al.*, 2020). In this model, the primary induction is incremental and calculated at canopy scale. The daily increment of primary induction in calculated by a concave function of the soil surface temperature and a calibrated parameter representing the optimal temperature for primary induction.

5.2. Simulation of reproductive tiller proportion and its consequences on plant perenniality

The models CATIMO (Bonesmo and Bélanger, 2002) and OSYAQ (Herrmann and Schachtel, 2001) do not explicitly make any difference between the functioning cycle of vegetative and reproductive tillers. Variations in tiller demography are therefore implicit and the increase in reproductive tillers is derived from the decrease in the biomass quality for herbivores as calibrated from biomass harvests performed throughout the season. Few models consider the role of environmental conditions on the proportion of reproductive tillers. In the model developed by Fiorelli (2001), the proportion of reproductive tillers increases with nitrogen availability. In more detailed models, the population of tillers is distributed in groups according to their status, *e.g.* vegetative and reproductive in the model of Groot and Lantinga (2004), GrazeGro (Barrett *et al.*, 2005) and SISTAL (Mazel *et al.*, 2005) ; vegetative, non-elongating reproductive and elongating reproductive in BASGRA (Höglind *et al.*, 2016) and BASGRA_NZ (Woodward *et al.*, 2020) ; or vegetative, reproductive and senescent in Fiorelli's (2001). In the model of Fiorelli *et al.* (2001), the size of the tiller population is considered constant as new tillers permanently replace the reproductive ones, which is representative of the established swards but not of the early stages of sward development. For models which dynamically simulate tiller demography (GrazeGro, SISTAL and BASGRA), tiller appearance is dependent on the rhythm of leaf production and stops at canopy closure, approximated using a leaf area index threshold. The transition of tillers from a developmental group to another is based on different hypotheses. In Groot and Lantinga (2004), initial tillers are undifferentiated, those appeared before the end of the vernalization period become reproductive according to their order of emergence and a constant daily rate. In SISTAL (Mazel *et al.*, 2005), the probability of any tiller to become reproductive is defined by its date of initiation: tillers initiated before the end of November remain vegetative and those initiated before the end of August have the highest chance to become reproductive. In the model GrazeGro (Barrett *et al.*, 2005), all tillers appeared before March 1st are considered to be primary induced and will therefore become reproductive. The model BASGRA (Höglind *et al.*, 2016) simulates plant development for several years and it is the only one which explicitly accounts for the frost-induced mortality of vegetative tillers. The

reproductive transition of the tillers in BASGRA is more sequential, a first transition from vegetative to non-elongating reproductive tillers occurs after a primary induction (temperature threshold) and depends on temperature and photoperiod, the subsequent transition in elongating reproductive tillers occurs at a constant daily rate if the photoperiod is sufficiently long. In the model BASGRA_NZ, the transition is similar to the model BASGRA, but the primary induction is more complex. Primary induction of tillers occurs at a daily rate depending on the temperature.

Modelling the reproductive tiller proportion throughout the season also requires consideration of tiller mortality. Tiller mortality due to cutting is inconsistently implemented in grassland models. In GrazeGro (Barrett *et al.*, 2005), all reproductive tillers are removed after cutting by grazing or mowing. In BASGRA (Höglind *et al.*, 2016), which distinguishes two categories of reproductive tillers, the mortality by cutting only applies to elongating tillers, assuming that the apices of non-elongated tillers are located below the cutting point. In the model of Groot and Latinga (2004), which has a geometrical representation of tillers, only the reproductive tillers whose apex is above the cutting height are removed. The model SISTAL (Mazel *et al.*, 2005) is the only one to integrate the mortality of vegetative tillers that occurs during the reproductive period. Aftermath heading is also accounted for in few models which assume that some individual reproductive tillers may survive after mowing or grazing. In the model of Groot and Lantinga (2004), aftermath heading is an emergent property resulting from the height of the apex and the cutting height. In BASGRA (Höglind *et al.*, 2016), reproductive tillers can remain non-elongated, thus avoiding mortality by cutting. Interestingly, some models also include some effects of winter, in particular freezing risks, which allow to simulate the complete annual cycle of the plant (Höglind *et al.*, 2016).

5.3. Towards more comprehensive models of grassland reproductive phenology

Current models of grassland are mostly based on empirical rules, which raises the question of their ability to simulate the phenology of various genotypes in contrasted environments. In order to further improve our ability to predict the phenology

of grasses and its effects on grassland productivity and management, we propose to develop more comprehensive models integrating the role of the environment × genetics interactions on the phenology and growth processes at the individual tiller scale. We have seen that the floral induction is a critical event for the onset of flowering which is highly dependent on genetic × environment interactions. To our opinion, a fine implementation of this process in models is essential to better anticipate the phenology of grasslands in current and future climates. However, it would require a better knowledge of the floral induction, in particular concerning the cardinal temperatures and photoperiods associated with the primary and secondary floral inductions of each species. The determination of induction equations independent of the experimental conditions would require the use of experiments under constant induction conditions combined with experiments under fluctuating conditions. Finally, a method for an early determination of the floral transition would also be required (*e.g.* phytohormone dosage, non-destructive observation of the apex) to replace the late determination of the reproductive state often observed at the date of heading.

There is growing evidence for strong interactions between the reproductive development of perennial grasses and their morphogenesis. These interactions are poorly accounted for in current models despite their consequences on biomass quality and quantity. For instance, the rhythm of leaf appearance is an important variable for the determination of the heading date as it determines the final number of leaves, the duration of their expansion and the length of the pseudostem from which the spike will emerge. Architectural models based on coordination rules between successive leaves (*e.g.* Verdenal *et al.* (2008)) would be appropriate to account for the temporal evolution and the intraspecific diversity of the rhythm of leaf appearance in relation with the growing conditions. According to the studies reviewed above, the increase in leaf growth rate usually observed in spring should be implemented in models as a direct function of temperature and photoperiod *i.e.* independently of the floral transition. Finally, the modelling of tiller appearance and their reproductive status is the key point to predict the environmental history of each tiller, the number of spikes, the proportion of stem in the harvested biomass and the tiller demography. Therefore, it seems that the tiller is the relevant scale to model the reproductive development of perennial grasses. The individual-based models describing the tillering dynamics therefore appear as promising tools to better integrate the growth conditions actually

experienced by individual tillers (Lafarge et al., 2005; Mazel et al., 2005; Verdenal et al., 2008; Rouet et al., 2020). In addition, the topological and geometrical relations between tillers represented in these models are adapted to further assess the hypothesis of a signaling system responsible for the transmission of the floral induction between tillers. Individual-based models coupled with an explicit description of plant architecture in 3D also give the opportunity to determine precisely the environment perceived by each individual tiller, leaf and apex (Godin and Sinoquet, 2005). It also allows to explicitly represent the heterogeneity of both plant structures and environment within the canopy by attributing different genetic characteristics to the plant (DeJong *et al.*, 2011).

6. Conclusion

Agriculture is facing new issues, requiring more efficient and sustainable agrosystems based on species and cultivars adapted to the future climatic conditions. More intelligent management, using more powerful numerical applications are a key for the sustainability of future agriculture. In perennial grasses, these objectives strongly depend on the reproductive phenology as the earliness and proportion of reproductive tillers affect spring production and grassland perenniality. Computer plant modelling is a promising tool to understand current plant functioning, to simulate changes due to future conditions and test genetic and management solutions. The accuracy of the models depends on the knowledge we have about the development of plants in interaction with their environment.

The present review highlights that two main scales have to be considered to fully address the whole plant reproductive development. The floral induction and the growth of reproductive organs mainly proceed at tiller scale. This is in accordance with the fact that morphogenesis (leaf production and elongation) and metabolism are highly independent between the tillers of a cohort (except in the early stages). The floral induction depends on the environmental conditions and determines the morphogenesis and, at the same time, the heading date of the tiller. Accounting for the plant scale is also necessary to understand the tiller demography, from apex initiation to death. This review also highlighted some points that would require further

investigations such as a better quantification of the inductive requirements for floral induction. Also, in some species and conditions, the extent to which the reproductive status of tillers could be inherited from other tillers of the plant should be better assessed and quantified.

Current models of perennial grasslands have been developed for an agronomic use, based on empirical relations. These models do not allow to simulate the dynamics of floral transition at tiller scale in perennial grasses, which limits our ability to study how genotype × environment interactions affect plant phenology. The rough representation of the tiller population along the whole year also limits our ability to study the perenniality of plants and the competition between them. As a step further, future models should better account for the dual floral induction process. There is also a lack in the representation of the interactions between reproductive development and morphogenesis at tiller and plant scale. Representing the whole plant scale is also crucial to account for processes determining the demography of tillers and therefore plant perenniality, among which tillering regulation, the coordination between leaf production and tiller initiation. Including such aspects in future models is crucial to improve our ability to predict the reproductive phenology of grasslands in contrasted climatic conditions and management.

Résumé du chapitre 1

Le développement reproducteur des graminées pérennes est un processus avec de nombreux impacts agronomiques et écologiques. Il est responsable d'une augmentation de la production de biomasse par les prairies ainsi que d'une diminution de leur qualité fourragère.

Le développement reproducteur est déclenché par l'induction florale qui est dépendante des conditions de température et de photopériode. A l'échelle de la talle, l'induction florale enclenche une accélération de la production de *primordia* à l'apex qui formeront des feuilles ou des épillets. En parallèle, la vitesse de croissance des feuilles s'accélère. La date d'épiaison, c'est-à-dire le moment d'émergence de l'épi hors de la pseudotige ne se produit qu'une fois ensemble des feuilles ligulées, ce qui met en évidence l'importance du nombre final de feuille de la talle. Le développement reproducteur d'une talle trouve son issue dans la mort de la talle.

Une plante est un ensemble de talles produites à des moments différents à partir d'une talle-mère grâce au processus de tallage. Au cours du développement floral, seule une partie des talles présentent un développement reproducteur, les autres restant végétatives et assurant la pérennité de la plante. En majorité les talles reproductrices sont apparues avant ou pendant l'exposition aux conditions inductrices, mais, certains résultats expérimentaux ont mis en évidence des transferts d'induction, notamment secondaire, à des talles n'ayant pas été exposées aux conditions inductrices. Toutefois les molécules et processus impliquées dans le transfert d'induction restent à explorer.

Dans la littérature, les modèles de graminées pérennes intègrent des modèles phénologiques empiriques qui ne permettent pas de bien rendre compte des interactions entre l'induction florale et la morphogénèse.

Dans le chapitre 2, nous proposons une expérimentation pour étudier les effets de différents calendriers d'induction florale sur la morphogénèse et la date d'épiaison des talles chez *Lolium perenne*.

Chapitre 2

Effet de la durée des phases d'induction florale sur la date d'épiaison et la morphogénèse chez *Lolium perenne*.

1. Introduction

The reproductive development of perennial grasses is monocarpic and the floral transition is irreversible (Gillet, 1980; Heide, 1994). In *Lolium perenne*, most experimental studies showed that the floral transition requires two successive induction phases under the control of different environmental factors. The primary induction is completed after an exposure to low temperatures and short photoperiods for several weeks while the secondary induction is reached after a few days of exposure to elevated temperatures and long photoperiods (Heide, 1994). Different combinations of temperature, photoperiod and exposure duration have been tested to determine the environmental window favorable to induce flowering (Aamlid *et al.*, 2000). These experiments are very useful for determining effective thresholds of temperature or photoperiod under constant conditions, but do not allow the definition of continuous response laws for floral induction that could be applied in natural and fluctuating conditions. In addition, such studies have focused on floral induction but do not allow inferring the heading date from the date of floral transition.

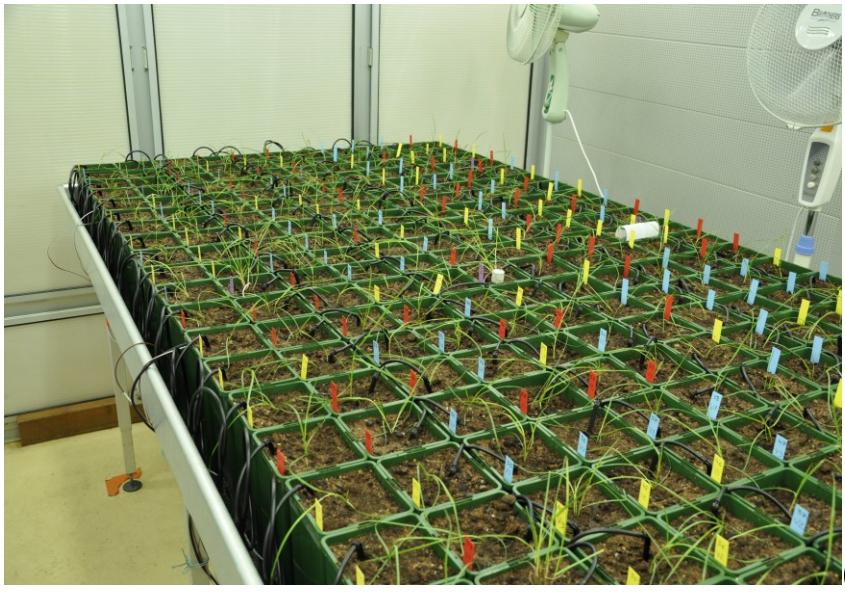
In grasses, the heading date results from a combination between the duration of floral induction and the growth of reproductive organs, which ultimately lead to the emergence of the spike from the pseudostem. Before floral transition, the tiller is vegetative and the apex produces vegetative phytomers (a leaf, an internode and a lateral apex). During these vegetative stages, the rate of leaf emergence and leaf dimensions define the length of the pseudostem from which the spike will emerge. After floral transition, the apex produces reproductive phytomers (a spikelet and an internode), which are derived from an initial structure common to leaves: the primordium. The heading of the spike therefore depends on apex activity and growth processes during both vegetative (length of the pseudostem, number of leaves) and reproductive (number of spikelets, peduncle length) stages. As a consequence, the duration of floral transition appears as a key factor for integrating the interactions between vegetative and reproductive morphogenesis.

The aim of the present chapter was to study how the duration of the floral induction affects the reproductive morphogenesis and the heading date of *Lolium*

perenne tillers. To that purpose, leaf production, leaf elongation and heading dates were monitored in three cultivars of perennial ryegrass exposed to different regimes of temperature and photoperiods. Specifically, we assessed (i) the relation between the floral transition and the acceleration of leaf elongation (Davies, 1971; Parsons and Robson, 1980), (ii) the relation between the rates of leaf emergence and primordia production during the reproductive phase, (iii) the interaction between the genetic variability and the environmental conditions.

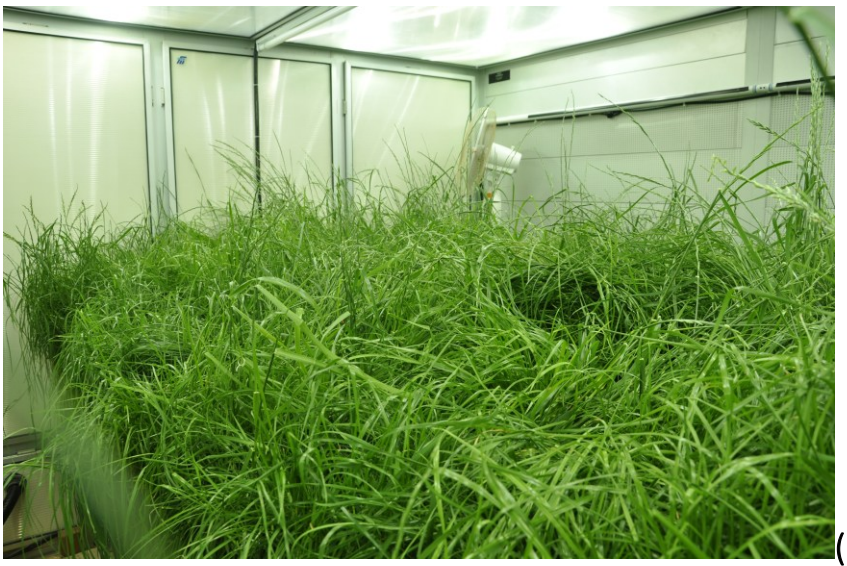
2. Materials and methods

The overall principle of the experiment was to grow three perennial ryegrass cultivars, from seedling to flowering, with varying durations of exposure to inductive conditions (Figure 2.1). Four inductive treatments were defined, with temperature, photoperiod and phase duration as factors. Briefly, the treatments differed in the duration of a non-inductive period (elevated temperature and short days) after the end of the primary induction and prior to the secondary induction. As such, plants stayed in a vegetative growth for variable durations before the beginning of the secondary induction. During tiller development, leaf length and leaf emergence rate were monitored at regular intervals as well as the heading date for each inductive treatment.


(a)



(b)



(c)

Figure 2.1: Experimental setup.
(a) plants of treatments 1, 2 and 3 during primary induction (low temperature and short days). (b) plants of treatment 0 maintained in non-inductive conditions (high temperature and short days). (c) Plants of treatments 0, 1, 2 and 3 at heading.

2.1. Plant material

The experiment was conducted on Bronsyn, Carvalis and Tryskal, three cultivars of *Lolium perenne* differing in heading earliness. These cultivars are registered in the French catalog of cultivars and have been characterized by the French Variety and Seed Study and Control Group (GEVES) (Table 2-1). Bronsyn is the

earliest cultivar of the catalog, Carvalis is classified as having an intermediary earliness, while Tryskal is a late heading cultivar. The cultivars were all appropriate for cultivation in temperate areas and were supposed to require winter conditions to become competent for flowering. Indeed, no heading was reported during the year following sowing in early spring in the GEVES network of experiments, but all flowered following at least one winter.

As the experiment aimed to study precisely the effects of environmental conditions on the reproductive phenotype, we started to grow plants from seeds. This ensured that all tillers were submitted to the same environmental conditions and that they had the same age but this introduced some genetic diversity between individuals. Seeds were provided by seed companies, harvested in summer 2018 and stored in the dark at ambient temperature, thus ensuring that they did not start the primary induction.

Table 2-1: Details of the cultivars of Lolium perenne used in the experiment.

Spring growth, heading date, flexibility (number of available days for grassland exploitation) and aftermath heading (score between 1 and 9, 9 corresponding to a cultivar with an important aftermath heading) are the average of the observations made in different sites and years. Herbe Book https://www.herbe-book.org/ 2019 edition.

Cultivar	Breeder	Country	Registration year	Ploidy	Main use	Spring growth	Heading date	Flexibility (days)	Aftermath heading
Bronsyn	Agriseeds Ltd	New-Zealand	2001	2n	Forage	March 28th	May 5th	38.7	4.2
Carvalis	Carneau Frères SA	France	2010	2n	Forage	April 4th	May 22th	55.1	2.4
Tryskal	RAGT R2N	France	2010	2n	Forage	April 10th	June 6th	65.5	2.1

2.2. Growth conditions

First, seeds were germinated in Petri dishes in the dark at a mean temperature of 18°C. After 4 days, seedlings were sown in micro-sods of peat and placed in a greenhouse for 4 weeks in November (Figure 2.2). Air temperature was held over 15°C and light was added in the morning and evening to ensure a photoperiod of 13 hours (Sodium lamps, 400W) to avoid the start of primary induction.

After that preliminary growth phase, plants were transplanted in 3L plastic pots (l: 12, w: 12, h: 20) filled with a substrate composed of loam PELTRACOM (60%), superficial soil from Lusignan, France (30%), sand (10%) and controlled-release fertilizer (12/14M; N-P-K: 14-18-11). Plants were arranged in a randomized block design in different growth chambers (model 97132/7NU, Froids et Mesures, Beaucouzé, France) (Figure 2.1). Then, plants were progressively moved from one chamber to another depending on the induction treatment (see details below). When all plants were gathered in the same growth chamber, the density was 70 plants.m^{-2}. Irrigation was provided in both chambers according to canopy growth to ensure optimal growing conditions. Light was provided by HQI lamps (POWERSTAR, HQI-T 400WD lamps, OSRAM, Munich, Germany) with a Photosynthetic Photon Flux Density of 240 µmol m^{-2} s^{-1}. The target photoperiod and temperature regimes are detailed below, while actual measurements of temperature are available in Supplementary 2-2.

2.3. Temperature and photoperiodic treatments

In growth chambers, plants were exposed to four regimes of inductive conditions with different durations and levels of temperature and photoperiod (Figure 2.2). Chamber 1 was set with “high temperature and long day” conditions (HT – LD: 18°C - 16h) for the whole experiment. In Chamber 2, conditions were first “low temperatures and short days” (LT – SD: 6°C – 8h) and then “high temperature and short days” (HT – SD: 18°C - 8h).

In treatment 0 (T0), 78 plants (26 per cultivar) were continuously exposed to the HT – LD conditions of the Chamber 1. This treatment was used as a control because the HT – LD conditions were not expected to allow the floral transition due to the absence of cold temperature exposure. In the three other treatments (T1, T2 and T3), all plants were first exposed to conditions that were supposed to trigger floral induction. Plants of these treatments were exposed first to LT – SD conditions for 9 weeks (Chamber 2), which was expected to complete the primary induction requirement (Aamlid *et al.*, 2000; Paina *et al.*, 2014). Then, the temperature of Chamber 2 was raised up to 18 °C but photoperiod was maintained short (HT - SD). Plants of T1, T2 and T3 were successively transferred from Chamber 2 (HT - SD) to Chamber 1 (HT – LD) with different delays. Plants of T1 were immediately transferred to HT – LD after LT – SD (*i.e.* no delay between the completion of the primary induction and the exposure to long days). In T2 and T3, plants were maintained under HT – SD in Chamber 2, respectively for 3 and 6 weeks, before being transferred to HT – LD (Chamber 1). Long day conditions were the same than those used by Paina *et al.* (2014), except for temperature (18°C instead of 20°C).

The photoperiod extension of 8h in Chamber 1 was applied using LED tubes (Philips, MAS LEDtube UN 1500mm UO 24W840 T8) whose surface was partially covered (75%). LED tubes were turned on for 4 hours just before the HQI lights were switched on and 4 hours after HQI lights were switched off. The supplementary irradiance provided by LED tubes was sufficiently low (+8 µmol $m^{-2}.s^{-1}$ of PPFD) to assess that the photosynthetic activity was not significantly increased in comparison to plants maintained under short day conditions.

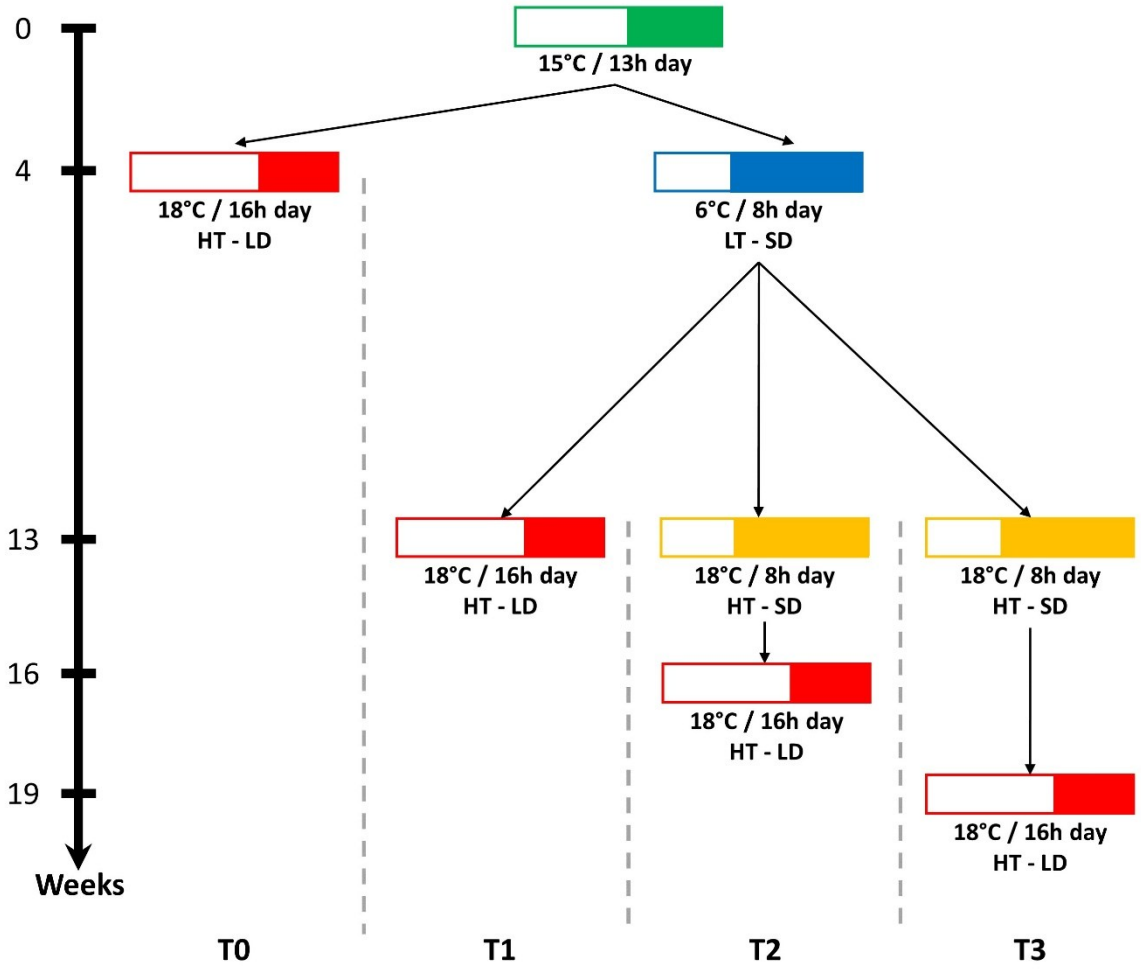


Figure 2.2: Diagram representing the inductive treatments imposed to the Lolium perenne cultivars. Temperature and photoperiod regimes differed from the 4th week. LT-SD: 6°C/8h day, HT-SD: 18°C/8h day, HT-LD: 6°C/8h day

2.4. Measurements

Measurements were performed to characterize (i) the dynamic of vegetative morphogenesis all along the experiment, (ii) the effects of the induction treatments on leaf appearance and heading date and (iii) the effects of the induction treatments on the final morphology of the main tiller.

From the date of transplantation (4 weeks after sowing), the visible length of every leaf of the main tillers was measured with a ruler every 2 or 3 days with a precision of 1 mm. Lamina length and collar height were measured. In order to assess the elongation rate variations of successive leaves during the whole experiment, the results presented below are expressed as 'tiller elongation' that we defined as the

cumulated elongation of all visible leaves produced by a tiller. Leaf elongation measurements stopped when internode elongation started as it was not possible to distinguish internode and sheath elongation from the non-destructive measurements used in the study. The appearance and ligulation dates of each leaf were registered. Finally, the heading date, defined as the date when at least one spikelet emerged from the pseudostem, was monitored.

After tiller growth had stopped for several days and spikes were entirely emerged, tillers were collected to measure the number of long internodes (*i.e.* longer than 1mm) and the number of spikelets. The length of internodes and peduncle were also measured for plants of T1. Results about the internodes are presented in Supplementary 2-3.

2.5. Statistical analyses

Analysis of variance and non-linear regression were performed with R software (*R Core Team* 2021). Analyses of variance (ANOVAs) were performed following a one-factor linear model such that

$$y_{ij} = \mu + T_i + V_j + \gamma_{ij} + \varepsilon_{ij}$$

Here, y_{ij} is any measured variable for treatment (*i, j*), μ represents the mean value of *y*, *T* signifies the additive main effect of the inductive treatment *i*, *V* signifies the main additive effect of the variety *j*, γ is the nonadditive interaction effect of treatment (*i, j*), and ε is the random error.

The normal distributions of the residuals of ANOVAs were tested using the Shapiro–Wilk test. Homoscedasticity was checked by random distribution of the residuals. Median comparisons where realized with the test of Wilcoxon-Mann-Whitney (values not distributed normally). In all cases, H_0 was rejected when p-value was lower than 0.05. In the text, values given correspond to the median values and the standard error associated. All the boxplots of this chapter were made with the style of Tuckey (-1.5*IQR, 2nd quartile, median, 3rd quartile, +1.5*IQR).

3. Results

3.1. Heading date

As expected, no plants of T0 exhibited any reproductive development during the experiment (180 days). This result confirmed that the cultivars required winter-like conditions to flower. In Bronsyn, 77, 81 and 58% of plants achieved floral transition and produced a spike in T1, T2 and T3, respectively (Figure 2.3).

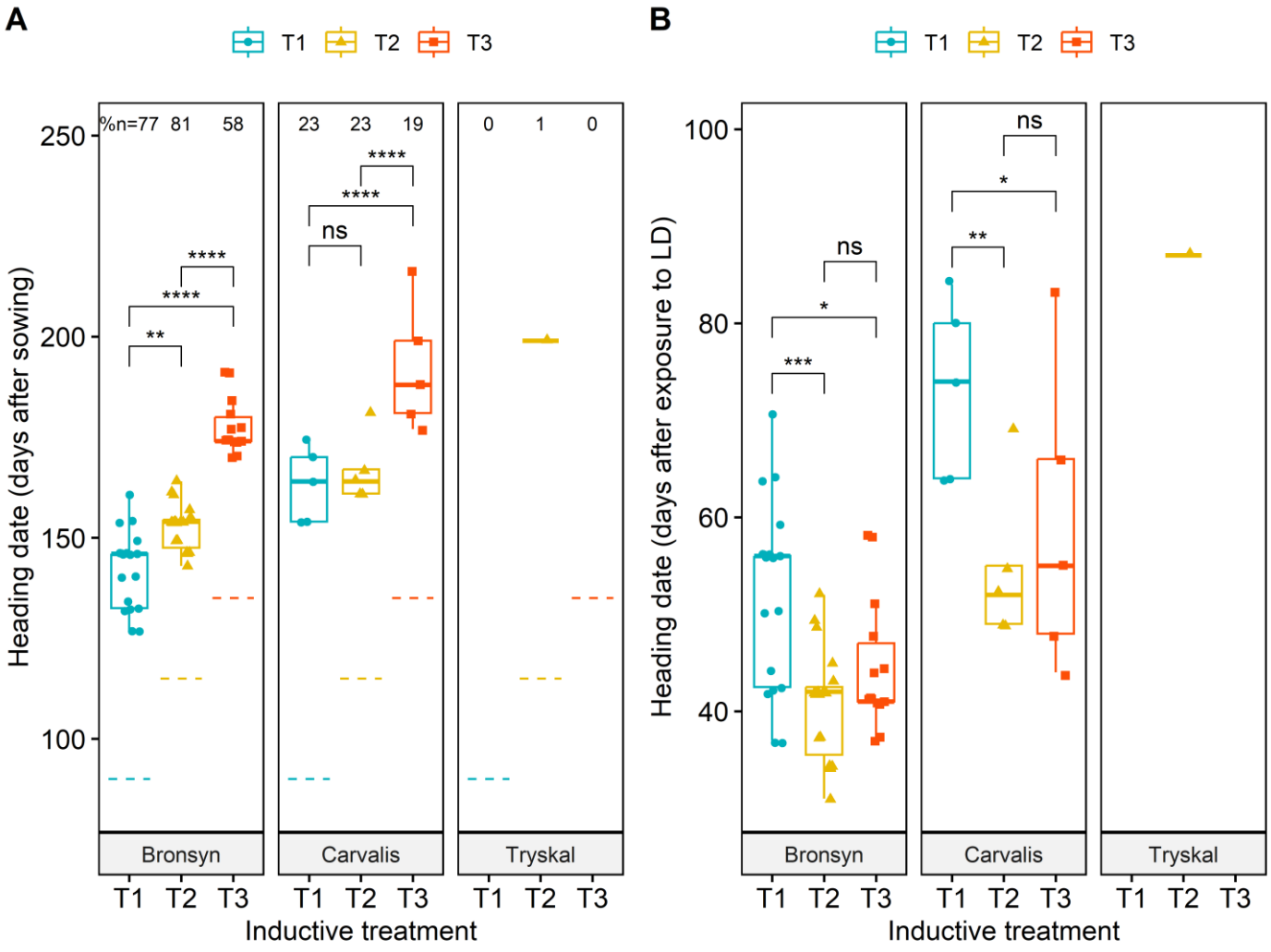


*Figure 2.3: Heading dates in cultivars Bronsyn, Carvalis, and Tryskal for the different inductive treatments T1 (blue circles), T2 (yellow triangles), and T3 (red squares). (A) Heading date calculated from sowing. (B) Heading date calculated from the exposure to long photoperiods. The percentage of headed plants for each treatment is indicated above each boxplot in A. The start of exposure to long days is indicated by dashed lines in A for each treatment. Statistical differences between treatments are shown in A (ns: non-significant, *: P < 0.05, **P < 0.01, ***P < 0.001, ****P < 0.0001).*

In Carvalis, heading ratios were significantly lower (23% in T1, 23% in T2 and 19% in T3). Surprisingly, only one plant of cultivar Tryskal achieved the floral transition and reached the heading stage. This was confirmed through tiller dissection of every non-headed plants, which revealed no sign of floral transition on the apex (absence of double-ridges or white stripes). The cultivar Tryskal was not considered for the following analyses on the reproductive development but different hypotheses explaining that behavior are proposed in the discussion. The comparison of heading dates between cultivars Bronsyn and Carvalis from the same treatment highlights that Bronsyn always headed earlier than Carvalis (*treatment T1: $W = 15$, $p < 0.05$, treatment T2: $W = 13.5$, $p < 0.05$, treatment T3: $W = 14$, $p < 0.05$*) (Figure 2.3.a). This ranking was in accordance with the observations by the GEVES group in natural conditions (Figure 1.2). The delay between the heading dates of the two cultivars were respectively 21 ±5 days in T1, 11 ±9 days in T2 and 14 ±7 days in T3.

For the Bronsyn and Carvalis cultivars, the average heading date was postponed in relation to the duration spent in HTSD conditions. Consequently, heading occurred later in T3 than in T2 and later in T2 than in T1. This delay was significant between all treatments in Bronsyn and only between T1–T3 and T1–T2 in Carvalis. Despite plants spending 6 weeks in HT–SD (T3), no heading was observed under short days, confirming that exposure to long photoperiods is necessary to trigger the floral transition. Interestingly, the delay between the transfer to HT–LD conditions and the heading date was not proportional to the duration of the HT–SD period (Figure 2.3b). In fact, when calculating the heading date from the start of exposure to long photoperiods, the average delay to heading in Bronsyn was 56 days for T1, 42 days for T2, and 41 days for T3. A similar nonlinear response to the duration of exposure to long days was observed for Carvalis (T1: 77 days, T2: 54 days, and T3: 55 days).

3.2. Final number of leaves and number of spikelets per spike

In average, the final number of leaves on headed tillers increased from T1 to T3 (Figure 2.4.a), which is in accordance with the results on heading dates (Figure 2.3.a). This result was expected as plants of T2 and T3 were exposed to non-inductive

conditions and therefore remained vegetative for a longer period than plants of T1. Counting the number of leaves produced from the date of exposure to long photoperiod allowed the comparison between treatments in similar conditions (Figure 2.4.b).

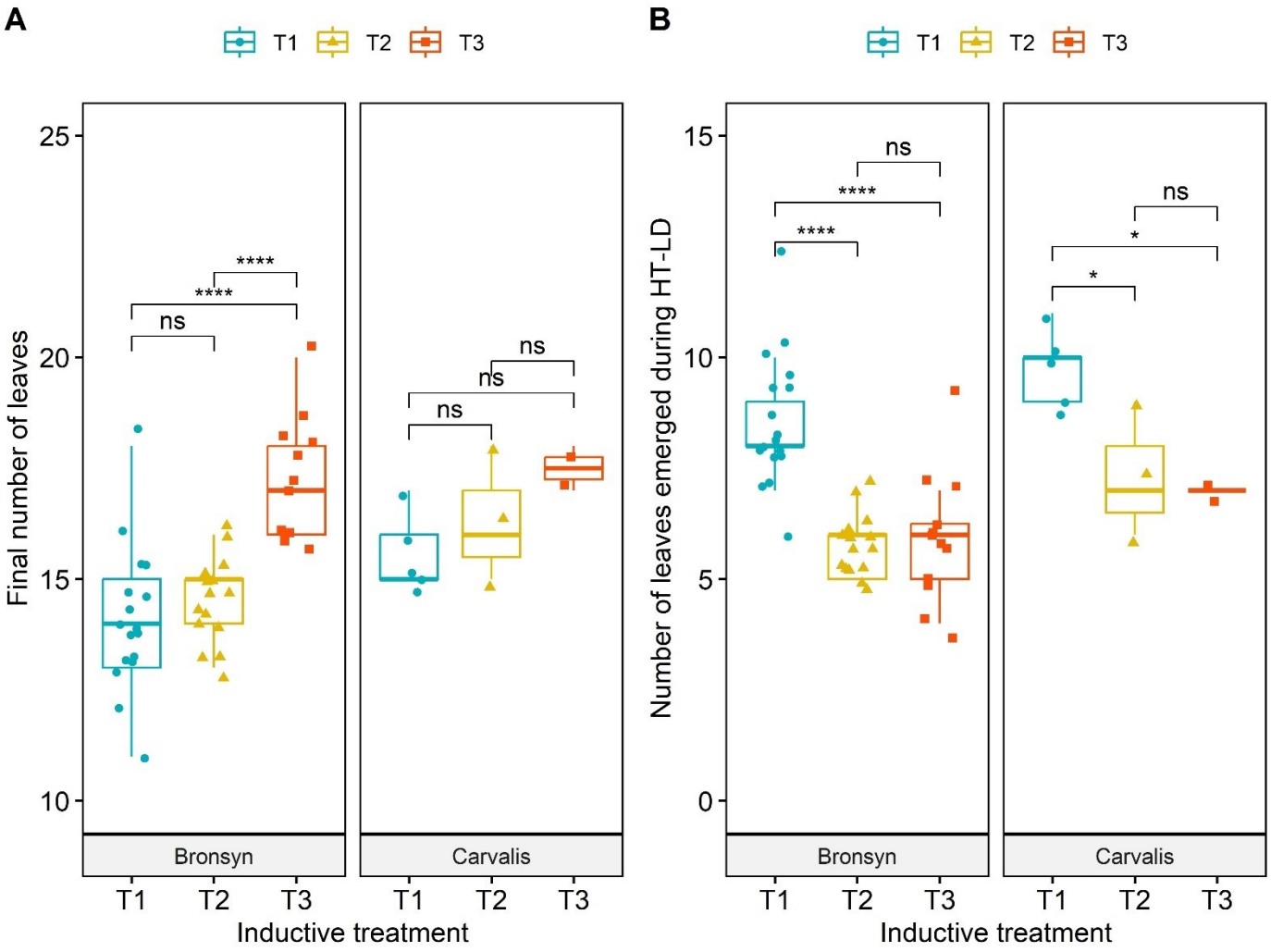


Figure 2.4: Final number of leaves (A) and number of leaves that have emerged since the transfer to high temperature-long day (HT–LD) conditions (B). *Results are shown only for Bronsyn and Carvalis plants that reached the heading stage. The inductive treatments are denoted as T1 (blue circles), T2 (yellow triangles), and T3 (red squares). Statistical differences between treatments are shown in A (ns: non-significant, *P < 0.05, **P < 0.01, ***P < 0.001, ****P < 0.0001).*

The final count of leaves on the headed tillers varied from 11 to 20 for Bronsyn and 15 to 18 for Carvalis. On average, the final leaf count for the headed tillers increased by three leaves between T1 and T3 in both cultivars (Figure 2.4A), although statistical differences were only significant for T3 in Bronsyn. The number of leaves that emerged during the HT–LD period exhibited high variability across treatments and cultivars, ranging from 4 to 14 leaves (Figure 2.4B). In T1, the number of leaves that

emerged during the HT-LD period constituted 57% and 66% of the final leaf count for Bronsyn and Carvalis, respectively. For both cultivars, the number of leaves that emerged during this period was significantly higher in T1 compared to T2 and T3 (*T1–T2: W = 285.5, P < 0.001 and T1–T3: W = 198, P < 0.001 for Bronsyn; T1–T2: W = 14, P = 0.07, and T1–T3: W = 10, p < 0.05* for Carvalis). There was no significant interactive effect between the varieties and the treatments (*P = 0.44*). For Bronsyn, T1 plants produced an average of two more leaves than T2 and T3 plants during the HT–LD period. The number of leaves that emerged during this period was identical between T2 and T3 treatments for Bronsyn (~6 leaves; *W = 105.5, P > 0.05*). For Carvalis, T1 plants produced an average of three more leaves than those of T2 and T3 during the HT–LD period.

The average number of spikelets per spike varied from 14 to 32 across treatments and cultivars (Figure 2.5).

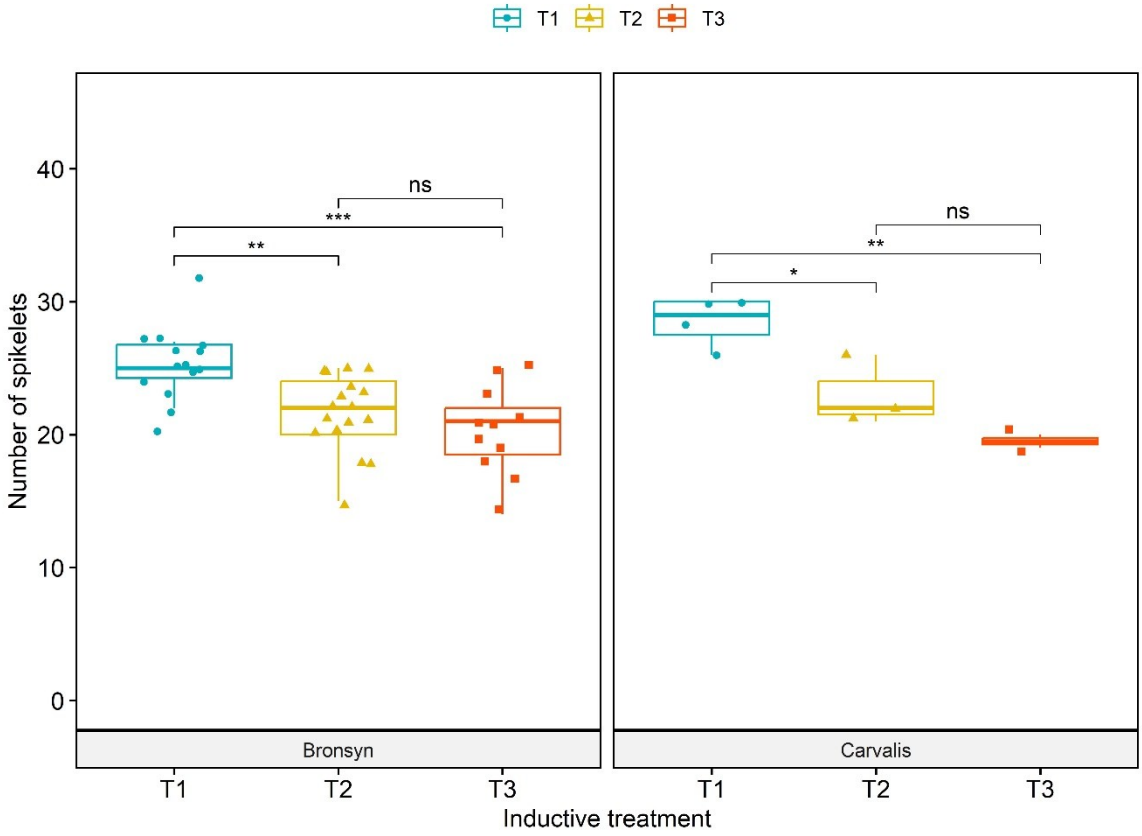


Figure 2.5: Number of spikelets per spike for cultivars Bronsyn and Carvalis. *The inductive treatments are denoted as T1 (blue circles), T2 (yellow triangles), and T3 (red squares). Statistical differences between treatments are shown in A (ns: non-significant, *P < 0.05, **P < 0.01, ***P < 0.001, ****P < 0.0001).*

The analysis of variance of spikelet number revealed neither significant differences between cultivars nor interactive effect between the varieties and the treatments (*P = 0.33*). Similar to the observation for leaves, the longer the exposure to HT–SD conditions, the fewer the spikelets. In Bronsyn, the number of spikelets was higher in T1 compared to T2 and T3 (*P < 0.01*). The differences between treatments were similar for Carvalis, with a decrease from 28 ± 1.7 spikelets in T1 to 19 spikelets in T3 (*P < 0.01*). Both the number of leaves that emerged during the HT–LD period and the number of spikelets per spike were significantly higher in T1 compared to T2 and T3.

Hence, both the number of leaves produced during the HT-LD period and the number of spikelets per spike were significantly higher in T1 while T2 and T3 were very close. With the hypothesis that changes in apex functioning immediately occurred when plants started to be exposed to long photoperiods, these results suggested a faster production of primordia in treatment T1 than in treatments T2 and T3.

3.3. Leaf elongation rate and leaf ligulation rate

Based on individual leaf length dynamics, linear regressions were performed on the total tiller length (sum of all leaf lengths) across four 3-week periods corresponding to the treatment application schedule (**Figure 2.6**). For T0 plants, exposed solely to HT–LD conditions, tiller elongation rates tended to increase during the experiment, particularly for Bronsyn *(period 1–2: W = 99, P < 0.01 and period 1–3: W = 71, P < 0.01*). After three weeks in T0 conditions, Bronsyn's elongation rate was significantly higher than that of Carvalis (*P < 0.01*) and similar to Tryskal (*P = 0.08*). For T1, T2, and T3 plants, a notably low leaf elongation rate was observed during exposure to low temperature (LT–SD) (*mean ± SD of all cultivars = 0.54 cm day−1 ± 0.04*) with no significant difference between treatments (*P = 0.42*) or varieties (*P = 0.65*). The leaf elongation rate then sharply increased to 5.4 cm day−1 ± 0.08 when the plants were transferred to high temperature (HT–SD and HT–LD). The leaf elongation rate of tillers exposed to HT remained remarkably stable as long as plants were not transferred to long day conditions (HT–SD; orange bars). In these HT-SD conditions, plants of cultivar Bronsyn showed the highest rate of leaf elongation compared to Carvalis and

Tryskal (*P < 0.001*). For T1 and T2 plants, leaf elongation rate increased for several weeks

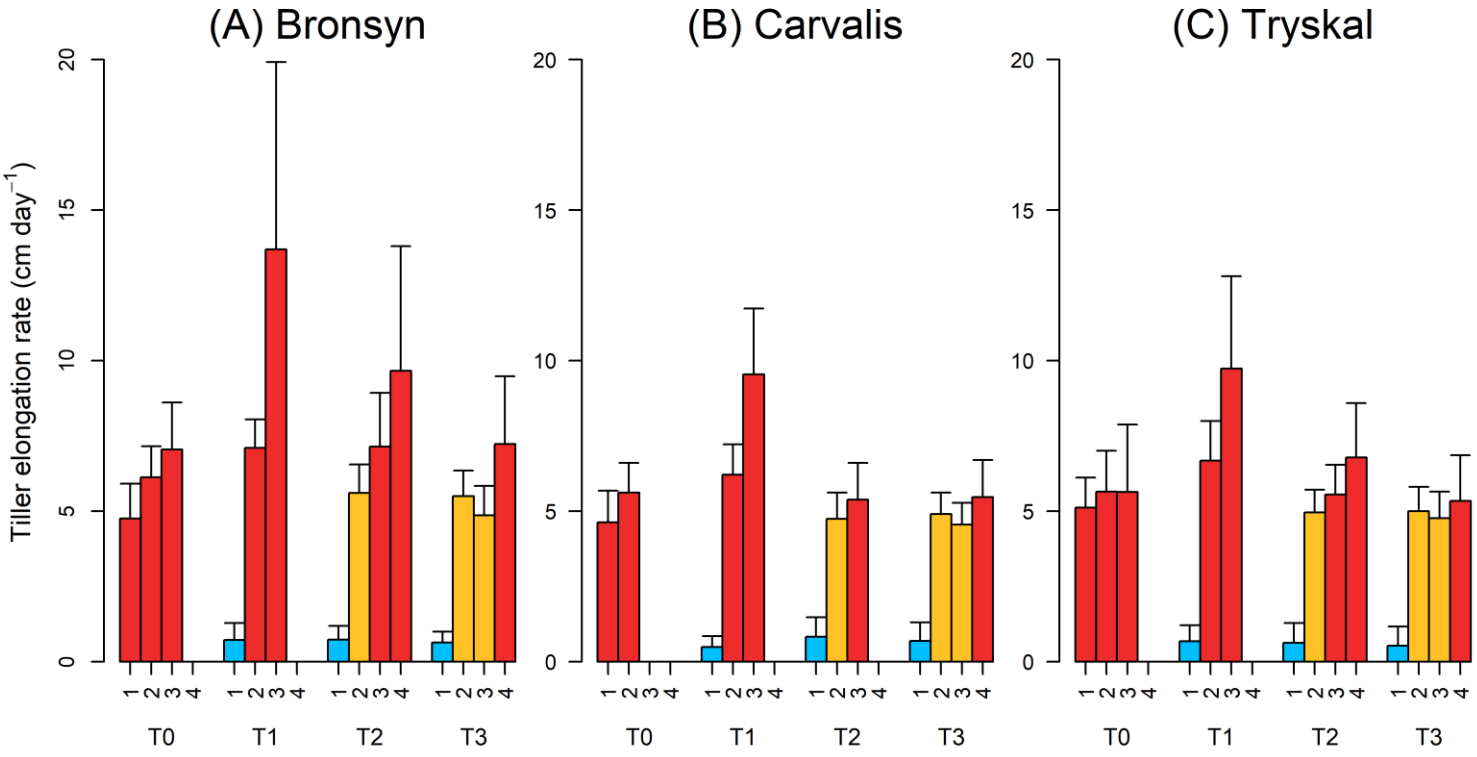


Figure 2.6: *Dynamics of tiller elongation rate of cultivar Bronsyn (A), Carvalis (B), and Tryskal (C). Results are presented for each inductive treatment (T0, T1, T2, and T3). Based on the dynamics of individual leaf length, linear regressions were performed on the total length of the tillers, considering four 3-week periods corresponding to the treatment application schedule. For clarity, the low temperature–short day (LT–SD) conditions are represented by blue bars, high temperature–short day (HT–SD) by orange bars, and high temperature–long day (HT–LD) by red bars. The value of the bars is the mean + SD.*

after transfer to HT–LD. For all cultivars, exposure to long days and high temperature immediately after the LT–SD period (T1 period 2; red bars in **Figure 2.6**) significantly *(P < 0.001*) increased the rate of leaf elongation compared to plants exposed to high temperature but remaining under short days (T2 period 2 and T3 periods 2–3; orange bars in **Figure 2.6**). The same dynamics were observed when T2 and T3 plants were transferred to long days (*T2, period 2 vs. 3: P < 0.01, except for Tryskal; T3, period 3 vs. 4: P < 0.05*). For T1, T2, and T3, the maximal leaf elongation rate was delayed approximately proportionally to the time spent under HT–SD (during period 3 for T1, during period 4 for T2 and later for T3). In Carvalis and Tryskal cultivars, which had few reproductive tillers, the mean acceleration of leaf elongation was significantly lower

than for Bronsyn, especially in T2 and T3. The above analyses of variance revealed no significant effect between the varieties and the treatments.

The impact of the inductive treatments on the dynamics of the leaf appearance rate (LAR) exhibited similarity across the three cultivars (**Figure 2.7**). For T0 plants, consistently exposed to HT–LD throughout the experiment, the LAR gradually declined from approximately 0.146 to 0.09 leaves per day (l day^{-1}) over four weeks for all cultivars. During their exposure to low temperature (LT–SD), plants of T1, T2, and T3 demonstrated a notably low LAR of about 0.035 l day−1 which was similar across all cultivars and treatments (*P = 0.22 and 0.35*, respectively). This rate significantly increased to around 0.16 l day−1 when plants were exposed to high temperatures (*P < 0.001*), subsequently decreasing progressively as the tillers aged across all cultivars and treatments. Contrary to the results shown for leaf elongation rate (**Figure 2.6**), the photoperiod did not influence LAR, as no significant differences were observed among T1, T2, and T3 (*period 2: P = 0.54*).

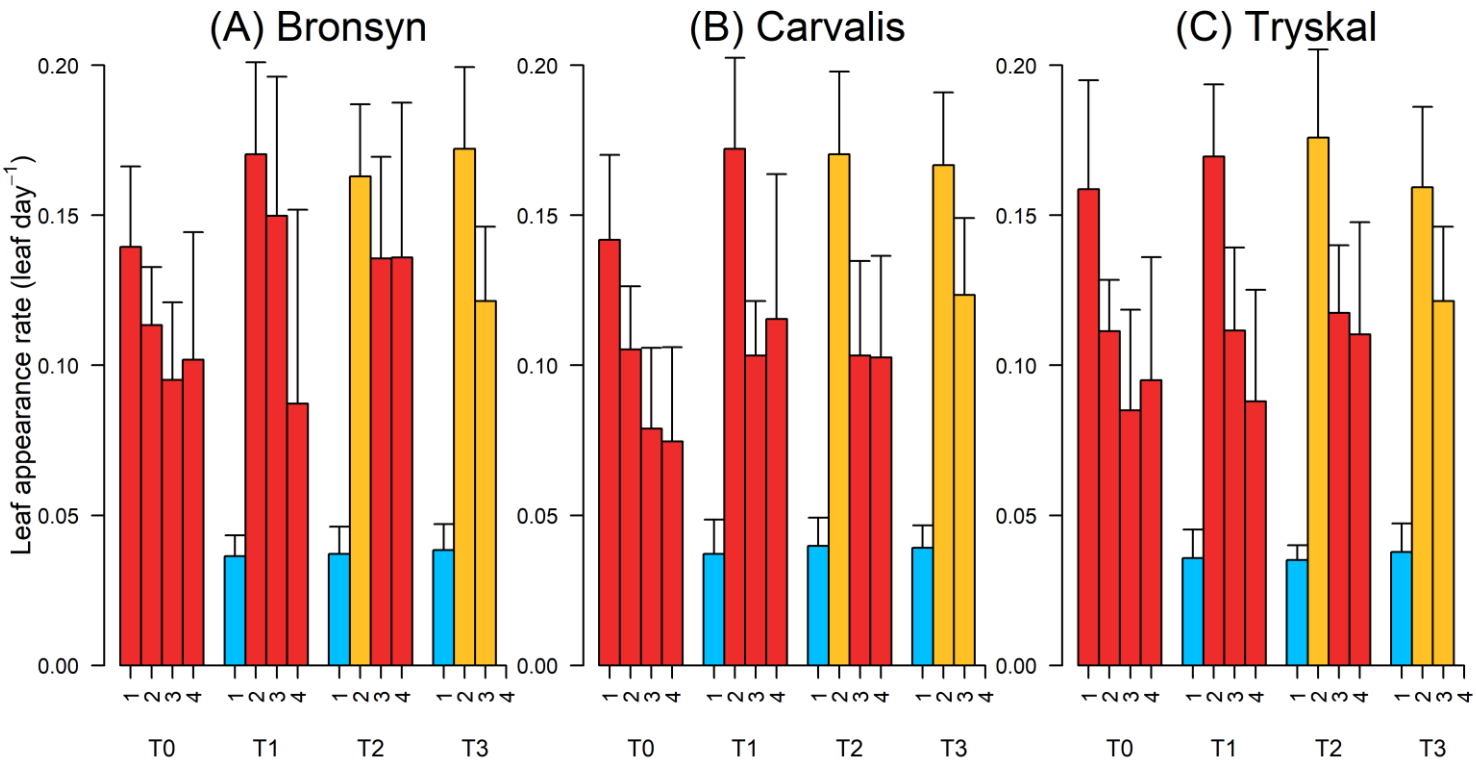


Figure 2.7: *Dynamics of leaf appearance of cultivars Bronsyn (A), Carvalis (B), and Tryskal (C). Results are presented for each inductive treatment (T0, T1, T2, and T3). Linear regressions were performed on the total length of the tillers, considering four 3-week periods corresponding to the treatment application schedule. For clarity, the low temperature–short day (LT–SD) conditions are represented by blue bars, high temperature–short day (HT–SD) by orange bars, and high temperature–long day (HT–LD) by red bars. The value of the bars is the mean + SD.s*

.

4. Discussion

4.1. A dual floral induction but different requirements among cultivars

In *Lolium perenne*, it was shown that populations and cultivars differed in floral induction requirements (for review see Chapter 1). Within that intraspecific diversity, some populations, usually found in the Mediterranean area, seem to have a unique induction phase, as no specific requirements for cold temperature were found (Aamlid *et al.*, 2000). In this study, we chose cultivars appropriated for temperate areas with cool winters and moderately dry summers. Therefore, they were expected to have a dual floral induction consisting of a primary and secondary induction (Heide, 1994). Indeed, observed heading dates (Figure 2.3) and tiller dissections showed that without any exposure to low temperatures and short photoperiods (LT - SD) tillers remained vegetative and produced up to 20 leaves (T0). Although the proportion of reproductive plants highly differed among cultivars, floral transition of the apex and heading were only observed after consecutive exposure to LT – SD and HT – LD conditions. These plants also exhibited a delay in heading when plant exposure to long days was delayed (T2 and T3) in comparison to those exposed to long days immediately after exposure to low temperature (T1). These observations confirmed the requirement of low temperature followed by long days for the floral induction of the studied cultivars. However, a fourth treatment combining LT-SD followed by HT-SD in a longer experiment would be required to conclude on the strict requirement for long photoperiods.

Establishing quantitative responses of primary and secondary inductions to temperature and photoperiod was beyond the scope of this study. However, the low proportion of heading plants in cultivars Carvalis and Tryskal raised the question of the inductive requirements for floral transition in those plants. The photoperiod set to induce secondary induction (16h) was longer than that existing in the GEVES trials in France, where the studied cultivars regularly flower. For instance, in Lusignan (latitude:

46.4333, longitude: 0.1167) the maximum photoperiod is 15.8h at summer solstice *i.e.* long after observed heading dates. The average temperature set to 18°C in the HT – LD condition was also higher than that observed in France during the completion of secondary induction (~ late winter – early spring). Regarding the LT - SD conditions, they were expected to allow completion of primary induction in all cultivars (Aamlid *et al.*, 2000; Paina *et al.*, 2014) compared to the natural conditions observed in the GEVES trials in winter. The photoperiod (8h) was lower than the minimum photoperiod in Lusignan (8.6h at winter equinox, minimum daylength) and the temperature was equivalent to the mean winter temperature in Lusignan (5°C compared to 5.1°C). Finally, the duration of the low temperature period (9 weeks) exceeded the average number of days with a mean temperature lower to 5°C in Lusignan (8 weeks for a period between Sept. 15th and July 30th for years 2001 to 2016). One possible explanation for the low proportion of heading in Carvalis and Tryskal, could be be the lack of very low temperatures (<5°C). Indeed, short and few episodes with very low temperature might have a stronger effect than a longer exposure to moderate low temperatures. More investigations would hence be necessary to determine quantitatively the response of the primary induction to low temperatures. Another reason for the low proportion of heading could have been the existence of a minimal developmental stage before which plants become competent for the primary induction (Cooper, 1960; Bommer, 1961; Heide, 1994). However, this was unlikely because tillers exposed to the LT-SD conditions were beyond the 3-leaf stage and *Lolium perenne* primary induction has been shown to respond at earlier stages (Heide, 1994).

4.2. Convergence of the heading dates among treatments

As expected, our results show that the heading date was delayed by 8 to 28 days when plants were maintained in short days and high temperature (HT-SD) between the primary and secondary inductive conditions (Figure 2.3). Thus, the earlier plants were submitted to long days after primary induction, the earlier the floral transition and the earlier the date of heading. However, expressing the date of heading as the number of days since exposure to long days revealed that plants maintained

under HT-SD conditions reached the heading stage faster compared to plants that were immediately transferred to long day conditions after primary induction. This relationship between the duration of the HT-SD conditions and the time of heading after exposure to long days was non-linear. Our results also highlighted that the reduced time to heading for the plants that were transiently exposed to short days, occurred for large plants having a high number of leaves as they were allowed to remain vegetative for a long period. The apices of these large plants appeared to be able to respond rapidly to secondary inductive conditions, thereby rapidly stopping leaf production (Figure 2.4) in favor of reproductive organs.

In different temperate cultivars of *Lolium perenne*, Cooper (1960) observed similar relationships between heading dates and number of leaves emerged under continuous days. He also observed a variable heading ratio between cultivars from 0% to 81%. For this author, the cause of these observations was an incomplete primary induction due to the insufficient inductive effect of the cold conditions (germinated seeds for 0, 4 and 8 weeks in a refrigerator to 0-3°C). He assumed that adding a following treatment by short photoperiod (4 and 8 weeks, 8 hours of day) tended to have an additional inductive effect and allowed a full induction of plants. This hypothesis was supported by the absence of reduction in time to heading for *Lolium multiflorum* individuals whose heading rate was already 100% without any short photoperiod treatment.

4.3. Balance between leaf and spikelet production: clues on apex dynamics

During the floral induction, the terminal apex of tillers undergoes major changes marking the transition from vegetative to reproductive stages (Gillet, 1980; Thomas, 1980). The exact period and the underlying processes driving the conversion of leaf primordia production to spikelet production are still under investigation. Many authors agree that the general structure of the apex is almost invariant in terms of size, mitotic index and number of primordia during the vegetative stages (Gillet, 1980; Gonthier and Francis, 1989; Kemp *et al.*, 1989). Gonthier and Francis (1989), who performed tiller dissections after exposure to different inductive treatments, noticed that this apparent

permanent state was conserved during the primary induction. In the present study, similar results were observed from apex observations on plants that were kept under non-inductive conditions (data not shown). The constant apex structure and morphology during vegetative stages likely arises from a coordination between the initiation of primordia and their differentiation into leaves.

From the start of secondary inductive conditions, authors observed an increase in the primordium initiation rate (lower plastochron), thus leading to an accumulation of primordia on the apex (Gonthier and Francis, 1989; Kemp *et al.*, 1989). Accumulated primordia are assumed to undergo two ways of differentiation: basal ones could develop into leaves, while distal ones eventually form a double-ridge and develop into spikelets (Gillet, 1980). Our results showed a correlation between the number of leaves emerging during the secondary induction conditions and the number of spikelets per spike (Figure 2.4 and Figure 2.5). However, our results did not allow us to determine when the leaf/spikelet differentiation took place during the secondary induction phase. Some studies based on destructive observations of apices suggested that the first primordium to be transformed into a spikelet appears a few plastochrons after exposure to long days (Gonthier and Francis, 1989).

4.4. Leaf growth and floral induction

For plants in T2 and T3, the initial acceleration of leaf elongation was attributed solely to the effect of temperature, while the more pronounced increase in leaf elongation rate for T1 plants resulted from the combined effects of temperature and photoperiod increases. This acceleration of leaf elongation around the time of floral transition aligns with our observations and has been consistently reported in literature (Davies 1978; Parsons and Robson 1980). Parsons and Robson (1980) proposed a causal link between the increase in leaf elongation rate and the floral transition. Conversely, Davies (1971) suggested that the acceleration of leaf elongation was independent of the floral transition and was driven by the same environmental factors as the floral induction, i.e. the photoperiod. To properly verify the independence of the effects of photoperiod and floral transition on leaf elongation rate, an additional treatment involving plants exposed to high temperature and short photoperiod before

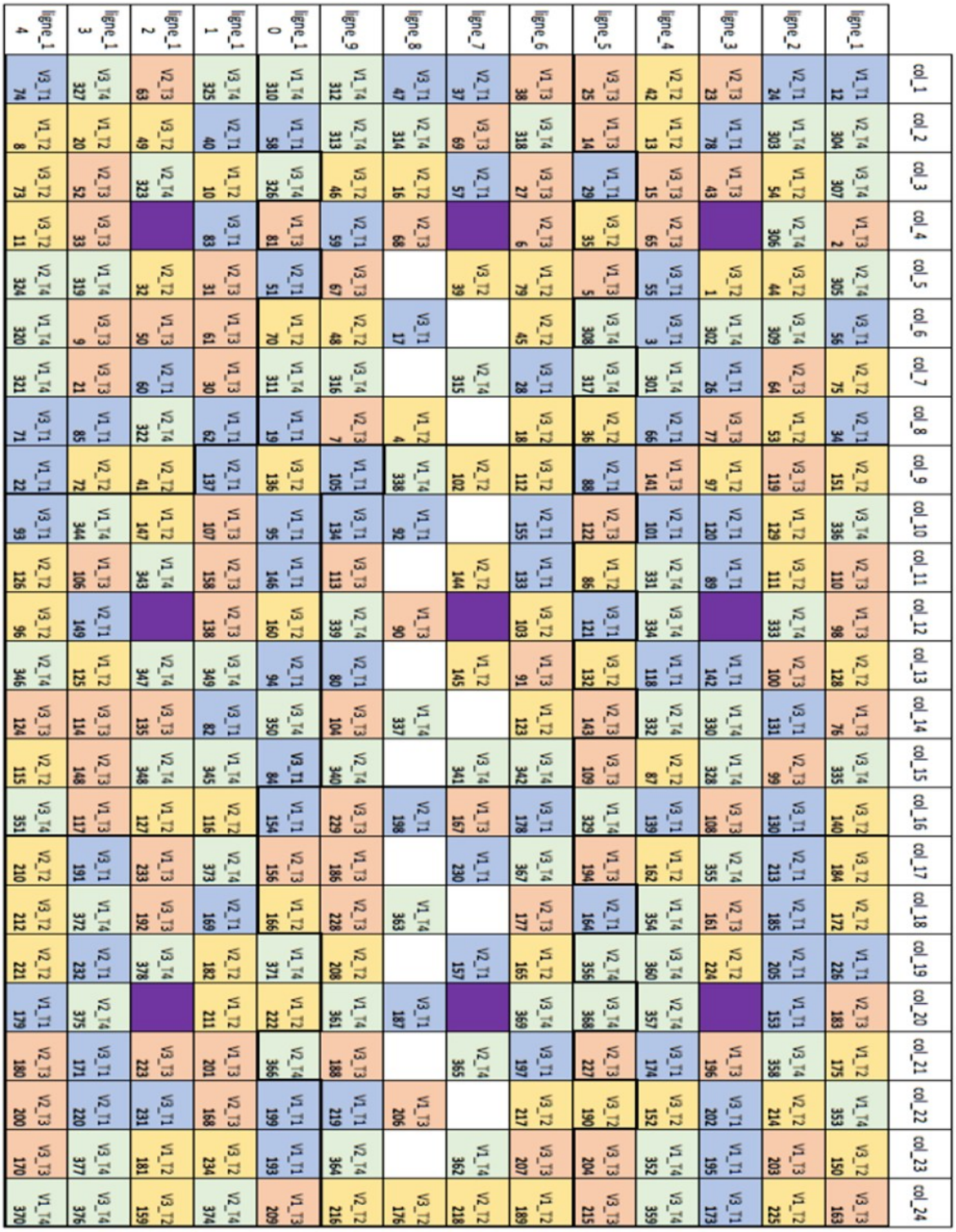
being transferred to high temperature and long photoperiod would have been necessary. However, our results indicated that the leaf elongation rate of plants in short days (HT–SD in T2 and T3) was slower than that of plants immediately transferred to long days (HT–LD in T1). This suggests that the floral transition may have an additive effect on the increase in leaf elongation induced by exposure to long days. The underlying mechanisms by which the floral transition or the photoperiod itself controls leaf elongation remain unclear to date but they may involve major phytohormones. For instance, it has been shown that KNOX proteins are key players in auxin, gibberellin, and cytokinin biosynthesis in the meristems during floral transition and inflorescence morphogenesis (McSteen and Leyser 2005; Colasanti and Coneva 2009; Zhang and Yuan 2014). At the same time, it appears that the same set of hormones actively regulates the rate of cell division in the leaf growth zones of maize plants (De Vos et al. 2020).

5. Conclusion

Perennial ryegrass demonstrated significant interactions between leaf growth and reproductive development, influenced by both genetic and environmental factors. Our findings confirmed that the floral transition only occurs following sequential exposure to low temperatures and long photoperiods even for the cultivars with low proportions of reproductive tillers. We noted that the date of exposure to a long photoperiod impacted the final count of leaves and spikelets. Additionally, the rate of leaf and spikelet production noticeably escalated following the plants' exposure to long photoperiods. Our results also suggest a direct, positive influence of photoperiod on leaf elongation rate, an effect that is further amplified in plants undergoing the floral transition. Finally, this work demonstrated original GxE interactions between the vegetative and reproductive development with strong consequences on plant fitness.

6. Supplementary Chapter 2

Supplementary 2-1: Plant repartition in Chamber 1



	col_1	col_2	col_3	col_4	col_5	col_6	col_7	col_8	col_9	col_10	col_11	col_12	col_13	col_14	col_15	col_16	col_17	col_18	col_19	col_20	col_21	col_22	col_23	col_24
ligne_1	V1_T1 12	V2_T4 304	V3_T4 307	V1_T3 2	V2_T4 305	V3_T1 56	V2_T2 75	V2_T1 34	V2_T2 151	V3_T4 336	V2_T3 110	V1_T3 98	V2_T2 128	V1_T3 76	V3_T4 335	V3_T2 140	V3_T2 184	V2_T2 172	V1_T1 226	V2_T3 183	V1_T2 175	V1_T4 353	V3_T2 150	V3_T3 163
ligne_2	V2_T1 24	V1_T4 303	V1_T2 54	V2_T4 306	V3_T2 44	V3_T4 309	V2_T3 64	V1_T2 53	V3_T3 119	V1_T2 129	V3_T2 111	V2_T4 333	V2_T3 100	V3_T1 131	V2_T3 99	V3_T1 130	V2_T1 213	V2_T1 185	V2_T1 205	V1_T1 153	V3_T4 358	V2_T2 214	V1_T3 203	V1_T2 225
ligne_3	V2_T3 23	V1_T1 78	V1_T3 43	V3_T2 1	V1_T4 302	V1_T1 26	V3_T3 77	V1_T2 97	V2_T1 120	V2_T1 101	V2_T3 122	V1_T1 142	V1_T4 330	V2_T4 328	V3_T3 108	V2_T4 355	V2_T3 161	V1_T4 354	V3_T4 360	V2_T4 357	V3_T1 174	V3_T1 196	V1_T1 195	V3_T1 173
ligne_4	V2_T2 42	V1_T2 13	V3_T3 15	V3_T2 65	V3_T1 55	V1_T4 3	V1_T4 301	V2_T1 66	V1_T3 141	V2_T1 101	V2_T4 331	V3_T4 334	V1_T1 118	V2_T4 332	V2_T2 87	V3_T1 139	V1_T2 162	V1_T4 354	V3_T4 360	V2_T4 357	V3_T1 174	V3_T2 152	V1_T4 352	V3_T4 359
ligne_5	V3_T3 25	V1_T3 14	V1_T1 29	V3_T2 35	V1_T3 5	V3_T4 308	V3_T4 317	V2_T2 36	V2_T1 88	V2_T3 122	V1_T2 86	V3_T1 121	V3_T2 132	V2_T3 143	V3_T3 109	V1_T4 329	V1_T3 194	V2_T1 164	V2_T4 356	V3_T4 368	V2_T3 227	V3_T2 190	V3_T3 204	V3_T3 215
ligne_6	V1_T3 38	V3_T4 318	V3_T3 27	V2_T3 6	V1_T2 79	V2_T2 45	V3_T1 28	V3_T2 18	V3_T2 112	V2_T1 155	V1_T1 133	V3_T2 103	V1_T3 91	V1_T2 123	V3_T4 342	V3_T1 178	V2_T3 177	V1_T2 165	V3_T4 369	V3_T1 197	V3_T2 217	V3_T3 207	V1_T2 189	
ligne_7	V2_T1 37	V3_T3 69	V2_T1 57		V3_T2 39		V2_T4 315		V2_T2 102		V2_T2 144		V1_T2 145		V3_T4 341	V1_T3 167	V1_T1 230		V2_T1 157		V2_T4 365		V1_T4 362	V2_T2 218
ligne_8	V3_T1 47	V2_T4 314	V2_T2 16	V2_T3 68		V3_T1 17		V1_T2 4	V1_T4 338	V1_T1 92		V1_T3 90		V1_T4 337		V2_T1 198				V1_T3 206			V3_T2 176	
ligne_9	V1_T4 312	V2_T4 313	V3_T2 46	V2_T1 59	V3_T3 67	V2_T2 48	V3_T4 316	V2_T3 7	V1_T1 105	V3_T1 134	V3_T3 113	V2_T4 339	V2_T1 80	V3_T3 104	V2_T4 340	V3_T3 229	V1_T3 186	V2_T3 228	V2_T2 208	V1_T4 361	V3_T3 188	V1_T1 219	V2_T4 364	V2_T2 216
ligne_10	V1_T4 310	V1_T1 58	V3_T4 326	V1_T3 81	V2_T1 51	V1_T2 70	V1_T4 311	V1_T1 19	V3_T2 136	V1_T1 95	V1_T1 146	V3_T2 160	V2_T1 94	V3_T4 350	V3_T1 84	V1_T1 154	V2_T3 156	V1_T2 166	V1_T4 371	V1_T2 222	V2_T4 366	V1_T1 199	V1_T1 193	V1_T3 209
ligne_11	V3_T4 325	V2_T1 40	V1_T2 10	V3_T1 83	V2_T3 31	V1_T3 61	V1_T3 30	V1_T1 62	V2_T1 137	V1_T3 107	V2_T3 158	V1_T4 343	V3_T4 349	V3_T1 82	V1_T4 345	V2_T2 116	V2_T4 373	V2_T1 169	V2_T2 182	V1_T2 211	V1_T3 201	V2_T3 168	V3_T2 234	V2_T4 374
ligne_12	V2_T3 63	V3_T2 49	V2_T4 323		V2_T2 32	V1_T3 50	V2_T1 60	V2_T4 322	V2_T2 41	V1_T2 147	V1_T4 343		V2_T4 347	V3_T3 135	V2_T4 348	V1_T2 127	V1_T3 233	V3_T3 192	V3_T4 378		V3_T3 223	V3_T1 231	V1_T2 181	V3_T2 159
ligne_13	V3_T4 327	V1_T2 20	V2_T3 52	V3_T3 33	V1_T4 319	V3_T3 9	V3_T3 21	V1_T3 85	V2_T2 72	V1_T4 344	V1_T3 106	V2_T1 149	V1_T2 125	V3_T3 114	V1_T3 148	V1_T3 117	V3_T1 191	V1_T4 372	V2_T1 232	V2_T4 375	V3_T1 171	V2_T1 220	V3_T4 377	V3_T4 376
ligne_14	V3_T1 74	V1_T2 8	V3_T2 73	V3_T2 11	V2_T4 324	V1_T4 320	V1_T4 321	V3_T1 71	V1_T1 22	V3_T1 93	V2_T2 126	V3_T2 96	V2_T4 346	V3_T3 124	V2_T2 115	V3_T4 351	V2_T2 210	V3_T2 212	V2_T2 221	V1_T1 179	V2_T3 180	V2_T3 200	V3_T3 170	V1_T4 370

Supplementary 2-2:

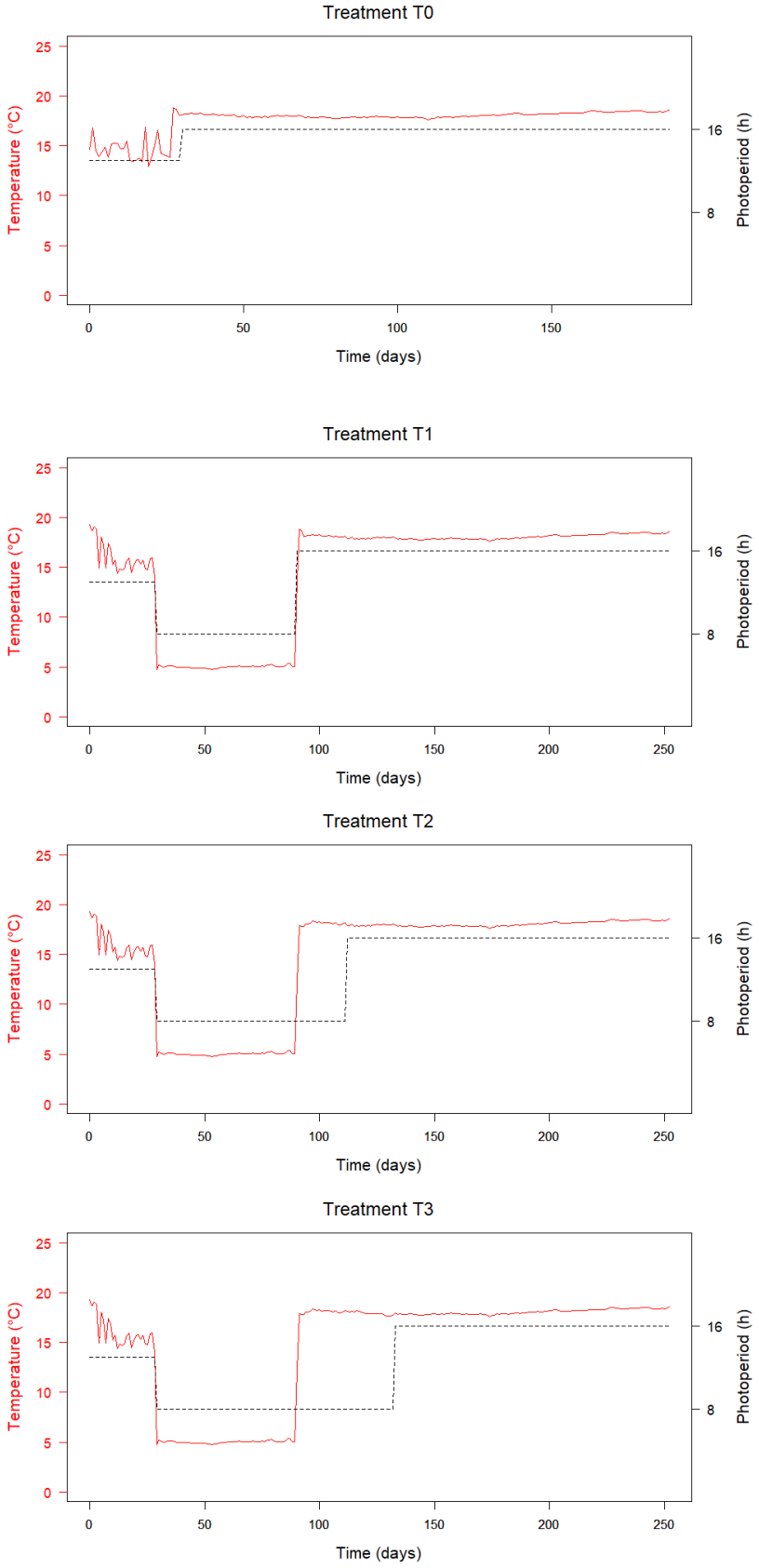


Figure 2.8: Temperature and photoperiod for the four treatments.
Temperature (red) is the mean value of temperature measured in 9 locations of the chamber. Photoperiod (dashed line) is the setpoint photoperiod.

Supplementary 2-3: Internode length pattern

For Bronsyn and Carvalis, tillers had at 3 to 6 long internodes in addition to the peduncle (Figure 2.9). In average, Bronsyn exhibited 5.2 ±0.7 long internodes against 5.8 ±0.8 in Carvalis. Internodes *n*-5, *i.e.* the oldest ones, were slightly elongated (0.7 cm and 2.0 ±0.5cm in Bronsyn and Carvalis, respectively) and only observed in 3% of Bronsyn's tillers against 22% in Carvalis. In contrast, internodes *n-3* were elongated in 88 and 100% of the tillers of Bronsyn and Carvalis, respectively. The slightly higher number of internodes observed in Carvalis was associated with smaller internodes compared to Bronsyn, thus leading to similar total length of tillers at maturity (52.9 ±9.3 cm for Bronsyn and 54.0 ±11.6 cm for Carvalis). In every plants of both cultivars, peduncles were significantly longer than the other internodes and represented 27 ±5% of the total length of the culm.

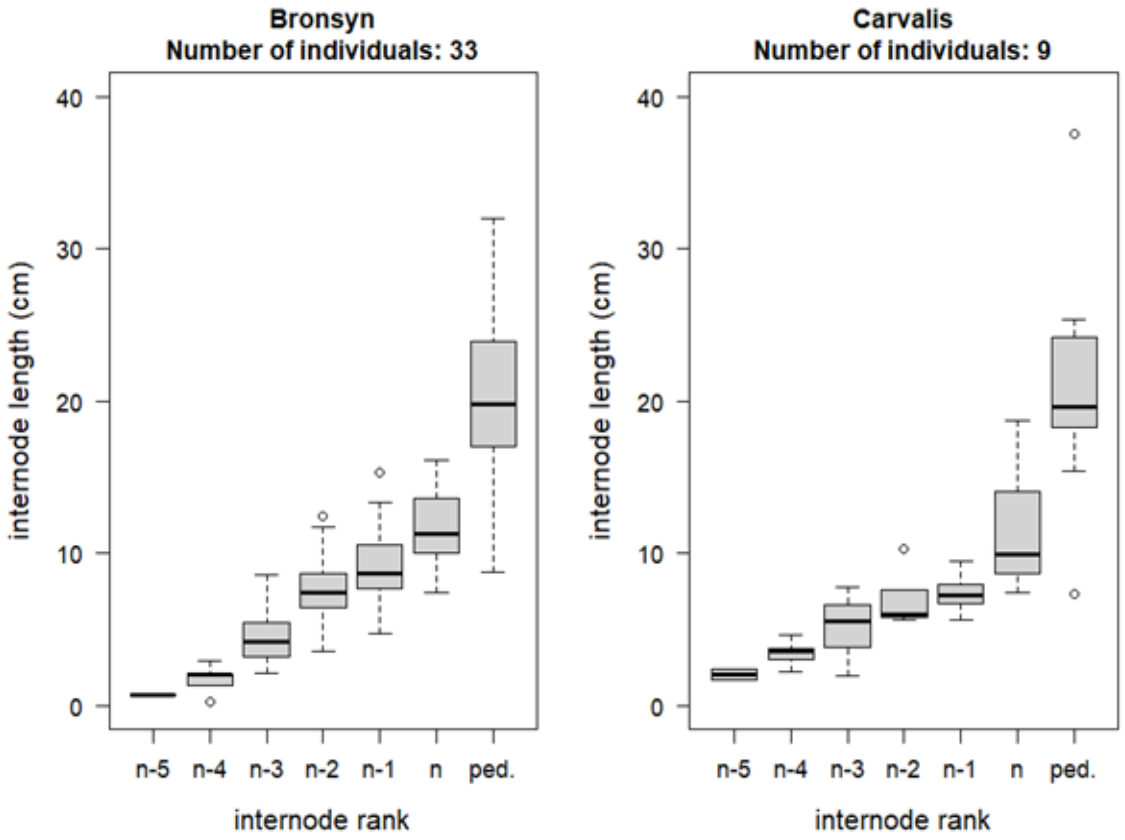


Figure 2.9 Length of internodes depending on their rank for cultivars Bronsyn, Carvalis exposed to treatment T1.
3 tillers per plant (including the main tiller) were measured. Internode rank is given relatively to the last internode. "ped." corresponds to the peduncle.

Résumé du chapitre 2

Les connaissances actuelles sur les processus d'induction florale sont majoritairement qualitatives et ont permis d'identifier les facteurs environnementaux nécessaires à l'induction florale. Leurs effets sur la morphogénèse de la plante sont en revanche peu connus. Pourtant, après l'induction florale, c'est la morphogénèse de la talle (production de feuilles, production d'épillets) qui détermine la date d'épiaison.

Dans ce chapitre, nous avons développé une stratégie pour saisir les effets des conditions d'induction florale sur la morphogénèse à l'échelle de la talle. Plutôt que d'étudier l'effet d'un grand nombre de combinaisons de températures et de photopériodes, nous avons choisi d'étudier l'effet du calendrier d'induction florale, c'est-à-dire de la répartition dans le temps des inductions primaires et secondaires.

Dans un premier temps, cette étude a permis de valider la nécessité d'une induction à deux phases chez les variétés étudiées. Elle a toutefois mis en évidence des besoins inductifs très différents entre variétés, conduisant à des taux d'épiaison très contrastés. L'étude de l'allongement foliaire en fonction des conditions d'induction florale a montré une corrélation entre l'état reproducteur et l'accroissement de vitesse d'allongement des feuilles. L'étude non-destructive du nombre de phytomères a fourni des indices permettant d'inférer les dynamiques de production de primordia par l'apex durant les phases végétatives et reproductives. Enfin, elle fournit un jeu de données très complet à l'échelle de la talle, qui est utilisable pour la calibration de modèles.

Dans le chapitre 3, nous proposons un modèle pour rendre compte du développement reproducteur chez *Lolium perenne*. La construction du modèle est fondée sur les observations et hypothèses formulées dans la littérature (Chapitre 1), ainsi que sur les résultats expérimentaux de ce chapitre.

Chapitre 3

L-GrassF, un modèle structure-fonction du développement reproducteur des talles de graminées pérennes.

1. Introduction

The reproductive development of perennial grasses involves major phenological events, which highly affect their physiology, morphology and ultimately the agro-ecological functioning of grasslands. The underlying biological processes, such as floral induction, spikelet production and flowering are highly determined by the genetic × environment interactions, thus highlighting the necessity to improve the prediction of grassland phenology to cope with agro-ecological challenges and climate change. For this purpose, computer modelling gives interesting opportunities (Durand *et al.*, 2016). Nevertheless, existing models use empirical relations based on calendar or thermal time to infer phenological stages, thus limiting their genericity and ability to cope with new environmental conditions (Chapitre 1).

The aim of this study is to propose an original and generic model of perennial grass phenology, accounting for the interactions between the environmental factors, floral induction and tiller morphogenesis. We developed a functional-structural plant model (FSPM) at tiller scale, named L-GrassF, which accounts for the floral induction of individual tillers and the interactions with morphogenesis. The model represents the complete development of a tiller from its initiation to the heading of the spike, which allows us to simulate the reproductive development in relation to the vegetative development. The model simulates the main phenological stages (floral transition, heading date) and morphological variables (*e.g.* final leaf number and dimensions, number of spikelets per spike). As a first assessment of L-GrassF, the model was calibrated using the experimental data described in Chapitre 2 in order to evaluate the ability of our approach to simulate the effect of the photoperiodic treatments. Finally, we realized a Principal Component Analysis on simulated individuals to explore their repartition in the parameter space and identify potential interactions between parameters.

2. Model description

2.1. Model overview

The model L-GrassF is a functional-structural plant model (FSPM) accounting for the reproductive development in perennial grasses. The visible expression of reproductive phenology, which is used to manage grasslands or describe the species variability is heading, which is therefore the ultimate target of the model. It occurs as the first spikelet emerges from the sheath of the last leaf produced by the apex. However, this stage is highly determined by processes that occur long before, such as vegetative growth and floral induction. L-GrassF therefore simulates the vegetative (appearance and elongation of leaves, tillering) and reproductive development (floral transition, internode and spike production, heading) of individual tillers from their initiation to heading (Figure 3.1). L-GrassF was developed from L-Grass, an existing individual-based model describing the aerial vegetative development in *Lolium perenne* (Verdenal *et al.*, 2008; Verdenal, 2009).

The initial version of L-Grass was built by Verdenal (2008; 2009) to simulate aerial vegetative stages only. It describes dynamically leaf growth, tillering and the effects of defoliation. The model is based on the L-system formalism, which allows a 3D and botanic representation of plant dynamics (Prusinkiewicz, 2004). In L-Grass, the plant is composed by individual tillers which can be decomposed as a succession of phytomers: an internode, an axillary bud and a leaf. Each leaf is made of a lamina and a sheath, separated by the collar. The successive nested sheaths constitute the pseudostem of the tiller through which grow the leaves before emergence. The rhythm of leaf initiation is coordinated to previous leaf emergence and leaf elongation is driven by self-regulation rules, *i.e.* leaf final dimensions and elongation rate are highly affected by the length of the pseudostem. In L-Grass, the time of tiller emergence is coordinated with that of the leaves on the mother tiller, while the probability of tiller emergence is negatively regulated by leaf area of neighboring plants. The model was calibrated for *Lolium perenne* and is able to produce contrasted plant morphologies from turf to forage phenotypes. Using the L-systems, the plant is modelled as a dynamic network

of organs, called modules, that is written as a string of characters. The string is rewritten at each time step according to the morphogenetic rules described above and modules can be interpreted geometrically to provide a 3D representation of the plant architecture. The initial version of L-Grass was implemented in the L-Studio simulation platform (Prusinkiewicz *et al.*, 2000) using a L + C modelling language (Karwowski and Prusinkiewicz, 2003). Later, it was implemented in L-Py, a L-Systems framework in Python distributed in the OpenAlea platform (Boudon *et al.*, 2012).

L-GrassF was developed from the version of L-Grass implemented in the L-Py framework. Several adaptions were made on the initial version of the model and they are detailed below. Briefly, some functions involved in leaf elongation were adapted to extend the model to reproductive stages. In addition, the time unit of the model was converted from thermal time to astronomic time and temperature-dependent processes were adapted by integrating a nonlinear function of temperature. A sub-model of floral induction was developed at tiller scale and was implemented as two successive phases: a primary induction depending on temperature (Figure 3.1,3) and a secondary induction depending on photoperiod (Figure 3.1, 4). Floral induction dynamically affects tiller morphogenesis (Figure 3.1, 5, 6, 7) thereby determining the final morphology of the tiller (final number of leaves, number of long internodes and spikelets). Heading date is an emergent property of the model and corresponds to spike emergence out of the pseudostem (Figure 3.1, 8). L-GrassF was calibrated on *Lolium perenne* but the underlying processes implemented are generic to grasses. The code of the model is open source, available on GitHub (https://github.com/openalea-incubator/lgrass), and released under a CecILL-C license.

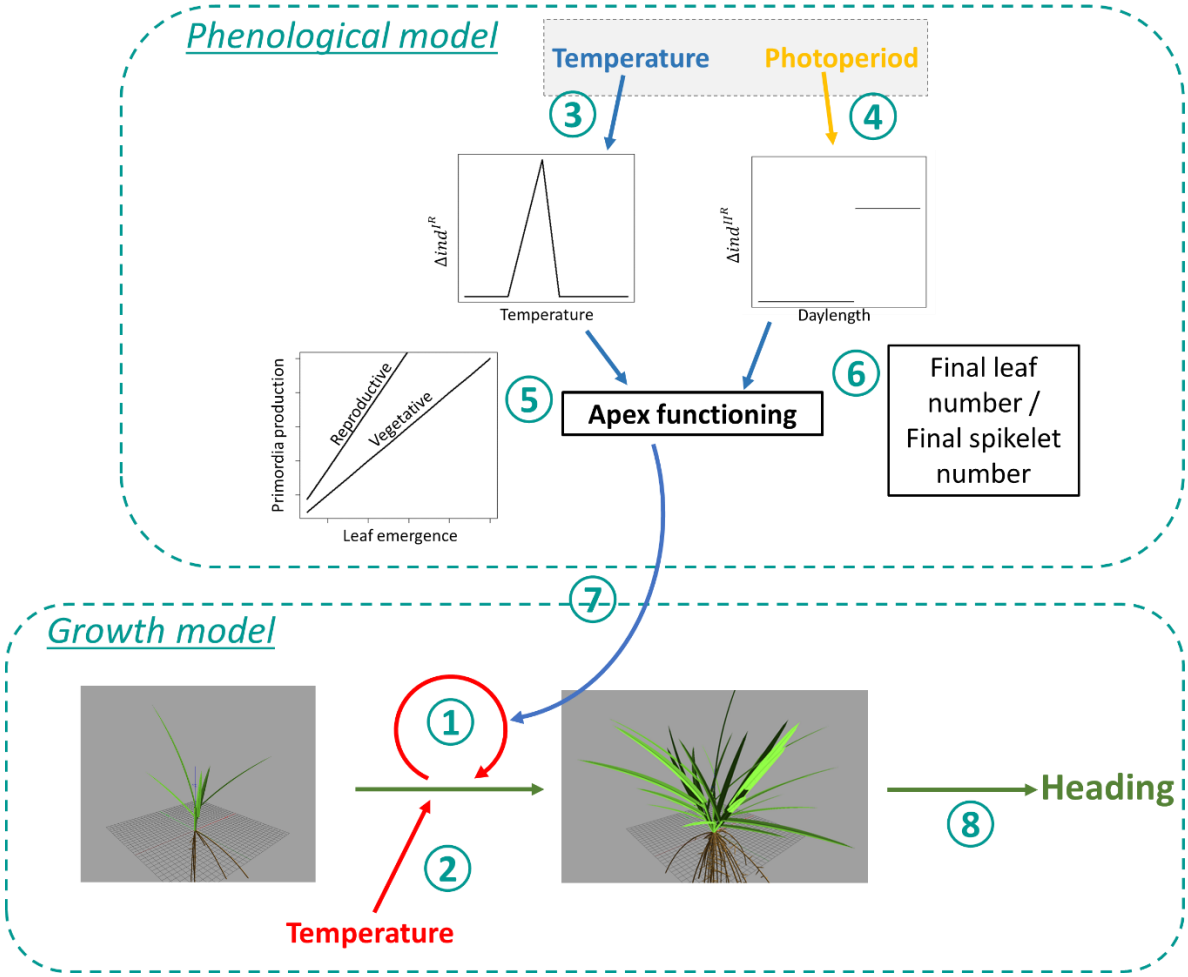


Figure 3.1: Overview of L-GrassF functioning.
The model accounts for tillering as well as leaf initiation, leaf elongation (1). L-GrassF includes a phenological model, which calculates the rate of primary and secondary induction according to temperature and photoperiod (3, 4). The completion of floral induction defines the rate of primordium initiation at the apex (5). At floral transition, the final number of leaves and spikelets is defined (6). Finally, the model simulates the heading of the spike from the ligulation date of the flag leaf of the tiller (8).

2.2. Time unit of the model and temperature effects

In the previous version of the model, the time unit used was the thermal time (Verdenal *et al.*, 2008). This unit is a useful tool for studying plant development under constant temperature or in a range where the studied processes follow a linear function of temperature (Bonhomme, 2000). However, since the model was intended to be used in contrasting environments with a variable temperature range, and that some processes, such as floral induction, were directly dependent on temperature, it appears

that thermal time was not a relevant time unit anymore. For this reason, L-GrassF was modified in order to express time-related parameters and the time step of the model in astronomic time unit (hours).

In L-GrassF, the time step (*dt*) is of one hour. Leaf *n* age (Age_n), which is the time variable used to calculate leaf elongation and senescence, is expressed in hours and modulated by a non-linear function of temperature (Eqn 3-1), leading to a kind of 'physiological age':

$$\frac{dAge_n}{dt} = \begin{cases} \left(\frac{T(t) - T_{min}}{T_{ref} - T_{min}}\right)^q \times \left(\frac{T_{max} - T(t)}{T_{max} - T_{ref}}\right); & if\ Tmin \leq T(t) \leq Tmax \\ 0 & else \end{cases} \qquad \textit{Eqn 3-1}$$

Where $T(t)$ is the mean temperature of the day (°C), T_{min} is the minimum temperature, T_{max} is the maximum temperature, q is a shape parameter and T_{ref} is the reference temperature (Table 3-1). The equation and parameters for *Lolium perenne* were obtained from (Zaka *et al.*, 2017, pers. comm.). According to the observations of Zaka (2016), we assumed that cardinal temperatures were identical for all genotypes of the species.

Previous parameters expressed in degree days (mainly related to the rates of leaf elongation and senescence, see below) were converted into hours using the temperature regimes that were set in the different experiments used to calibrate the initial version of L-Grass.

Table 3-1: Model parameters

Parameter	Description	Value	Unit	Related equation	Reference
Organ aging					
T_{min}	Minimum temperature	-2.88	°C	Eqn 3-1	(Zaka *et al.*, 2017, pers. comm.)
T_{max}	Maximum temperature	38.9	°C	Eqn 3-1	(Zaka *et al.*, 2017, pers. comm.)
T_{ref}	Reference temperature	23.97	°C	Eqn 3-1	(Zaka *et al.*, 2017, pers. comm.)
q	Shape parameter	1.56	Dimensionless	Eqn 3-1	(Zaka *et al.*, 2017, pers. comm.)
Leaf elongation					
Ω	Parameter to calculate LED^0 and LED	1.91	h mm^{-1}	Eqn 3-2	Adapted from (Verdenal et al., 2008)
a	Parameter to calculate LED^0 and LED	1.18 x 10^{-3}	h^{-1}	Eqn 3-2	Adapted from (Verdenal et al., 2008)
b	Parameter to calculate LED^0 and LED	-0.1	Dimensionless	Eqn 3-2	(Verdenal et al., 2008)
$R_{sα}$	Parameter to calculate LED^0 and LED	0.2	Dimensionless	Eqn 3-2	(Verdenal et al., 2008)
Hidden phase					
Age_{max}	Leaf age threshold	0.76 x LED^0	h-1	Eqn 3-2	(Verdenal et al., 2008)

Visible phase

T_{01}	Parameter to calculate Y_m	2.718	mm	Eqn 3-4	(Verdenal et al., 2008)
T_{02}	Parameter to calculate Y_m	2.718	mm	Eqn 3-4	(Verdenal et al., 2008)
k_1	Parameter to calculate Y_m	2.249 x 10^{-2}	h^{-1}	Eqn 3-4	Adapted from (Verdenal et al., 2008)
k_2	Parameter to calculate Y_m	3.375 x 10^{-2}	h^{-1}	Eqn 3-4	Adapted from (Verdenal et al., 2008)
Tb_1	Parameter to calculate Y_m	144	h	Eqn 3-4	Adapted from (Verdenal et al., 2008)
Tb_2	Parameter to calculate Y_m	27.98	h	Eqn 3-4	Adapted from (Verdenal et al., 2008)
L	Parameter to calculate Y_m	30	mm	Eqn 3-4	(Verdenal et al., 2008)
Floral induction					

Primary induction

$T_{min}^{I^R}$	Minimal temperature for primary induction	-3	°C	Eqn 3-6	(Woodward *et al.*, 2020)
$T_{opt}^{I^R}$	Optimal temperature for primary induction	4	°C	Eqn 3-6	(Woodward *et al.*, 2020)
$T_{max}^{I^R}$	Maximal temperature for primary induction	12	°C	Eqn 3-6	(Woodward *et al.*, 2020)

$\Delta ind_{max}^{I^R}$	Maximal daily increment for primary induction	0.1	Dimensionless	Eqn 3-6	Calibrated on data
Secondary induction					
PP_{min}	Minimal photoperiod for secondary induction	16	h	Eqn 3-7	Calibrated on data
Reproductive morphogenesis					
$index_{tiller,n}^{I^R}$	Threshold of the primary phase for leaf elongation increase	1	Dimensionless	-	Calibrated on data
$index_{tiller,n}^{II^R}$	Threshold of the secondary phase for leaf elongation increase	1	Dimensionless	-	Calibrated on data
kY_m^0	Multiplicative factor of Y_m^0	1	Dimensionless	-	Calibrated on data

2.3. Vegetative morphogenesis

This section describes tiller functioning during the vegetative stages. Although this part of the model is mainly based on the initial L-Grass model, we had to adapt some functions in order to further extend the model to reproductive stages.

2.3.1. Dynamics of apex functioning

In L-GrassF, each tiller has a module called "apex" declared in the L-systems string which represents the terminal apical meristem. Based on the initial version of L-Grass, the dynamics of apex functioning during vegetative stages is coordinated with leaf emergence *i.e.* the apex initiates a new phytomer of rank *n* (leaf, internode and axillary bud) at the emergence of leaf *n-1*. Thus, the phyllochron (duration between the appearance of two successive leaves) and the plastochron (duration between their initiation) are considered equal in the model but are not constant as they depend on the time taken by leaves to exceed the length of the pseudostem. The above implementation applies to vegetative tillers only. For tillers whose apices have started the secondary induction, we modified the coordination between leaf emergence and initiation (see details in the section about reproductive morphogenesis).

2.3.2. Leaf elongation

The elongation of a leaf is divided into two distinct phases. The first one occurs while the leaf is hidden in the pseudostem. This phase starts at leaf initiation and ends at leaf emergence. The second phase starts from leaf emergence and ends when the leaf has reached its final length.

Hidden phase

In the initial version of L-Grass, leaf elongation during the hidden phase followed a function inspired from the β integral (Yin *et al.*, 2003) which was bounded above by a potential length (Verdenal *et al.*, 2008). This approach implicitly assumed that leaves could not exceed this potential final length during the first phase of elongation. Although the dynamics of leaf elongation is beyond the scope of the present work, we implemented a revision of the model because: (i) there was no evidence for any maximal length that leaves cannot reach during the hidden phase of their initial elongation and even if it were the case this would raise the question of the environmental effect on that limit and whether it should be defined for each genotype, and (ii) when tillers stay vegetative and produce many leaves, the pseudostem may be longer than the potential final leaf length, preventing growing leaves from emerging and thus any new leaf from being initiated.

Consequently, in L-GrassF leaf *n* length (*Y*, mm) is initiated to 1mm and increases following a dual function depending on leaf age (Eqn 3-2). While leaf age is lower than a threshold (Age_{max}, h), leaf length follows the initial Beta function (Eqn 3-3) proposed in L-Grass and which tends to Y_m^0 (mm). However, if leaf age exceeds Age_{max}, leaf length is not bounded above by Y_m^0 anymore but follows a linear function of leaf age whose slope is equal to the Beta function derivative calculated at Age_{max}. This allowed us to avoid the initial limitation of leaf length for large plants while ensuring a continuity between the two functions (Figure 3.2).

$$Y_n(t) = \begin{cases} Beta(t) & if\ Age_n \leq Age_{max} \\ \dfrac{dBeta(Age_{max})}{dt} \times (Age_n(t) - Age_{max}) + Beta(Age_{max}) & else\ Age_n > Age_{max} \end{cases} \quad \textit{Eqn 3-2}$$

$$Beta(t) = Y_m^0 \left(1 + \frac{LED^0 - Age_n(t)}{LED^0 - Age_{max}}\right)\left(\frac{Age_n(t)}{LED^0}\right)^{\frac{LED^0}{LED^0 - Age_{max}}} \quad \textit{Eqn 3-3}$$

where Y_m^0 (mm) is the provisional final length of the Beta function of leaf elongation and LED^0 (h) is the provisional duration of the Beta function of leaf elongation (Table 3-1).

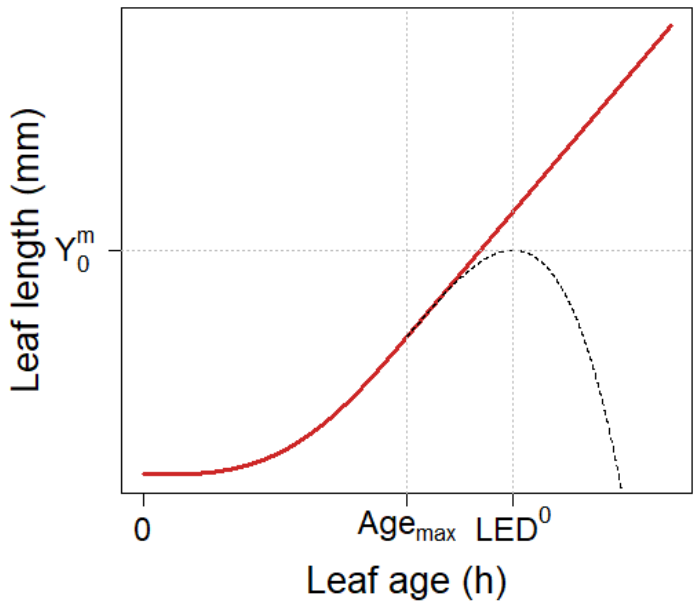


Figure 3.2: Dual function followed by leaves during the hidden phase.
While leaf age is lower than $\boldsymbol{Age_{max}}$*, leaf length follows a beta-like function (for information, the behavior of the function beyond* $\boldsymbol{Age_{max}}$*is illustrated by the dotted line). For leaves older than* $\boldsymbol{Age_{max}}$*, leaf length is assumed to increase linearly.*

Leaf emergence and final length determination

At each time step, the length of the hidden growing leaf is compared to that of the pseudostem, leaf emergence is thus defined when its length is higher than that of the pseudostem. The length of the pseudostem corresponds to the length of the sheath with the highest collar on the tiller. At leaf tip emergence, the model dynamically modifies the value of the parameters of the initial elongation function (Y_m^0 and LED^0; Eqn 3-3). Thus, while the rate of elongation was similar for all leaves during the hidden phase, the second phase is specific to each leaf and is thus determined by the duration of the first phase (Verdenal *et al.*, 2008).

In the initial version of L-Grass, the final leaf length (*Ym*, mm) increased with the duration of the hidden phase until a maximum reached for leaf age = Age_{max} and then strongly decreased, finally taking negative values, which were however never reached for the simulated vegetative stages. Because the model was not intended to simulate the morphogenesis of vegetative plants for long periods (max = 1500°C day, Verdenal *et al.* (2008)), the initial implementation would lead to inconsistent results when leaf age would be higher than Age_{max}: leaves would become rapidly shorter than

the pseudostem, preventing them to emerge. We therefore decided to revise the initial equation by defining a constant final length when leaf age exceeds Age_{max}. In other words, beyond a certain hidden growth duration, leaves will have a constant final length.

In L-GrassF, *Ym* values are thus recalculated as:

$$Ym_n = \begin{cases} C \times \left(T_{01} e^{k_1 (Age_n(t_{E_n}) + Tb_1)} - T_{02} e^{k_2 (Age_n(t_{E_n}) + Tb_2)} - L\right); & if\ Age_n(t_{E_n}) \leq Age_{max} \\ C \times \left(T_{01} e^{k_1 (Age_{max} + Tb_1)} - T_{02} e^{k_2 (Age_{max} + Tb_2)} - L\right) & else \end{cases} \quad \textit{Eqn 3-4}$$

Where $Age_n(t_{E_n})$ is leaf *n* age at its emergence (h), T_{01}, T_{02} (mm), k_1, k_2 (h^{-1}), Tb_1, Tb_2 (h) and *L* (mm) are parameters fitted to the data described in Verdenal *et al*. (2008). *C* is a multiplicative factor with no immediate biological meaning, but which allows to generate very contrasting architectures through a single parameter. By modifying the final leaf length (Figure 3.3), *C* was used to obtain different morphologies characterized by varied leaf lengths and leaf/tiller appearance rates (Verdenal *et al.*, 2008) (Figure 3.3). With the exception of C, all parameters were set to fixed values between cultivars in the following.

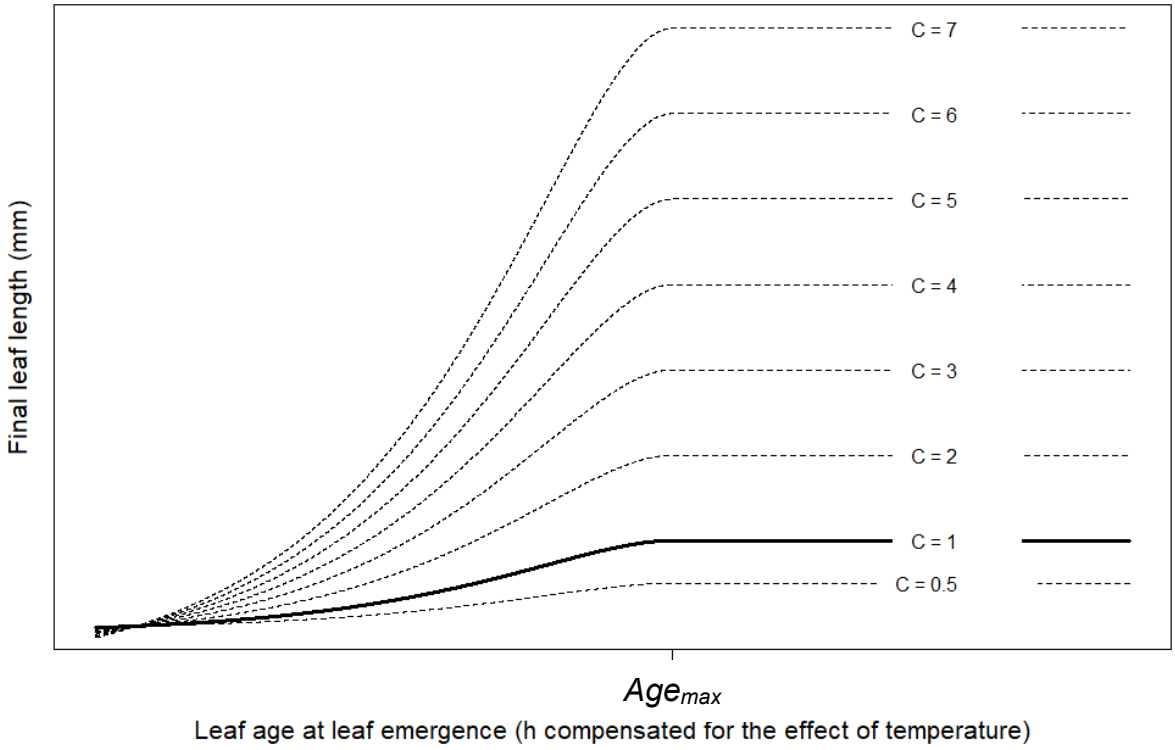


Figure 3.3: Determination of final leaf length as a function of leaf age at the time of leaf emergence. Final leaf length is assumed constant for leaves older than $\boldsymbol{Age_{max}}$*. The effect of the multiplicative factor C is shown to illustrate how this single parameter can affect the final length of individual leaves.*

Regarding leaf elongation duration (*LED*), the parameter is also recalculated at leaf emergence as in the original L-Grass model. Briefly, *LED* is estimated from the sheath length proportion of the leaf, which is itself calculated at leaf emergence by an affine function of leaf age *i.e.* the hidden phase duration (Verdenal *et al.*, 2008).

Visible phase

After leaf emergence, leaf length is calculated from the initial beta function (Eqn 3-3) using the updated parameters *Ym* and *LED* until leaf length reaches *Ym*.

2.3.3. Cutting

The model accounts for the cutting of the aboveground organs according to a horizontal plane. The organs are virtually divided into segments of 1mm length and those located above the cutting height are removed. If the cutting height is lower than the position of the pseudostem, the growth of the hidden leaves is affected. The determination of their emergence date and thus their final length are updated according to the length of the shortened pseudostem. If an apex is located above the cutting height, the tiller dies.

2.4. Floral induction

The visible expression of reproductive phenology used to manage grasslands or describe the species variability is heading. It is defined as the emergence of the first spikelet from the sheath of the last leaf produced by the apex. Long before, the tiller apex undergoes a series of changes, starting with floral induction. Floral induction is the process through which the apex of a vegetative tiller becomes reproductive. In L-GrassF, we assumed that the floral induction takes place in two phases in *Lolium perenne*: a primary and a secondary induction phase (Chapitre 1). The two phases are strictly successive, meaning that the secondary induction can only start the day following the primary induction completion. Each of the induction phase is represented in L-GrassF by an incremental variable (ind^{I^R}, ind^{II^R}, respectively) ranging from 0 at apex initiation to 1 when the induction requirements are completed. These variables are incremented daily according to the average temperature and photoperiod of the day. Both induction phases are irreversible and modify the apex status (Eqn 3-5). The consequences of the floral induction and the consecutive floral transition on apex dynamics and leaf elongation are detailed below.

$$apex_n^{status} = \begin{cases} vegetative & if\ ind_{apex,n}^{I^R} \leq 1 \\ primary\ induced & if\ ind_{apex,n}^{I^R} = 1 \\ reproductive & if\ ind_{apex,n}^{II^R} = 1 \end{cases} \qquad \text{Eqn 3-5}$$

2.4.1. Primary induction

In temperate cultivars of *Lolium perenne*, low temperature was identified as an obligatory requirement for floral induction. Although the photoperiod could modulate the effect of low temperatures (Heide, 1994), the primary induction is assumed to be only dependent on temperature in L-GrassF. In the literature, the primary induction is generally characterized by three cardinal temperatures: a minimum, optimum and maximum (He *et al.*, 2012; Woodward *et al.*, 2020). As little information exists about the induction rate between these cardinal temperatures, the progression of the primary induction is calculated daily according to a triangular response to daily air temperature (Figure 3.4).

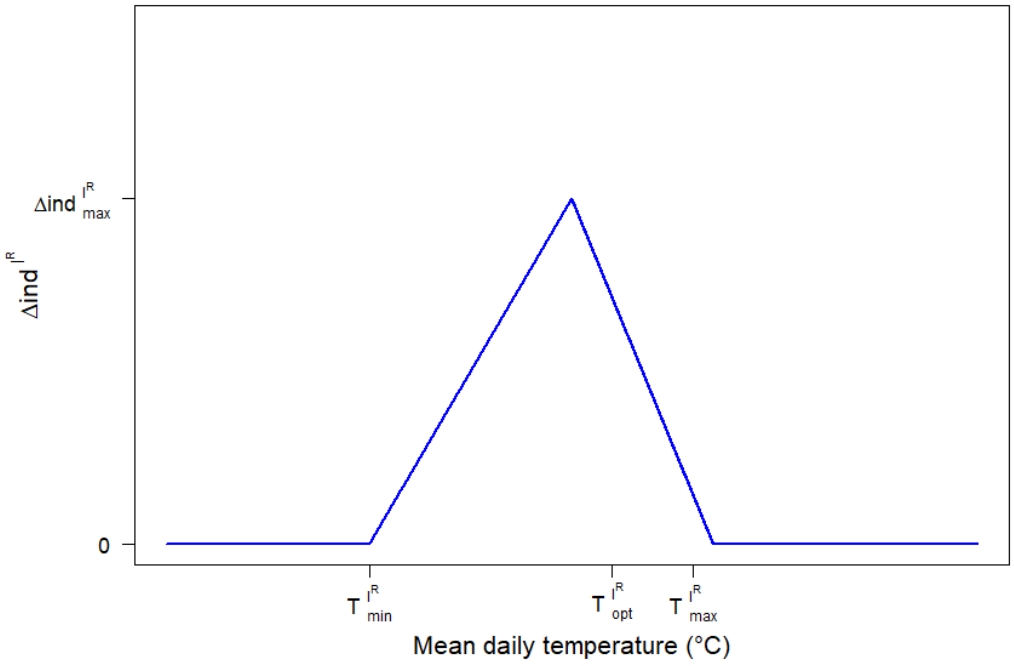


Figure 3.4: Response curve of primary induction to daily temperature.

The daily increment of the primary induction (Δind^{I^R}) increases linearly with mean air temperature from the minimum temperature ($T_{min}^{I^R}$, °C) to a maximum ($\Delta ind_{max}^{I^R}$) reached for an intermediate temperature $T_{opt}^{I^R}$. Above this temperature, Δind^{I^R} reduces to zero at the maximum temperature ($T_{max}^{I^R}$, °C), such that:

$$\Delta ind^{I^R}(day) = \begin{cases} 0 & if\ T(day) < T_{min}^{I^R}\ or\ T_{max}^{I^R} > T(day) \\ \Delta ind_{max}^{I^R} \times \dfrac{T(day) - T_{min}^{I^R}}{T_{opt}^{I^R} - T_{min}^{I^R}} & if\ T_{min}^{I^R} \leq T(day) \leq T_{opt}^{II^R} \\ \Delta ind_{max}^{I^R} \times \dfrac{T(day) - T_{max}^{I^R}}{T_{opt}^{I^R} - T_{max}^{I^R}} & if\ T_{opt}^{I^R} \leq T(day) \leq T_{max}^{II^R} \end{cases} \quad \textit{Eqn 3-6}$$

Where *T(day)* is the mean daily temperature. The progress toward full primary induction (ind^{I^R}) is simulated as a time integral:

$ind^{I^R} = \sum_{day=1}^{d} \Delta ind^{I^R}$, with $ind^{I^R} \in [0,1]$

2.4.2. Secondary induction

In the literature, the secondary induction is reported to be mainly dependent on the photoperiod and starts when it exceeds a given threshold (Heide, 1994). An interaction with the temperature was shown but of lower importance (Aamlid *et al.*, 2000). In L-GrassF, the secondary induction can only start when the primary induction is completed and at least one leaf of the tiller has emerged. This second criterion reflects the need for photoperiod-sensitive organs to perceive the signal. From Chapitre 2, we highlighted a relation between plant development (leaf number) and the duration of the secondary induction. Consequently, the completion of the secondary induction in L-GrassF is calculated daily as a function of the photoperiod of the day and the number of emerged leaves on the tiller (Eqn 3-7). Above a minimal photoperiod (PP_{min}, h), the daily increment of the secondary induction (Δind^{II^R}) increases with the number of leaves on the tiller (LN_{tiller}) until a maximum ($PPRM$):

$$\Delta ind^{II^R}(day) = \begin{cases} 0 & if\ PP(day) \leq PP_{min} \\ \min(PPRM, \quad PPRM \times \dfrac{LN_{tiller,n}}{\mathrm{LNM}} & else \end{cases} \quad \textit{Eqn 3-7}$$

where *PP* (h) is the photoperiod of the day*, PP_{min}* (h) is the minimum photoperiod for secondary induction*, PPRM* is the maximal daily increment of the secondary induction*, LN_{tiller}* is the number of emerged leaves of the tiller and *LNM* is the minimum number of leaves above which the secondary induction increment is maximal (PPRM)*.*

The progress toward full secondary induction (ind^{II^R}) is simulated as a time integral:

$ind^{II^R} = \sum_{day=1}^{d} \Delta ind^{II^R}$, with $ind^{II^R} \in [0,1]$. When the secondary induction is completed ($ind^{II^R} = 1$), the floral transition takes place.

2.5. Reproductive morphogenesis

2.5.1. Apex functioning dynamics

In accordance with the literature (Gillet, 1980; Thomas, 1980; Gonthier and Francis, 1989), the model accounts for an accumulation of primordia at the apex level during the floral induction (Figure 3.5). Until the secondary induction starts, we assumed the apex to be vegetative. As mentioned earlier, this means that leaf primordia are initiated with the same rate as leaf emergence. As soon as the secondary induction starts, the model accounts for an increase in primordia initiation rate as reported by Gonthier and Francis (1989). The primordia production rate is multiplied by a factor ρ, the apex producing ρ·primordia at each leaf emergence following the start of secondary induction (with ρ > 1). All primordia initiated during the secondary induction will develop into leaves, while those initiated after the secondary induction will later develop into spikelets. Consequently, the final number of leaves is determined at the time of floral transition *i.e.* the end of the secondary induction. After the floral transition, the initiation of spikelet primordia by the apex continues in coordination with leaf emergence until the last leaf starts to elongate. The stop of primordia initiation marks the death of the terminal apex and no supplementary organ is produced.

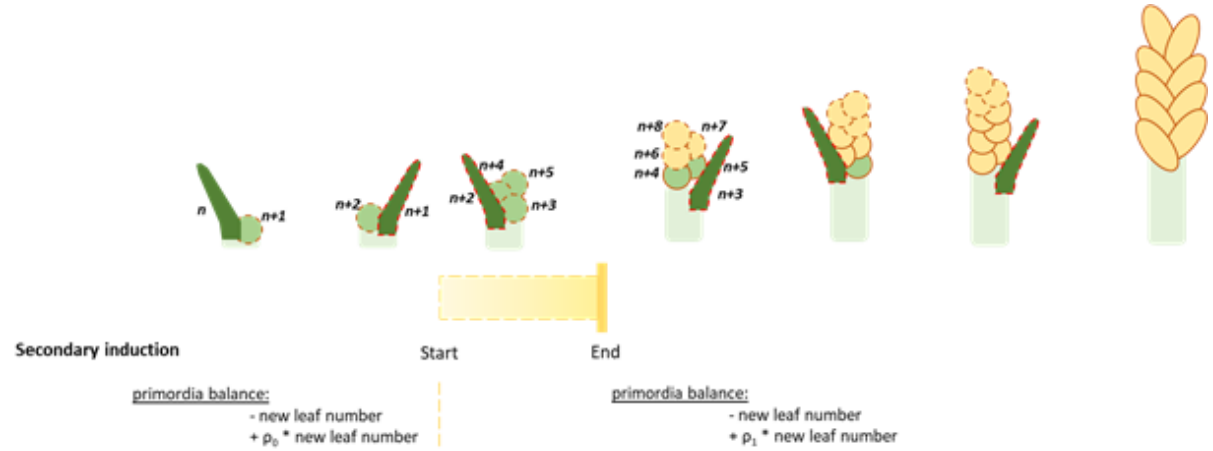


Figure 3.5: Dynamics of apex functioning during the floral induction process.

2.5.2. Leaf elongation

The literature reports an increase in leaf elongation rate around the period of floral transition, which frequently occurs in spring in temperate climates (Davies, 1971; Parsons and Robson, 1980). There has been a debate in the literature to know whether the increase in leaf elongation was directly caused by the floral transition or if these two processes were affected independently by common factors, which leads to an apparent synchronicity in most growth conditions (Davies, 1971; Parsons and Robson, 1980). Our experimental results presented in Chapitre 2 did not allowed to settle between the two hypotheses. We introduced in L-GrassF an independent regulation of leaf elongation rate in order to account for the behavior of reproductive tillers.

In L-GrassF, the increase in leaf elongation occurs when two successive phases are completed, the first one depends on temperature, assuming that this acceleration only occurs in primary induced plants, and the second one depends on photoperiod. Each phase is completed at the same rate than the primary and secondary induction, respectively (Eqn 3-6, Eqn 3-7). In order to implement the uncoupling between the floral transition and the increased leaf elongation as simply as possible, we only introduced two supplementary parameters ($index^{I^R}_{tiller,n}$, $index^{II^R}_{tiller,n}$) that determine the thresholds required for each phase completion. As a provisional choice, the value of these two parameters was set to 1, leading to an exact synchrony between leaf

elongation increase and floral transition. Further experiments with contrasting temperature and photoperiod would be needed to further calibrate these parameters.

The increase in leaf elongation rate is simulated by using two multiplicative factors (kY_m^0 and k_C) applied on Eqn 3-3 and Eqn 3-4. The factor kY_m^0 modulates the rate of leaf elongation during the hidden phase, while k_C affects the determination of final leaf length, which ultimately modulates leaf elongation rate. As an example, $kY_m^0 < 1$ increases leaf elongation rate and then reduces the duration of the hidden phase (earlier emergence). Therefore, the final length of the leaf will be shorter and its elongation rate will be higher during the visible phase, leading to a tiller with many short leaves. Similarly, $k_C > 1$ will increase final leaf length and leaf elongation rate. In this case, leaf initiation will decrease because of longer sheaths.

2.5.3. Internode elongation

The floral transition has been shown to trigger the elongation of internodes (Chapitre 1). However, the kinetics of internode elongation and their final dimensions are poorly described in the literature for perennial grasses. The frequency and non-destructive measurements performed in the experiment presented in Chapitre 2 did not allow us to determine morphogenetic rules to be implemented for internodes in the model. Although internode extension dramatically increases plant height and apex position, it does not affect, at least geometrically, the heading date as the distance between the spike and the highest ligule is not affected by the extension of lower internodes. As a consequence, internode elongation is extremely simplified in L-GrassF with the only objective of providing realistic 3D representations of reproductive tillers. Internode *n* elongation is triggered by the ligulation of leaf *n* while internode length increases linearly until its final length equals that of sheath *n*.

2.6. Heading of the spike

The heading date of a tiller is defined as the date when the terminal spikelet emerges from the pseudo-stem (Gillet, 1980; Thomas, 1980). In a majority of cases, the pseudostem at this date corresponds to the length of the last sheath of the tiller.

Therefore, the date of emergence of the terminal spikelet depends on the length of the flag leaf sheath, the elongation of the peduncle bearing the spike, the number of spikelets and the elongation of the short internodes bearing each of the spikelets. As for internodes, the literature on peduncle and spike elongation is very sparse and no simple rules could be found in the experimental dataset presented in Chapitre 2. Instead of simulating the heading of the spike from geometrical calculations involving uncertain elongation rules of the different organs cited above, we chose to use the date of flag leaf ligulation as a proxy for heading.

3. Model calibration

The model was calibrated using the experimental data on *Lolium perenne cv.* Bronsyn detailed in Chapitre 2. The number of reproductive plants in cultivars Carvalis and Tryskal was not sufficient to be used for calibration (respectively 17 and 1 reproductive plants). The parameters were calibrated for each individual plant measured in the experiment in order to represent the phenotypic variability in the growth conditions of the experiment. The model was initialized at sowing and ran for 5000 hours (208 days) using the measured temperature and photoperiod for each treatment of the experiment (Supplementary 2-2). Because L-GrassF accounts for the interactions between the vegetative and reproductive development, the calibration was performed on six parameters related to leaf elongation rate, final leaf dimensions, floral induction rate and apex dynamics (see details below). The calibration consisted in testing a large range of parameter combinations (Table 3-2). Each simulation takes nearly 15 minutes in a personal computer. In order to reduce the computational time, we deployed L-GrassF on a high-performance computing center (MESO@LR, Université de Montpellier, France) using Singularity containers to package the entire environment and libraries used.

In the experimental dataset, primary inductive conditions (low temperature and short photoperiod) were applied to young plants that had ~3 leaves (treatments T1, T2 and T3, Chapitre 2). Before calibrating the reproductive parameters on these plants, we performed a first calibration for two vegetative parameters *C* and Y_m^0. This calibration was performed on the non-induced plants which thus remained vegetative

(T0). Then, a single couple of parameters (*C* and Y_m^0) was attributed to each plant of T1, T2 and T3. Finally, the calibration of four reproductive parameters (k_C, *LNM*, *PPRM and ρ*) was performed for each plant of T1, T2 and T3.

Table 3-2: Range of parameters studied in the calibration process.

Parameter	Value range (Step)	Number of levels
C	2.25 – 7.25 (0.25)	21
$\boldsymbol{Y_m^0}$	45 – 115 (5)	15
ρ	3 – 7 (1)	5
k_C	0.05, 0.1 - 0.5 (0.2)	4
PPRM	0.17, 0.2 – 0.5 (0.1)	5
LNM	16 – 22 (2)	4

3.1. Calibration of the main vegetative parameters

The parameter *C* (determining the final leaf length) ranged between 0.5 and 7.75 and Y_m^0 (determining leaf growth during the hidden phase) ranged between 45 and 115mm (Table 3-2). The objective of this first step of the calibration was to identify a couple of (C-Y_m^0) values allowing to simulate the vegetative development of each plant of the treatment T0. Two output variables were used to identify the best set of parameters for each plant: (i) the Haun Stage (Eqn 3-8), which is a decimal index accounting for the dynamics of leaf development and emergence, and (ii) the leaf length profile along the tiller axis. A first screening was performed on the dynamics of each individual's Haun stage by selecting the parameter combinations which produced the lowest 10% RMSE (root mean square error; Eqn 3-9). This criterion was chosen first for the screening of parameters as the rate of leaf emergence and ligulation plays a central role in the model *e.g.* on secondary induction rate, final leaf number, spikelet production and heading date. About 10% of the simulations were selected after the first screening, then a second screening on RMSE was performed to find the best set of parameters describing individual leaf length along the simulated period.

$$Haun\ stage = \sum_{i=1}^{n} \frac{lamina\ length\ of\ leaf_i}{final\ lamina\ length\ of\ leaf_i} \qquad \textit{Eqn 3-8}$$

$$RMSE = \sqrt{\frac{1}{n}\sum_{i=1}^{n}(S_i - O_i)^2} \qquad \textit{Eqn 3-9}$$

where n is the number of individuals, S_i and O_i are respectively the simulated and observed value of the i^{th} individual for the variable considered

3.2. Calibration of reproductive parameters

The couple (C-Y_m^0) identified during the first calibration phase were considered representative of the diversity of phenotypes existing within the variety Bronsyn in our experimental conditions. These couples of parameters were then attributed to each plant of T1, T2 and T3 according to their morphological similarity with T0 plants. The chosen criteria to affect the couple of parameters was the cumulated length of leaves per tiller as it integrates the information on both leaf number and length.

The reproductive parameters (ρ, k_C, *LNM* and *PPRM*) were then calibrated using a complete factorial design (Table 3-2). Three output variables were used to determine the best quadruplet of parameters: the date of flag leaf ligulation, the rank of the flag leaf and the final number of spikelets. A screening based on RMSE was performed by successively selecting the quadruplets giving the best predictions of the output variables. When several sets of parameters gave the same RMSE for the three variables, the mean value of the variable parameter was taken.

3.3. Statistical analyses

Analysis of variance and non-linear regression were performed with R software (*R Core Team* 2021). Analyses of variance (ANOVAs) were performed following a one-factor linear such that

$$y_i = \mu + T_i + \varepsilon_i$$

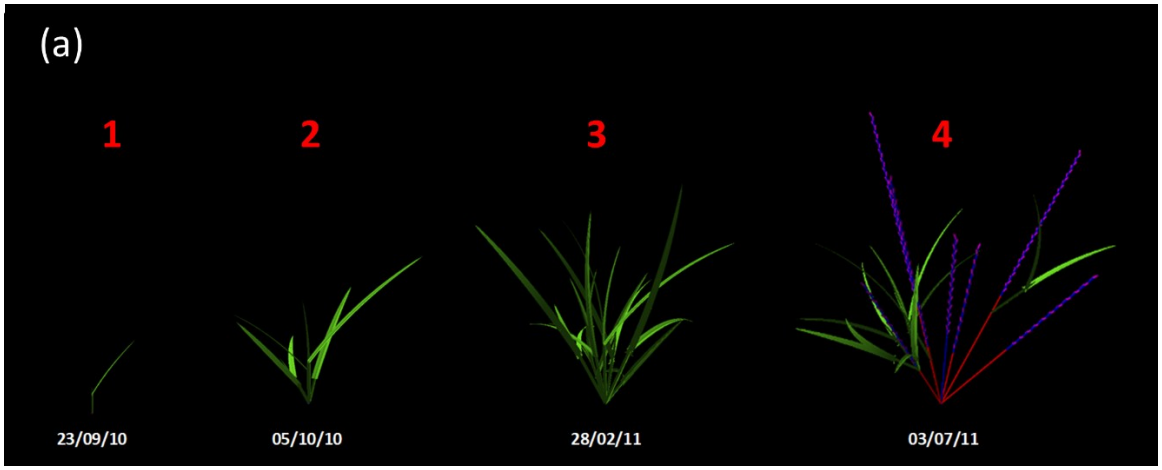
where Y is any dependent variable, μ *is the mean value of Y,* T_i *is the effect of treatment i and* ε *is the random error.*

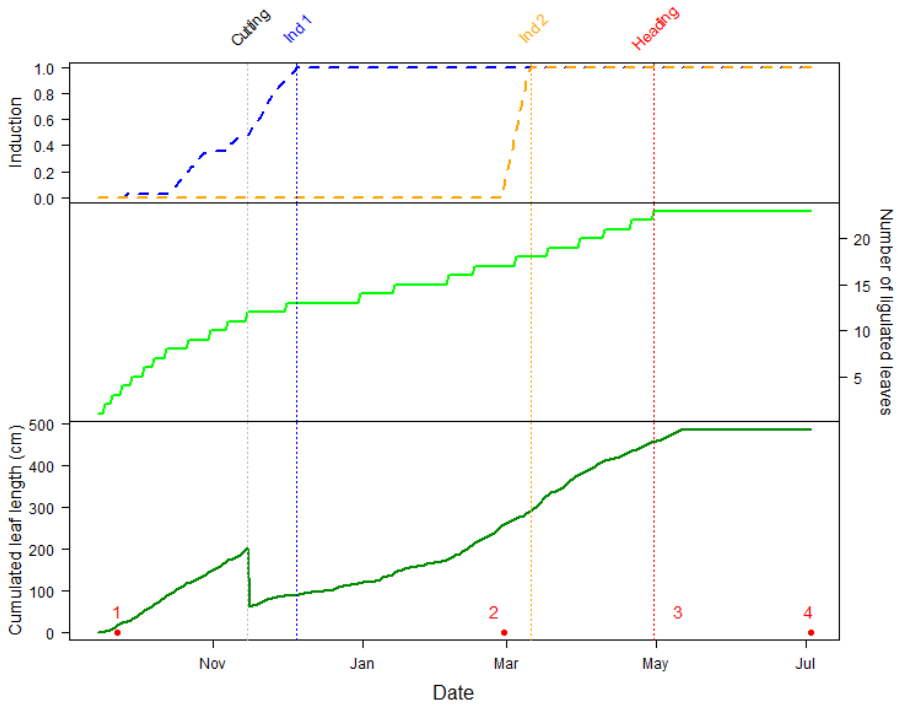
Normal distributions of the residuals of ANOVAs were tested using the Shapiro–Wilk test. Homoscedasticity was checked by random distribution of the residuals.

A Principal Component Analysis (PCA) was performed in order to explore parameter dispersion in the calibrated phenotypes. The individuals represent each plant phenotype of the variety Bronsyn which have been simulated, while the main quantitative variables are the parameters that were calibrated in the previous step (ρ, k_C, *LNM* and *PPRM*). Additional quantitative variables simulated by the model were added to the PCA: time to heading from the start of the secondary induction, number of spikelets. Finally, an additional qualitative variable corresponding to the treatment (modalities T1, T2 and T3) was added to analyze if the treatments were responsible for a bias on the parameter values. The PCA was performed using R language and the library FactoMineR (Lê *et al.*, 2008).

4. Results

4.1. 3D model output





(b)

Figure 3.6: Dynamic 3D representations of plant architecture from L-GrassF *(a) and dynamics of apex induction, number of ligulated leaves and cumulated leaf length (b). Stages 1, 2, 3 and 4 are notified in the two figures. The model was run with the environmental conditions of Lusignan, with sowing on September 15th 2010, cutting at 5cm on November 15th 2010.In this simulation, tillering was activated for illustration only as the present study focused on the main tiller. Green structures are leaves, red structures are internodes and purple structures are spikelets*

The geometrical interpretation of the L-systems modules allows for 3D representations of the plant state and architecture at each time step of the model (Figure 3.6). Although this aspect of the model was not used in the present study (except for visual assessment of the model during its development), the architectural representation of plants can be used to calculate light interception at organ level.

4.2. Simulation of tiller vegetative development

The first calibration realized on the vegetative plants of the treatment T0 allowed us to identify a couple of (Y_m^0 - *C*) parameters for each plant. This calibration also revealed a negative correlation between these two vegetative parameters (Figure 3.7). As a consequence, we chose to use that relation in the following simulations in order to simplify the model calibration by removing the independent variation of Y_m^0.

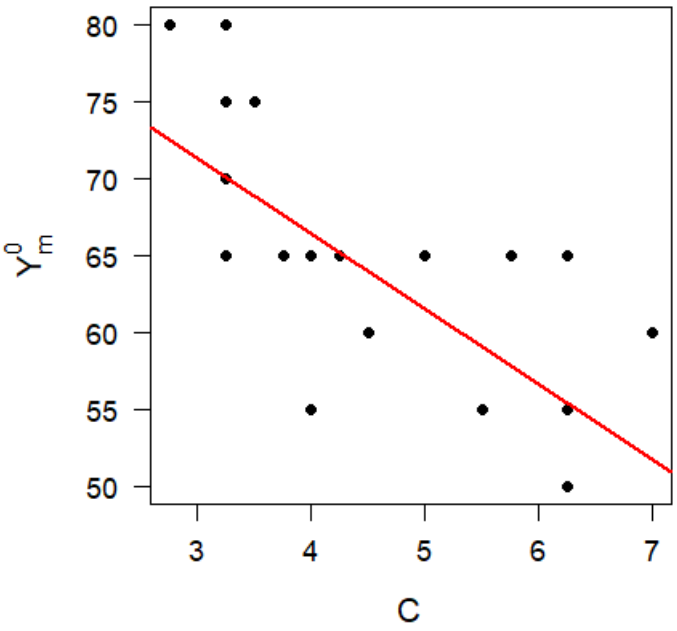


Figure 3.7: Relation between the vegetative parameters $\boldsymbol{Y_m^0}$ *and C.*
Each point represents an individual plant of the treatment T0. Equation of the linear regression: $\boldsymbol{Y_m^0}$ *= -4.88 × C + 85.99. R² = 0.50*

4.3. Simulation of tiller reproductive development

Despite the large range in the heading dates that were observed among the treatments, the calibration of the model allowed us to accurately simulate that variable (Figure 3.8.a ; *R^2 = 0.99 and RMSE = 2.45 days*). The excellent representation of the heading date variability by the model, which was the main target of the calibration, can be explained by the fact that this variable was used first to determine the best set of parameters associated with each plant. The quality of the simulation on the flag leaf rank, which corresponds to the final number of leaves, was clearly lower (Figure 3.8 ; *R^2 = 0.27*) as the simulated flag leaf rank was systematically overestimated by 2 to 8 leaves (except for one plant) compared to the observations (*RMSE = 5.02 leaves*). Nevertheless, the ranking between the treatments was similar to the observations. Further investigations on the simulated dynamics of leaf emergence showed that the overestimation of the flag leaf rank mainly resulted from the specific experimental treatments used in the early stages. Indeed, the number of leaves was overestimated very early, indicating that the model poorly accounted for the early and abrupt changes in the growth conditions in particular when the seedlings were transferred from the greenhouse (~15°C) to the primary inductive conditions (~5°C) and when transferred from the primary inductive conditions (~5°C) to high temperature conditions (~18°C). Part of the overestimation of the number of leaves can also originate from the initialization of the model at a date corresponding to the transfer of germinated seeds (coleoptile and radicle emerged) instead of the actual germination date which was not measured. In addition, the model does not account for the difference in the initial states of seeds (size, weight) observed within the populations, which could explain a part of the uncaptured variability (Ahmed, 2015). Finally, the simulation of the spikelet number gave contrasting results (Figure 3.8.c), in particular the model tended to underestimate the number of spikelets for plants with few spikelets *i.e.* plants of treatments T2 and T3 (*R^2 = 0.25*). Overall, the prediction quality for this variable was therefore limited (*RMSE = 8.60 spikelets*).

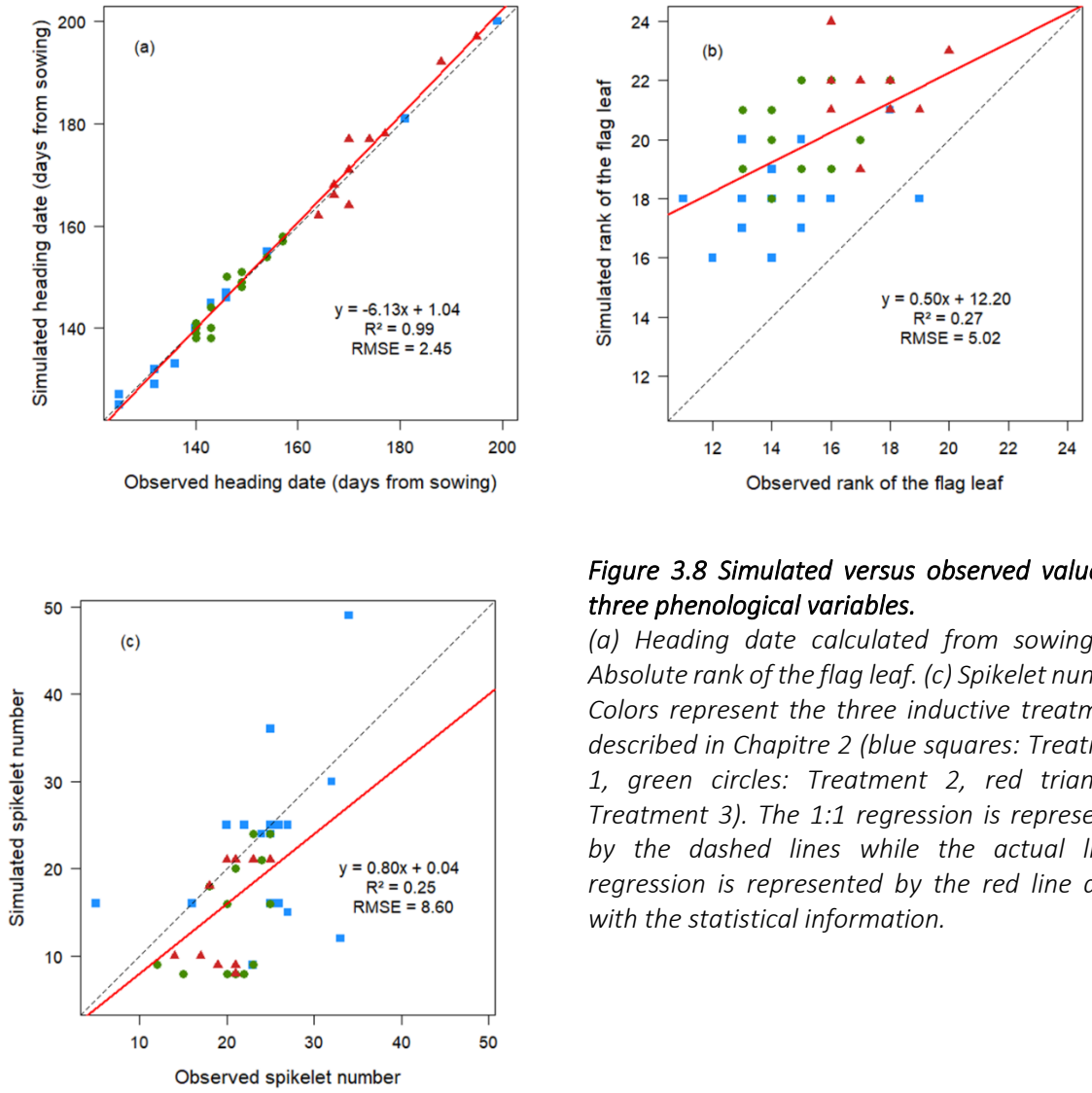


Figure 3.8 Simulated versus observed values of three phenological variables.

(a) Heading date calculated from sowing. (b) Absolute rank of the flag leaf. (c) Spikelet number. Colors represent the three inductive treatments described in Chapitre 2 (blue squares: Treatment 1, green circles: Treatment 2, red triangles: Treatment 3). The 1:1 regression is represented by the dashed lines while the actual linear regression is represented by the red line along with the statistical information.

4.4. Intra-varietal diversity of model parameters

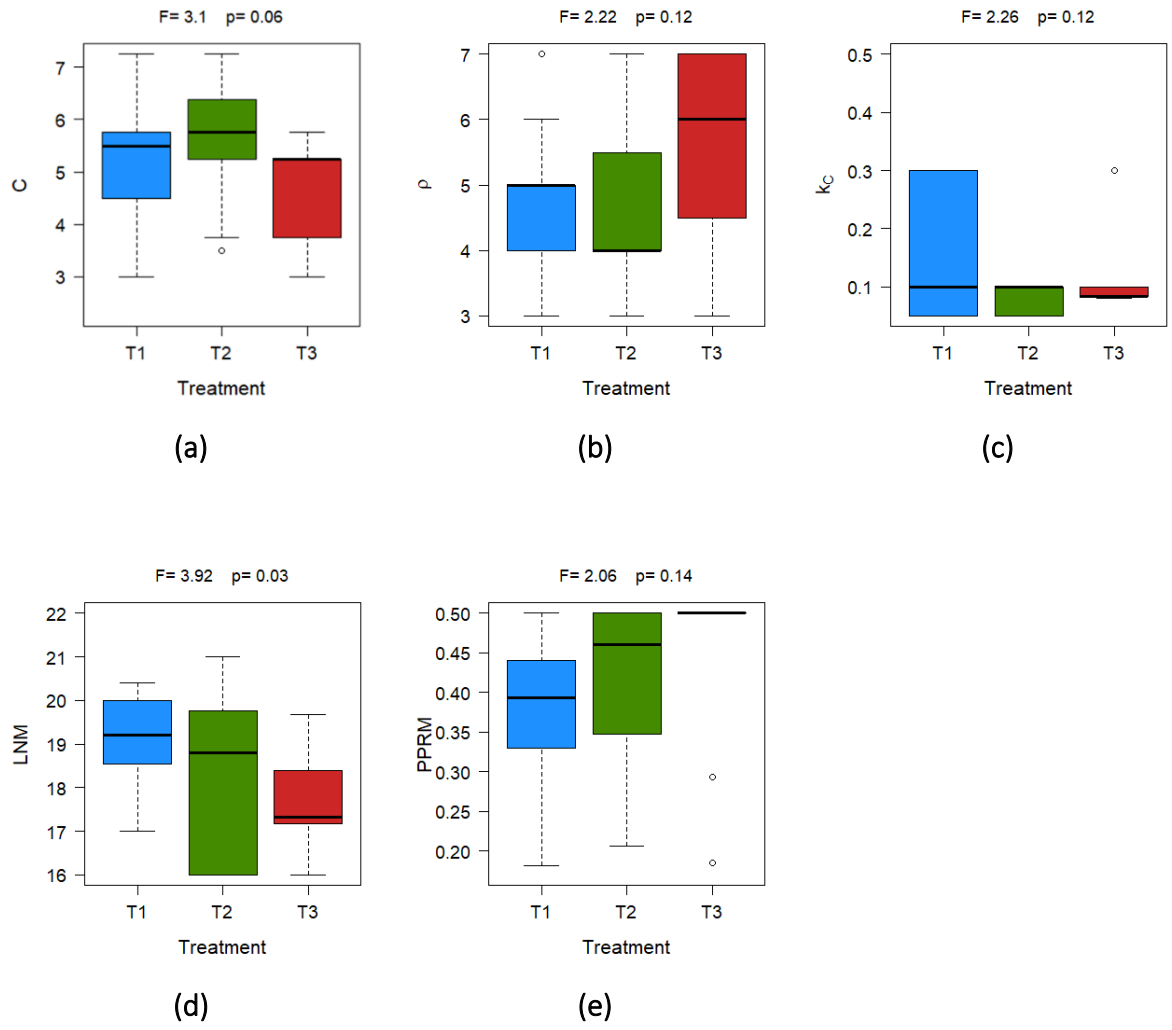


Figure 3.9: Variability of the calibrated parameter values within the variety 'Bronsyn' and between treatments.
(a) C, (b) ρ, (c) k_C, (d) LMN and (e) PPRM

The calibration of the model for each individual plant allowed to account for the phenotypic diversity. Overall, the parameters identified for each plant did not show significant differences between treatments (Figure 3.9), indicating that the calibration was independent of the treatments ($p > 0.05$, *except of LNM*). However, trends can be observed for some parameters. Concerning LNM, the median decreased from 19 ±1.1 to 17 ±1.1 leaves between T1 and T3, respectively ($p < 0.05$). That small gradient in LNM can be explained by the fact that in plants subjected to late secondary inductive conditions (T3), the number of leaves was often higher than the minimum threshold (LNM) required to induce the maximal rate of secondary induction. LNM had therefore

no effect on the rate of secondary induction for these plants. PPRM also slightly increased from T1 to T3 (*T1: 0.39 ± 0.10, T2: 0.46 ± 0.10, T3: 0.50 ± 0.11*), indicating that the calibration procedure has affected a higher maximal secondary induction rate for plants that were lately exposed to long photoperiods.

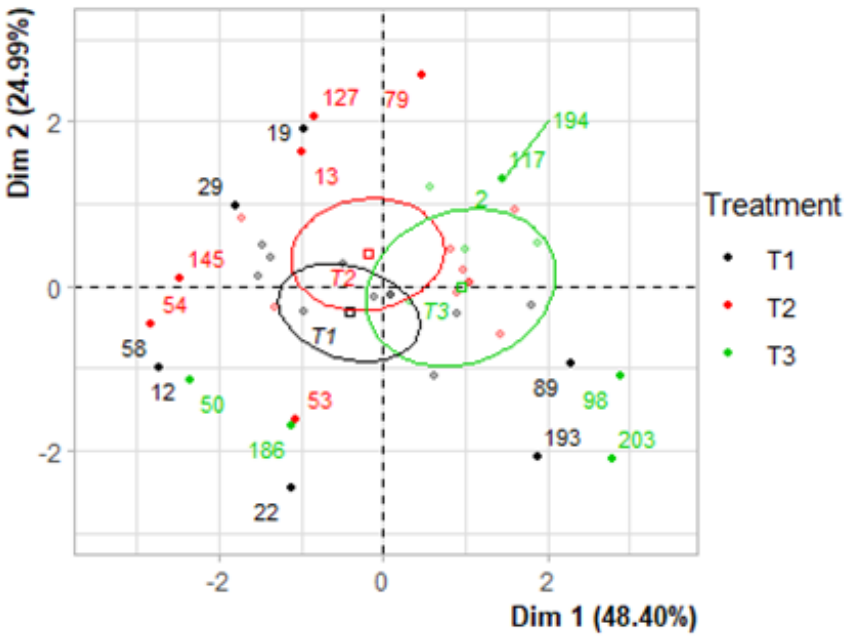


Figure 3.10: Plot of the individuals on the first plan obtained by PCA.
The labelled individuals are those having the greatest contribution to the construction of the plan. The individuals are colored according to the treatment used for the simulation (see above). Squares are the barycenter of individuals in each treatment and ellipses the confidence ellipses.

The first two axes of the PCA explain 73% of the dataset total inertia, with 48% explained by the first axis and 25% explained by the second axis (Figure 3.10). This high inertia percentage means that the variability of the individuals was well represented in this plane. This percentage was also higher than the reference value of 57.1% (0.95-quantile of the inertia percentages distribution obtained by simulating 10000 random datasets of 5 dimensions based on a normal distribution), meaning that not all variables in the dataset are independent. The confidence ellipses associated with the treatments are not significantly different, which is consistent with the results shown in Figure 3.9 This allows an analysis of the individuals regardless of the treatment associated with the plant.

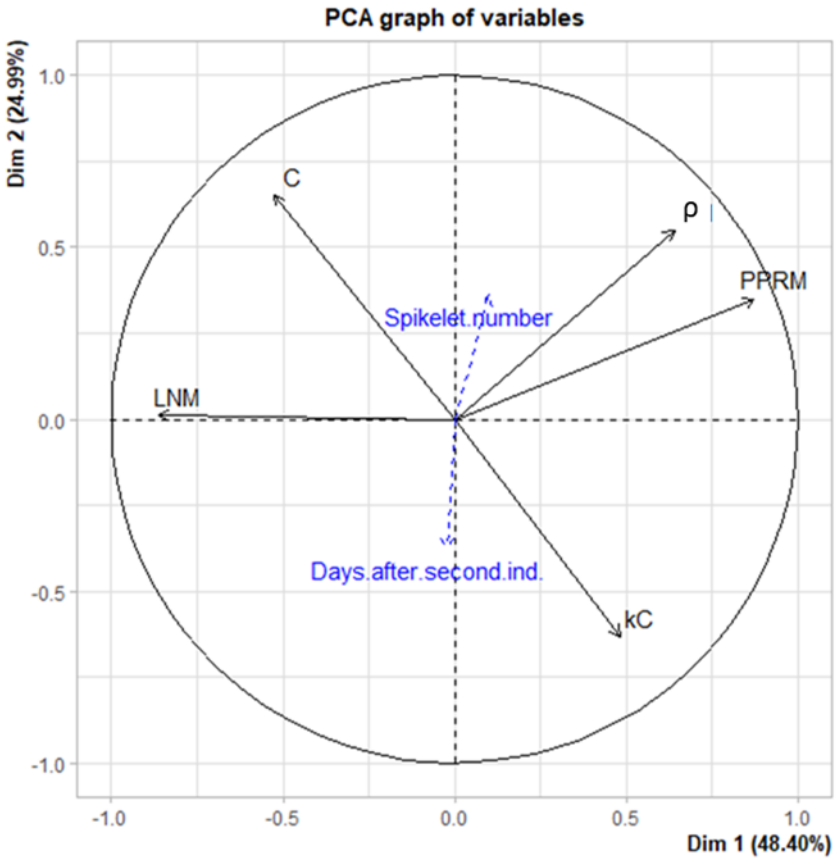


Figure 3.11: Plot of the variables (PCA).
Variables in black are the active variables, corresponding to the parameters of the model. Variables in blue are the additional quantitative variables (not used for the analysis), corresponding to phenological outputs of the model.

The first dimension of the PCA (Figure 3.11) was mainly determined by parameters associated with the secondary induction (PPRM and LNM) and its consequences on primordium emission (ρ). In Figure 3.10, plants located on the right-hand corner of the plot (*e.g.* 89, 98, 193, 194 and 203) were characterized by a fast-secondary induction leading to a high maximal induction rate (PPRM) and a low minimum number of emerged leaves to reach PPRM (LNM). At the same time, these plants initiated primordia at an elevated rate (ρ), thus increasing the final number of leaves and spikelets. On the left-hand corner, plants (*e.g.* 12, 29, 54, 58 and 145) have the opposite characteristics. The second dimension was mainly determined by parameters associated with leaf elongation rate and leaf final length (C and k_C). With the same age, plants located in the higher part of the plot (*e.g.* 13, 19, 79, 127) tended to produce longer leaves during the vegetative development and shorter leaves after floral transition. Plants of the lower part of the plot (*e.g.* 22, 53, 186, 193) have the

opposite characteristics. The supplementary quantitative variables representing time to heading from the start of secondary induction (*Days.after.second.ind*) and spikelet number are correlated with the third axe of the PCA and little to the secondary axes. Their low correlation with the two first axes of the PCA indicates a high interaction between parameters.

5. Discussion

5.1. A sequential model of floral induction

The environmental factors responsible for the floral induction have been well identified in perennial grasses. These are mainly temperature and photoperiod (Heide, 1994, Chapitre 1). Despite their important consequences for the success of reproductive development, attempts to finely predict the reproductive phenology are sparse. In this study, we developed a sequential two-phase model of floral induction as it was identified in *Lolium perenne* by Heide (1994). This kind of representation is similar to the propositions made by Woodward (2020) for forage grasses and in the model Sirius developed for wheat (Brooking, 1996; Jamieson *et al.*, 1998; He *et al.*, 2012; Brown *et al.*, 2013). Based on the literature, we assumed that for *Lolium perenne*, the primary induction is mainly dependent on temperature and the secondary induction on photoperiod. However, some interactions between these two factors have been reported during the two phases (Heide, 1994; Aamlid *et al.*, 2000). Some authors even suggest that an incomplete primary induction could be compensated by specific secondary induction conditions (Cooper, 1960; Heide, 1994). Qualitatively, the effects of temperature, photoperiod and their interactions during each phase are well known. Nevertheless, there is a lack of quantitative assessments of floral induction response to temperature and photoperiod, in particular in natural conditions. The decision to simplify our representation of the floral induction as two independent phases, each explained by a single variable, was made to account for the observations on floral induction in a sufficiently realistic way while avoiding an over-parameterization of the model compared to our quantitative knowledge of the processes. Because the

conditions of primary induction were identical in all treatments of the experiment (except T0), the calibration of $\Delta ind_{max}^{I^R}$ was not possible at this step. For the secondary induction, both LNM and PPRM were calibrated. LNM was incorporated to the model especially to account for the behavior of plants from T2 and T3. This adaptation of the model reached its goal as heading dates were well simulated and the global overestimation of the final number of leaves was reduced for individual of these treatments in comparison to individuals of T1. For PPRM, we found high values in comparison to the range explored. This is in accordance with the literature which agrees on the fact that the secondary induction is generally really fast when the photoperiod is over the minimum photoperiod (Chapter 1).

5.2. Interaction between floral induction and vegetative morphogenesis

In current models of perennial grasses, the role of floral induction is often limited to a simple switch between a vegetative to a reproductive functioning (Chapitre 1). In addition, none of them really account for the various interactions between floral induction and morphogenesis. The main innovation of our model relies on the representation of floral induction at tiller scale in a dynamic botanical structure. It allows representing the botanical continuity between the vegetative and the reproductive development. This strategy increases our ability to understand the complexity of the processes conducting to heading. First, assigning the floral induction processes to the apex allows to precisely account for the environmental history each apex. Therefore, in a context where tillers were not initiated at the same date, the model will be able to account for their different reproductive behavior. The model also provides a control of the floral induction by the morphogenesis as primary induction needs the presence of an apex and secondary induction requires at least one leaf to be emerged on the tiller. Then, it allowed defining the concept of final number of leaves, which is interesting to account for the progression of the floral development and is also used for modeling phenology in wheat (Brooking *et al.*, 1995; He *et al.*, 2012). Nevertheless, in wheat, which is an annual plant, tillers complete their life cycle in less than a year which limits their vegetative development in time. For tillers of perennial grasses, this overall limit

does not have a biological reality. Thus, contrasting to the model Sirius (Jamieson *et al.*, 1998; He *et al.*, 2012), which defines a maximum final number of leaves after which only spikelets will be produced, the final number of leaves in L-GrassF is completely under control of the floral induction. This allows simulating vegetative tillers for period longer than a year if the conditions are not favorable to floral induction.

The explicit representation of the organs and their development is very useful to account for the experimental results. In the present study, it allowed to propose a new modeling hypothesis to account for the reduced delay between secondary induction and heading as observed in the large plants of treatments T2 and T3 in the experiment presented in Chapitre 2. Our proposition was to add a control of the floral induction by the morphogenesis through a minimum number of leaves required for maximal secondary induction rate.

The representation of apex dynamics for the production of leaf and spikelet was useful to build a link between the final plant morphology and the coordination between leaf emergence and primordia dynamics. In our case, it was especially useful as we did not have experimental observation of apices. Nevertheless, the model conducted to an overestimation of the final number of leaves and an underestimation of the number of spikelets meaning that supplementary rules should be added, such as a dynamic balance between leaf and spikelet primordia after their initiation instead of considering that spikelets are determined only after floral transition.

Generally, studies on floral induction in perennial grasses were conducted by applying various conditions of temperature and photoperiod (Heide, 1988; Aamlid *et al.*, 2000; Seppänen *et al.*, 2010). However, determination of the response laws of the inductions with this strategy is very complex. Indeed, it requires growing plants until relatively advanced stages of development, *i.e.* beyond the floral transition (double-ridge, white stripes or heading) to conclude on the efficiency of given conditions. It is also necessary to modify the combinations of variables during the primary induction (temperature and photoperiod), the secondary induction as well as the duration of exposure to each of these induction phases. The model was used here to simulate the progression of the induction processes and their consequences on plant morphogenesis. For this purpose, however, it was necessary to set some parameters of the induction functions ($T_{min}^{I^R}$, $T_{opt}^{I^R}$., $T_{max}^{I^R}$, $\Delta ind_{max}^{I^R}$ and PP_{min}). It was thus possible

here to determine the duration of the secondary induction and its daily increment ($PPRM$). Due to the geometry of perennial grass tillers, the elongation of internodes does not have a predominant role in the determinism of the heading date. Consequently, the heading date was determined by the date of flag leaf ligulation in L-GrassF. However, it would be interesting to account for the development of internodes and the growth of the ear as it strongly affect plant height and the source-sink balance (Parsons and Robson, 1981; Matthew, 2002). In the context of using the model to study forage production, a good representation of the internodes would also make it possible to account for the decrease in biomass quality associated with their growth. Simulating the precise height of the apices and spikes would provide a good account of the direct effects of cutting on tillers' mortality, thus improving our understanding on the demography of tillers. Coordination rules between internode elongation and leaf ligulation have been proposed for wheat and maize (Fournier and Andrieu, 2000; Zhu *et al.*, 2009; Gauthier *et al.*, 2020) and further experimentations would therefore be required to assess those coordination rules on perennial *Lolium perenne*.

5.3. Choice of the parameters to calibrate

The objective of the calibration was to evaluate the ability of the formalisms implemented in the model to reproduce the observations of an experiment conducted under controlled conditions. The model calibration was performed on 6 parameters (C, Y_m^0, ρ, k_c and LNM) while the model has a total of 30 parameters. The remaining parameters were fixed to a unique value, common to all individuals and varieties. Concerning the vegetative development, differences in vegetative growth between individuals was introduced through variations in parameters C and Y_m^0, which were shown to have major effects (Verdenal, 2009). Indeed, Verdenal (2008; 2009) showed that these parameters were the most sensitive and could produce a large diversity of phenotypes. Subsequently, we found that the two parameters could be linked by a unique affine function, which allowed us to reduce the number of parameters to be estimated. The parameter C does not have a direct biological meaning. Nevertheless, its main advantage was to produce contrasted phenotypes with high values of C producing ‘forage type’ and lower values producing ‘turf type’.

For primary induction, the cardinal temperatures (Eq. 6) were fixed and only the maximum induction rate ($\Delta ind_{max}^{I^R}$) was considered variable. This hypothesis is supported by studies (Aamlid *et al.*, 2000; Paina *et al.*, 2014) on floral induction, which showed that varieties of contrasting geographical origins could be induced by exposure to the same temperature but that the exposure duration was critical. For this specific study, the data set used to calibrate the model did not allow assessing the maximum rate of primary induction ($\Delta ind_{max}^{I^R}$) as plants were exposed to a single temperature regime during this induction phase. Therefore, we fixed $\Delta ind_{max}^{I^R}$ value to ensure a full primary induction at the end of the 9 weeks exposure to low temperature. Similarly, the threshold photoperiod for secondary induction (PP_{min}) was set higher than the "long photoperiod" condition of the experiment (16h). Indeed, a photoperiod of 16h being higher than the one existing in France before heading, we considered that the secondary induction was then realized at the maximum rate (PPRM). Due to these choices and the experimental framework, we were not able to simulate the plant of treatment T1, T2 and T3, which remained vegetative. As a conclusion, the choice to set some parameters to fixed values was made within the specific framework of this study, which considered only a single species and specific environmental conditions. Using the model on another species and in another environmental conditions would require the recalibration of these parameters.

Nevertheless, the limited set of 6 parameters gave good estimates of the vegetative and reproductive development observed in the experiment. We found that the set of parameters identified were independent from the treatment applied which supports the idea that the identified parameters represent a phenotype corresponding to the combination of a genotype in interaction with the local environmental conditions (local temperature, local radiation intensity).

6. Conclusion

The L-GrassF model allowed us to aggregate the main processes driving the reproductive development. The model would be useful to explore the effects of the genetic diversity and the environmental variability on reproductive development. It also

constitutes an interesting starting point for the elaboration of a model representing the reproductive development at plant scale. However, the datasets used in this study did not allow us to decorrelate the genetic and environmental effects. Therefore, using the identified values in other environments than the conditions of our experimental dataset must be made with caution. Finally, all parameters of the model have been calibrated with different experiments on *Lolium perenne* in optimum growth conditions.This study at tiller scale showed that our formalisms is adapted to describe the complexity of the reproductive development especially the interaction between floral induction and morphogenesis.

Résumé du chapitre 3

Chez les graminées pérennes, la simulation de la date d'épiaison par les modèles est souvent empirique (date calendaire ou cumul de temps thermique fixes), même si des développements récents améliorent la représentation de l'induction florale. Dans tous les cas, la morphogénèse végétative, pourtant capitale dans le déterminisme de la date d'épiaison, n'est jamais prise en compte.

Nous proposons un nouveau modèle à l'échelle de la talle qui intègre les processus d'induction florale ainsi que leurs conséquences sur la morphogenèse. La morphogénèse végétative de la plante découle des formalismes développés dans une version précédente du modèle appelé L-Grass. Toutefois, des modifications ont dû être apportées à certains formalismes pour rendre compte du développement végétatif de talles à des âges avancés. Le développement reproducteur a été développé *ex nihilo* sur les bases de la littérature et des observations faites au Chapitre 2. L'induction florale se déroule en deux phases : une induction primaire contrôlée par la température et une induction secondaire contrôlée par la photopériode. Le démarrage de l'induction secondaire est dépendant du développement de la talle par un nombre de feuilles émergées minimum. La durée de la phase d'induction secondaire ainsi que le rythme d'émergence des feuilles pilotent la production de primordia par l'apex, conditionnant le nombre final de feuilles de la talle ainsi que le nombre d'épillets. La date d'épiaison est une propriété émergente du modèle et est calée sur la date de ligulation de la feuille drapeau.

Le modèle L-GrassF a été calibré individuellement sur les talles mères des plantes reproductives de la variété Bronsyn issues de l'expérimentation présentée au Chapitre 2. La calibration a mis en évidence la nécessité d'un grand nombre de combinaisons de valeurs de paramètres pour représenter fidèlement la diversité phénotypique observée.

Dans le Chapitre 4, nous évaluons la capacité du modèle à simuler l'effet de la diversité génétique et de la variabilité environnementale sur la précocité d'épiaison.

Chapitre 4

Simulation des effets des interaction entre la diversité génétique et la variabilité environnementale sur la date d'épiaison de variétés de *Lolium perenne* cultivées sur plusieurs sites et années

1. Introduction

The French catalog of forage cultivars proposes a large number of species and cultivars which are evaluated and characterized by the French Variety and Seed Study and Control Group (GEVES). In the case of *Lolium perenne*, 144 cultivars are available presenting various phenology, forage productivity, forage quality, perenniality and disease resistance (GEVES, 2018). For sowing their pastures, farmers have to choose the most adapted cultivars to the local environmental conditions, which will optimize forage yield, forage quality and fit forage biomass dynamics to animal requirements. Two major aspects of grass phenology can be used to optimize pasture production and management: the spring start of grass growth and heading start. Presently, breeding programs have been mainly oriented towards varieties with an earlier spring start of grass growth and a later heading, thus increasing the harvest-period of high-quality biomass. For their choice on phenological criteria, farmers can use the ranking of the cultivars made on heading precocity by the GEVES. The ranking, based on an average heading date in contrasted French locations, allows to compare cultivars but does not provide the absolute heading date for a given location.

For this purpose, forage plant models accounting for the effects of the environmental conditions and management practices on plant phenology are required. The model L-GrassF is a functional-structural plant model (FSPM) which simulates the reproductive development of individual tillers in relation to temperature, photoperiod and plant management (see Chapitre 3). It integrates an explicit model of floral induction in interaction with the morphological development of the tiller.

In the present work, we analyzed the behavior of L-GrassF and its ability to simulate the heading date of different varieties of *Lolium perenne* cultivated under contrasted natural conditions. After a presentation of the dataset used for model evaluation, we present the results from a sensitivity analysis aimed at determining the parameters with the highest effect on the heading date. Then, the most sensitive parameters were calibrated for seven varieties on a subset of the dataset and finally L-GrassF was evaluated for its ability to predict the date of heading on a second and independent subset.

2. Materials and method

2.1. Experimental dataset for model evaluation

The dataset used in this study was provided by the GEVES. The assessment criteria of the varieties include the date of regrowth start in spring and the date of heading start. The former variable corresponds to the first date for which the height of stretched plants exceeds 20 cm. The latter variable is defined as the first date for which at least 10 spikes are visible per linear meter. The measurement consists of an approximate visual assessment of the number of headed tillers. The given values of these two variables correspond to the average of three replicates. Since the measurements are carried out each 3 days, there is a measurement uncertainty of 3 days on both variables. In the following, we refer to the date of heading start as the heading date. The sward management and measurements were theoretically identical in all locations and years. Seeds were sown in spring in common gardens, in six-meter-long rows with a seed density of 5g per linear meter with three repetitions per cultivar. The rows were mowed during the first summer and the early winter to allow homogeneity in height before the second spring. Plants were well fertilized during their whole development to avoid nutritive stress. No irrigation was provided which may have created water shortage in some cases.

In our study, we selected 7 control varieties (Bronsyn, Indiana, Bargala, Lactal, Milca, Carillon and Escal) within the most represented ones available in the dataset. The detailed characteristics of these varieties and indicative values for the variables of interest are given in Table 4-1. The dataset explores a period of 17 years (2001-2017) on 6 French locations (Table 4-2). However, not all combinations of variety × site × year were available in the dataset.

Because the model does not account for drought effects, the dataset was restricted to environmental conditions where water resources before heading were not limiting. Environments where a water shortage would have potentially affected plant growth were identified by a water balance approach.

Table 4-1: Details of the varieties of Lolium perenne present in the dataset

Cultivar	Breeder	Country	Registration year	Ploidy	Start of regrowth in spring (doy)	Heading start (doy)	Number of observations
Bronsyn	Agriseeds Ltd	NZ	2001	2n	68 – 98	124	35
Indiana	Force Limagrain SA / DFL Trifolium	FR / DK	2004	2n	82 – 98	135	36
Bargala	Barenbrug Holland BV	NL	2000	4n	82 – 92	135	32
Lactal	RAGT / R 2n	FR	2004	4n	92 – 105	142	26
Milca	Carneau Frères SA	FR	1996	2n	92 – 105	145	27
Carillon	Carneau Frères SA	FR	2002	2n	92 – 112	159	26
Escal	R 2n	FR	2005	4n	–	–	23

Table 4-2: Characteristics of the environmental conditions in the 6 sites of the dataset.
Temperatures and rainfall are means calculated for the period from 2001 to 2017

Location	Latitude	Longitude	Altitude (m)	Mean winter temperature (°C)	Mean spring temperature (°C)	Photoperiod at summer solstice (h)	Soil available capacity (cm)	Annual rainfall (mm)
Erdre-en-Anjou	47.573 °	-0.827 °	53	5.9	11.4	16.0	120	680
Exmes	48.771 °	0.126 °	205	4.5	9.8	16.2	50	755
Guyancourt	48.771 °	2.097 °	161	4.7	10.9	16.2	190	577
Lusignan	46.418 °	0.119 °	150	5.1	11.1	15.8	166	787
Ploudaniel	48.504 °	-4.328 °	85	7.2	10.4	16.1	161	1152
Theix	45.723 °	3.018 °	830	1.2	6.9	16.0	50	800



Figure 4.1: Location of the study sites in France.
(1) Erdre-en-Anjou, (2) Exmes, (3) Guyancourt, (4) Lusignan, (5) Ploudaniel and (6) Theix

2.2. L-GrassF

2.2.1. Overview of L-GrassF

For this study, we used the model L-GrassF which was described in details in Chapitre 3. The model simulates the reproductive development of individual tillers in relation to environmental conditions. It represents dynamically the botanical structure of the tiller, *i.e.* organ initiation and growth. All organs of the tiller are initiated by the apex and grow depending on the environmental conditions, coordination rules and apex status (either vegetative or reproductive).

In the model, floral induction is explicitly described as a two-phase process: a primary induction depending on temperature and a secondary induction depending on the photoperiod. Floral induction determines the floral transition and triggers changes of tiller development. During secondary induction, the rate of leaf initiation by the apex increases while spikelets are initiated after the floral transition. The floral transition also impacts the leaf elongation rate and leaf final length. The model simulates phenological variables (floral transition and heading date) and morphological variables (leaf lengths, emergence dates of leaves).

As detailed in Chapitre 3, a majority of L-GrassF parameters were calibrated on *Lolium perenne* and are considered as invariant between cultivars of this species. Therefore, in the model, the phenotypic variability is assumed to be handled by seven parameters. Two parameters are related to leaf elongation: *C* that determines the final length of leaves and k_C that modulates parameter *C* after secondary induction. Five parameters are related to reproductive development: (i) $\Delta ind_{max}^{I^R}$ is the maximum daily increment of primary induction reached when day temperature is optimum (ii) PP_{min} is the minimum photoperiod allowing for secondary induction, (iii) PPRM is the maximal daily increment of secondary induction, (iv) LNM is the minimum number of leaves allowing for maximal PPRM and (v) ρ is a multiplicative factor of the number of primordia initiated at leaf emergence from secondary induction start.

2.2.2. Model inputs and initial conditions of simulations

L-GrassF was used to simulate the heading date of seven ryegrass varieties on 14 years and 6 locations (situations without water shortage). To date very little is known on the heading date variability between tillers of the same plant and this aspect of the model has not been assessed yet. Therefore, each experimental trial was simulated as a unique tiller in L-GrassF. In all locations, virtual sowing was realized on September 15th and a cut at 5cm height was performed on November 15th. The sowing was set later than the actual sowing date to reduce simulation time. This operation did not affect the predictions of the simulation. Indeed, the mean temperature of days from spring to September 15th were barely lower than the maximum primary induction temperature (12°C), so simulating plant development would not have modified the floral transition. Concerning the vegetative development, the two months between sowing and the cutting date in our simulations allowed the tillers to reach a permanent leaf production regime. Cutting the plants on November 15th as in real practices reduced the pseudostem length to 5cm and allowed equalizing plants. In order to reduce the computational time, L-GrassF was run on a high-performance computing center (MESO@LR, Université de Montpellier, France). All simulations were realized using the meteorological base 'SAFRAN' provided by Météo-France. From this base, we used daily variables (daily mean temperature, daily rainfall, daily potential evapotranspiration). Photoperiod was calculated using the Python package 'ephem'.

Table 4-3: Parameters of the model studied in the sensitivity analysis and calibrated.

Parameter	Description	Range of values for sensitivity analysis	Range of values for calibration	Unit
$\Delta ind_{max}^{I^R}$	Maximum daily rate of the primary induction	0.015 – 0.07	0.0425	unitless
PP_{min}	Minimum photoperiod for secondary induction	10 – 12	11	h
LNM	Minimum number of leaves for secondary induction at maximum daily rate	15 – 25	20	leaf
ρ	Number of primordia initiated per leaf emerging	2 – 7	4.5	primordium.leaf^{-1}
C	Multiplicative factor for the leaf final length	2 – 7	2 – 7	unitless
k_C	Multiplicative factor of C	0.05 – 0.5	0.05 – 0.5	unitless
PPRM	Maximum daily rate of the secondary induction	0.1 – 1	0.1 – 1	unitless

2.3. Sensitivity analysis

A sensitivity analysis was performed to identify and hierarchize the influence of the seven targeted parameters of the model on heading date. To optimize the number of simulations of the sensitivity analysis, we used the factorial screening method of Morris (1991). Morris' method is based on a discretization of the variation range for each parameter and the use of trajectories to explore it. One trajectory corresponded to a set of simulations defined by a starting point, *i.e.* a unique combination of parameter values, and movements from this point to explore the parameter space. Each movement corresponded to the variation of a single parameter value by a fixed step number of levels. It is therefore an exploration method called One At a Time (OAT). Several trajectories were randomly drawn for an efficient exploration of parameter combinations. In our study, each value of the seven parameters studied were discretized in 6 levels and the step on each parameter was 3 levels. A total of 40 trajectories were realized. In the end, the sensitivity analysis consisted in 320 simulations whereas it would have required 279 936 simulations (6^7) with a complete factorial design.

For each parameter, the Morris method allowed to calculate sensitivity indexes. The elementary effect of parameter P_i (i in [1, 7]) was calculated by the difference in output heading date between two successive simulations of a trajectory differing on the value of the parameter P_i. A mean sensitive index μ_i was calculated as the mean value of the 40 elementary effects of the parameter P_i (Eqn 4-1). The mean of absolute values of the elementary effects μ_i^* was calculated to account for both positive and negative effects. The potential interaction between the parameter P_i and the other parameters and/or the linearity of the response of the output heading date to change in parameter P_i were indicated by the standard deviation of the elementary effect of the parameter P_i, noted σ_i.

$$\Delta_i^r = \frac{LGrassF(T_{i-1}^r) - LGrassF(T_i^r)}{\delta}$$

$$\mu_i = \frac{1}{R}\sum_{r=1}^{R}\Delta_i^r$$

Eqn 4-1

$$\mu_i^* = \frac{1}{R}\sum_{r=1}^{R}|\Delta_i^r|$$

$$\sigma_i = \sqrt{\frac{1}{R-1}\sum_{r=1}^{R}(\Delta_i^r - \mu_i)^2}$$

where $LGrassF$ is the model L-GrassF, T^r is the trajectory r, R is the number of trajectories and δ is the step between two level of parameter i.

The same sensitivity analysis was performed for three contrasted environmental conditions to test the independence between the results of the sensitivity analysis and the environmental conditions. Since the photoperiod dynamics was not significantly different between the three sites, they were classified depending on the temperature: a cold environment (Theix 2009-2010), an intermediate environment (Ploudaniel 2009-2010) and a warm environment (Ploudaniel 2015-2016). The daily temperature variations in these environments are given in Figure 4.2.

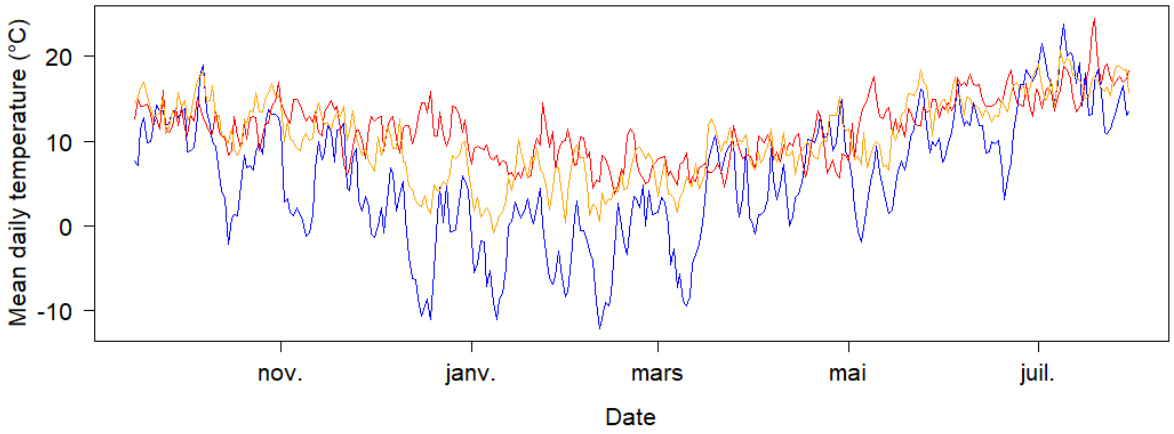


Figure 4.2: Daily temperatures, between September 15th and July 30th, in the 3 contrasted environmental contexts used for the sensitivity analysis
(blue: Theix 2009-2010, orange: Ploudaniel 2009-2010, red: Ploudaniel 2015-2016)

2.4. Calibration and validation

The objective was to identify sets of parameters which would be able to simulate the heading date of seven cultivars in any location of the GEVES' dataset. The experimental dataset was divided randomly into two subsets: 60% (n = 120) of the dataset for each variety was used for calibration and the remaining 40% (n = 85) for model validation. The calibration was made only on the three most sensitive parameters identified by the sensitivity analysis (C, k_C and PPRM). Other parameters were set to the mean value of the range used in the sensitivity analysis. A complete factorial plan with six levels for C, k_C and PPRM was set up, leading to 216 scenarios (6^3) which were run in each site-year combination. For each variety, the root-mean-square deviation (RMSE) was calculated for each combination of parameters and environments. The final set of parameters selected for the variety was the one which minimized the RMSE between observed and simulated heading dates. By mapping RMSE values in three-dimensional space (C, k_C, PPRM), we verified that this RMSE value corresponded to the global minimum of the explored space. The final sets of parameters identified for each cultivar were used for model validation.

2.5. Comparison of prediction methods

L-GrassF is intended to simulate the date and rate of leaf growth acceleration usually occurring at late winter, the heading date, the proportion of flowering tillers and the active vegetative tillers following each cutting. In this work, we limited the calibration of the model for each cultivar to heading date, and we compared the simulations from L-GrassF and those from current methods of prediction. The comparison was made on the validation dataset defined earlier and all cultivars were considered together. The cultivar Escal was not used in this part because the mean heading date calculated by the GEVES was not available. The three models used are the following:

Estimate 1: Mean heading date calculated by GEVES

For each cultivar of the French catalog of varieties, the GEVES indicates a value for the date of heading start (GEVES, 2006). This value used to rank cultivars depending on their precocity is calculated as the mean value of the heading dates measured in all GEVES' trials for several years. The mean value was calculated in 2006; therefore, the dataset used was partly different from the initial dataset we used in the study. This value can be used by farmers to predict the heading date of their pastures.

Estimate 2: Mean heading date calculated from our calibration dataset

This model is an adaptation that we made from the preceding one. Here, the mean heading date was calculated on the same dataset as the one used for the calibration of L-GrassF (60% of the initial dataset).

Model GDD 3: Constant sum of thermal time

Some models of the literature based the prediction of phenological stages from cumulated thermal time (Bonesmo and Bélanger, 2002; Jouven *et al.*, 2006; Jégo *et al.*, 2013). For each cultivar, we calculated the mean of the cumulated thermal time (base 0°C) between January 1st and observed heading dates from the calibration dataset. Using these values, we recalculated a simulated heading date for each combination location-year of the validation dataset.

2.6. Statistical analyses

Analysis of variance and non-linear regression were performed with R software (*R Core Team* 2021). Analyses of variance (ANOVAs) were performed following a one-factor linear model such that :

$$y_{ij} = \mu + C_i + \varepsilon_i$$

where Y is any dependent variable, μ is the mean value of Y, C_i is the effect of cultivar i, T_j is the effect of treatment j, $C_i \times T_j$ is the effect of the interaction between cultivar i and treatment j, and ε is the random error.

Normal distributions of the residuals of ANOVAs were tested using the Shapiro–Wilk test. Homoscedasticity was checked by random distribution of the residuals.

The root-mean-square deviation (RMSE) was calculated as:

$$RMSE = \sqrt{\frac{1}{n}\sum_{i=1}^{n}(S_i - O_i)^2}$$

*where **n** is the number of individuals, **S**$_i$ and **O**$_i$ are respectively the simulated and observed value of individual i for the variable considered*

All boxplot of this chapter were made with the style of Tuckey: -1.5*IQR, 2nd quartile, median, 3rd quartile, +1.5*IQR).

3. Results

3.1. Genetic diversity of heading date observed in the dataset

The analysis of the dataset revealed that the cultivars of our study presented a wide range of earliness, with more than one month between the earliest and the latest (Figure 4.3). An important variability of the heading date also existed within all the cultivars as shown by the boxplots (*sd = 23 days for Escal to 36 days for Indiana*). This expresses an interaction between genotypes and environments for the heading date. Despite the environmental variability, cultivar ranking according to their earliness was constant whatever the environmental conditions (results not shown). Therefore, predicting the heading date in *Lolium perenne* requires considering the genetic effect (supported by the cultivar), the environmental effect and their interaction.

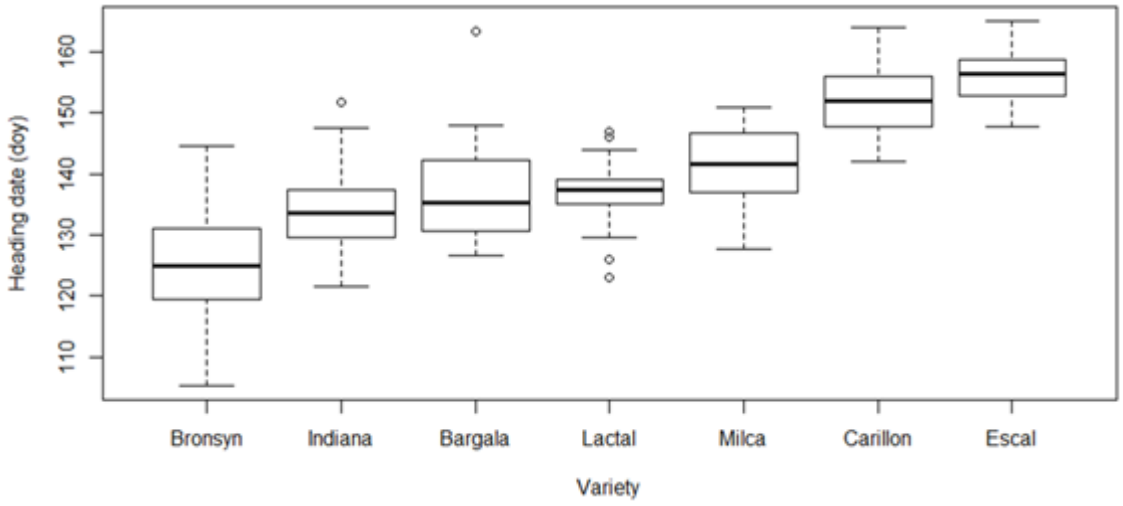


Figure 4.3: Heading date of the seven cultivars of Lolium perenne studied in various French locations for several years
Anova with model Yi = μ + Ci + εi ; F: 63.918, p < 0.05

3.2. Sensitivity analysis: the predominant effect of leaf growth and photoperiodic-related parameters

The Morris' method was used to study the sensitivity of the predicted heading date to seven parameters in L-GrassF (Figure 4.4). Three main groups of parameters were highlighted: C and kC were highly sensitive parameters, PPRM, PPmin and ρ had a moderate effect on heading date while LNM and $\Delta ind_{max}^{I^R}$ little affected the heading date. This pattern was similar across the three environments of contrasted temperature regimes.

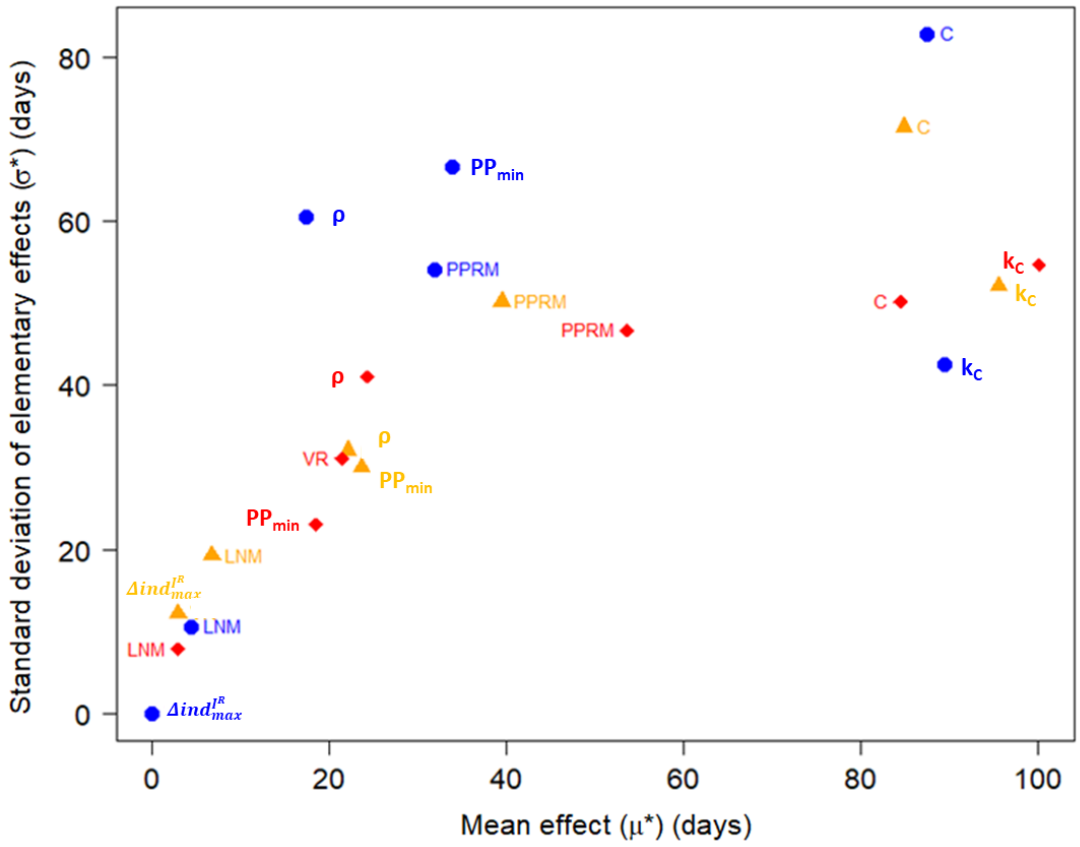


Figure 4.4: Morris sensitivity indices for the heading date.
Mean effects (μ) and standard deviation of the elementary effects (σ) of the parameters studied in the three sensitivity analyses (blue dots: Theix 2009-2010, orange triangles: Ploudaniel 2009-2010, red diamonds: Ploudaniel 2015-2016)*

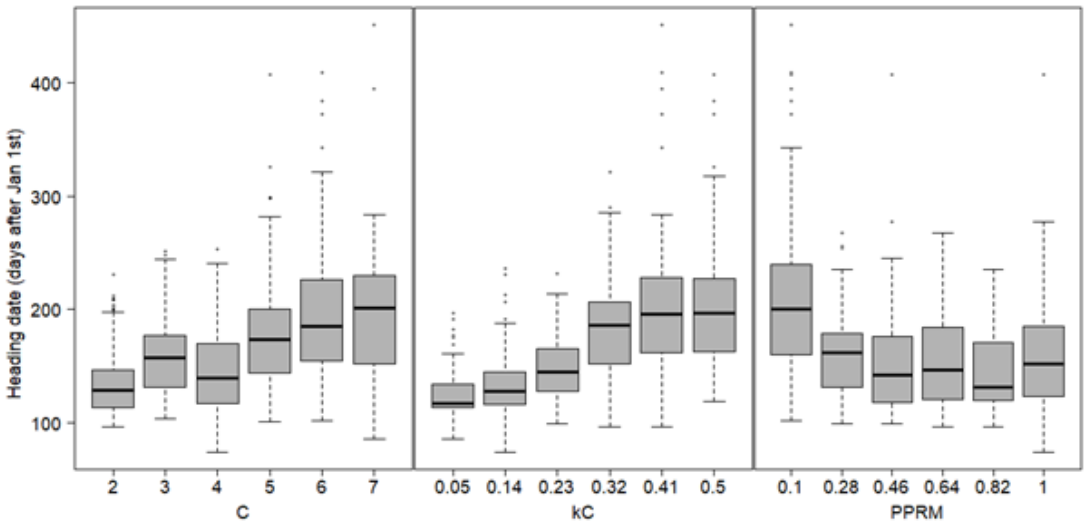


Figure 4.5: Boxplot of the heading date as a function of the values taken by the three most sensitive parameters (C, k_c, PPRM)

The parameters C and k_C, which are related to leaf elongation, presented a strong average effect of ~90 days whatever the environment (Figure 4.4). They positively affected the heading date (*i.e.* later heading) from 2 to 5 for C and 0.05 to 0.32 for kC (Figure 4.5). Beyond these ranges, their effect on the heading date showed a plateau. Their effect was also largely modulated by the value of the other parameters, reflecting an important interaction between the parameters (sdC ≃ 70 days and sdkC ≃ 50 days). The maximal rate of secondary induction (PPRM) had a smaller mean effect than C and kC but this effect was still significant in the three environments ([30-55] days; Figure 4.4). The only significant effect of PPRM was obtained for the value of 0.1 which led to late heading dates (Figure 4.5). Parameter PPmin appeared to have a strong mean effect ($\mu^* \simeq 35$ *days*) in the analysis performed in the coldest environment (Theix 2009-2010). The greater influence of this parameter in a cold environment is explained by the short duration of the primary induction in this case. The low temperatures of this environment led to an early completion of the primary induction which occurred before the days have reached the value of PPmin. Thus, PPmin was the only parameter responsible for the start of the secondary induction. On the contrary, in environments with medium (Ploudaniel 2009-2010) and high (Ploudaniel 2015-2016) mean temperatures, the start of secondary induction was strongly constrained by the completion of the primary induction, thus reducing the importance of PP_{min}. The maximum primary induction rate ($\Delta ind_{max}^{I^R}$) was little sensitive

($\mu^* < 25$) in comparison to other parameters but it highlighted an interesting feature. The sensitivity of $\Delta ind_{max}^{l^R}$ increased with increasing mean temperature of the environment meaning that in environments with a high temperature, the completion of the primary induction became constraining for the heading date. In the three analyses, the sensitivity of LNM was low, which can be explained by the advanced morphological stage of the plants when the secondary induction started characterized by a number of emerged leaves over the LNM values used in the analysis. It suggested the low importance of this parameter in natural conditions where sowing is often realized long before the flowering period. In the following, we limited our study to the three parameters that were the most sensitive: C, k_C and PPRM.

3.3. L-GrassF satisfactorily predicted heading date for contrasted environments and cultivars

The calibration and the validation of L-GrassF were realized on two subsets of the experimental dataset provided by the GEVES. Figure 4.6 compares the simulated heading dates in relation to the observed heading dates.

3.3.1. Calibration

The calibration allowed us to identify a combination of parameters for each of the seven cultivars of the dataset (Table 4.4). Using the optimal set of parameters for each cultivar, L-GrassF satisfactorily simulated the diversity of heading dates (Figure 4.6, grey dots). Overall, the RMSE was lower than seven days, except for Bronsyn, which showed a slightly higher RMSE (~ 8 days). The coefficients of determination obtained from the linear regressions between simulated and observed heading dates were low (< 0.60). This is due to the few data available and the low temporal range of heading dates observed within cultivars. For cultivar Escal and Carillon, we found the same set of parameters which is in accordance with their close observed heading dates (Figure 4.3).

Table 4-4: Values of parameters identified by calibration.
Parameters Rind1, PPmin, LNM and ρ were calibrated with the sensitivity analysis

Cultivar	C	kC	PPRM	*Rind1*	*PPmin*	*LNM*	*ρ*	RMSE	R^2
Bronsyn	3	0.23	0.64	*0.0425*	*11*	*20*	*4.5*	8.13	0.59
Indiana	7	0.14	0.64	*0.0425*	*11*	*20*	*4.5*	6.00	0.42
Lactal	5	0.23	0.64	*0.0425*	*11*	*20*	*4.5*	6.14	0.24
Bargala	7	0.14	0.64	*0.0425*	*11*	*20*	*4.5*	6.85	0.57
Milca	7	0.14	0.46	*0.0425*	*11*	*20*	*4.5*	6.73	0.30
Carillon	7	0.23	1.00	*0.0425*	*11*	*20*	*4.5*	6.36	0.23
Escal	7	0.23	1.00	*0.0425*	*11*	*20*	*4.5*	6.10	0.42

3.3.2. Validation

The validation of L-GrassF on the independent dataset showed variable results depending on cultivar (Figure 4.6). In Lactal, Bargala, Carillon and Escal, the model provided good overall estimates of the heading date (*RMSE < 7 days*) but the coefficients of determination were low (Table 4-4). This could be explained by the narrow range of observed heading dates for these cultivars, especially for Carillon. For Milca, the RMSE was quite high (9.42 days) and the determination coefficient was null, meaning that the model was not able to give a better prediction than the mean observed heading. For Indiana, the large range of observed heading dates (from 122 to 148) was well simulated by the model (0.55), but also produced a RMSE slightly lower than for other cultivars. For Bronsyn, the elevated RMSE was partly explained by one environment for which the model clearly overestimated the heading date (150 instead of 111) (Figure 4.6.a). Calculating the RMSE without this point reduced it from 13.46 to 8.72 days (-35%). We did not find any clear explanation for the model behavior in that situation which was not characterized by unusual environmental conditions.

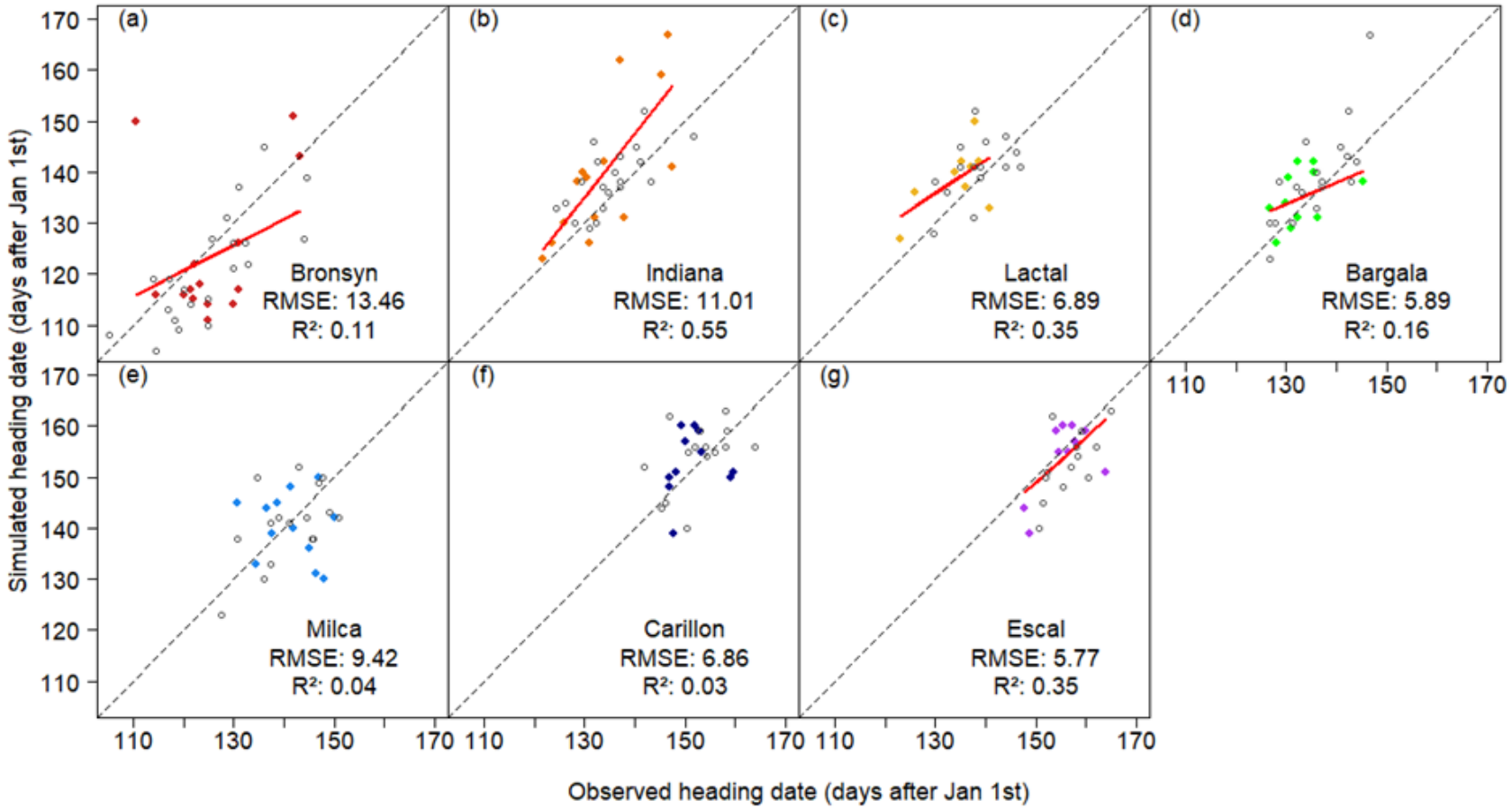


Figure 4.6: Comparison of observed and predicted values of heading date obtained with L-GrassF for seven cultivars.
(a) Bronsyn, (b) Indiana, (c) Lactal, (d) Bargala, (e) Milca and (f) Carillon, (g) Escal. Open grey circles are the results for the calibration procedure. Closed colored circles show the results for the model validation.

3.4. Comparison of prediction methods

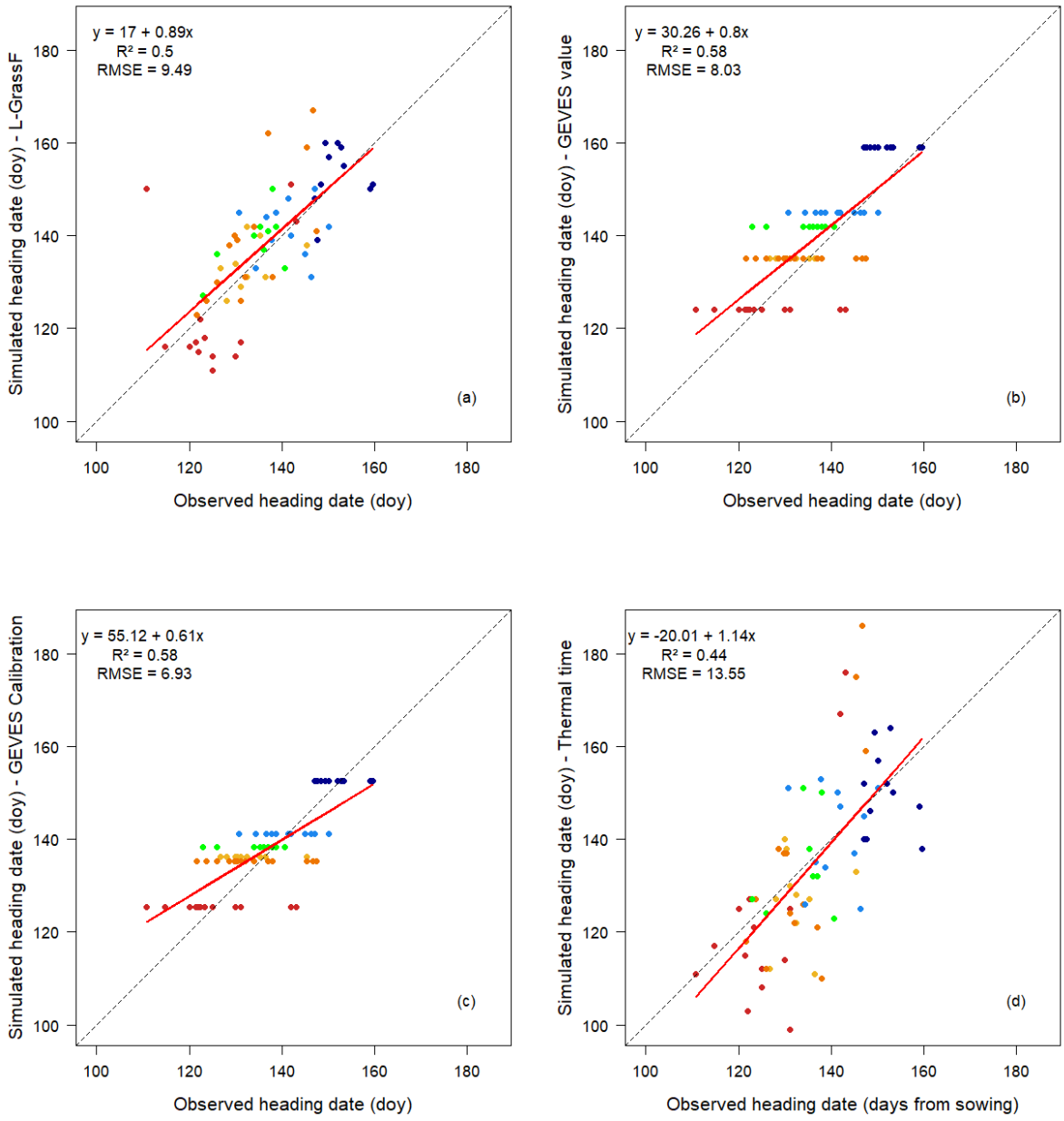


Figure 4.7: Comparison of observed and predicted values of heading date obtained with three models for cultivars Bronsyn, Indiana, Lactal, Bargala, Milca and Carillon.
(a) Values predicted with L-GrassF. (b) Values predicted by the mean value per cultivar given by GEVES (estimate 1). (c) Values predicted by the mean value per cultivar calibrated on the calibration dataset (estimate 2) (d) Values predicted by a constant thermal time sum from January 1st per cultivar. Colors correspond to cultivars.

The predicted heading dates obtained with L-GrassF (Figure 4.7.a), the indicator calculated by the GEVES (model 1, Figure 4.7.b), the mean value of the calibration dataset per cultivar (estimate 2, Figure 4.7.c) and a constant sum of thermal time from January 1st per cultivar calibrated with the calibration dataset (model GDD, Figure 4.7.d) were compared to observations. Among the four methods, the two models based on the mean heading date per cultivar (estimates 1 and 2) and L-GrassF gave similar results (*RMSE from 6.9 to 9.5 days*), considering the random error of 3 days on the observation. The models 1 and 2 provided a slightly better representation of variability between simulated and observed heading date ($R^2 = 0.58$) than did L-GrassF ($R^2 = 0.5$), due to a majority of observations close to the mean value. Nevertheless, estimates 1 and 2 were not able to predict the diversity of heading dates due to the environmental diversity. The model 3 was the significantly less accurate one (*RMSE = 13.6 days,* $R^2 = 0.44$). Exploring the behavior of the last method, we found that the model accuracy was particularly sensitive to the date used as reference for counting the sum of thermal time. Some reference dates between January 1st and observed heading dates gave a better accuracy even better than the other methods.

4. Discussion

4.1. Importance of the morphogenetic parameters

For the seven cultivars grown in the different environments studied, L-GrassF successfully simulated the diversity of heading dates. The sensitivity revealed the important role of the parameters C and k_C. As these two parameters were involved in leaf development, it reflected the importance of considering the morphogenetic development of the whole tiller to account properly for reproductive development. It also suggested that the main environmental variable correlated to heading date was the temperature. The effect of the other parameters of the model, in particular those of floral induction processes, was lower in the context of the study, revealing that under temperate conditions, and within the range of cultivars studied, the genetic variability

in the completion of floral induction was not determinant for the variability in heading date.

The preponderant role of parameters C and k_C could be exploited to identify the parameters associated with a genotype at an early stage. Indeed, final leaf length and the rhythm of leaf appearance during the vegetative development were unknown in the dataset but these variables can be easily measured in order to recalibrate the parameter C. The identification of k_C can also be realized early, during the spring, when leaf elongation rate increases.

4.2. L-GrassF satisfactorily predicted heading date despite large uncertainties on the dataset

Although all GEVES trials were theoretically managed following a common protocol, there were uncertainties about the practical application of this protocol for each year and location. The sowing dates in spring may have been different according to the local climatic conditions. For instance, it may have been delayed if the soil was not dry enough to allow access for farm machinery (Leclercq, pers.comm.). By initializing L-GrassF just before the first autumn (instead of the previous spring), we considered that the period preceding this date had no effect on the floral induction, in particular, because during that period, the temperatures were higher than the primary induction temperature threshold and because the development only affected the size of the vegetative organs. In order to homogenize organ sizes, a virtual cutting was made on the tillers on November 15th for all conditions. This cutting was analogous to the regularization cutting generally made by the GEVES just before winter (Leclercq, pers.comm., no precise date available). Practically, the GEVES cutting was unevenly made between the trials. Indeed, the cutting decision was made on a visual appreciation of plant height and, similarly to sowing, depended on the weather conditions.

Even if the size of the dataset used was large from an experimental point of view, it remained small from a statistical point of view (36 location-years combinations for the most represented variety). In addition, all cultivars were not present in all trials,

leading to an incomplete experimental design. The size and incompleteness of data was due to the high turnover of control cultivars in the GEVES trials. Indeed, control cultivars have to be the best for studying the range of candidate varieties for registration, which varies from year to year, mainly towards later heading cultivars. This decreased the accuracy of the calibration.

Despite all these uncertainties, L-GrassF was overall able to simulate the genetic and environmental variability in heading dates between cultivars, years and locations. The comparison between the accuracy of the different models highlighted that the performance of the model was equivalent to the other methods used for estimating heading dates.

4.3. Validity range of the model

L-GrassF was calibrated and validated in a reduced range of environments, corresponding to the northwest of France. Therefore, the range of latitude explored by the dataset did not provide significant differences in photoperiod between sites and the climatic contrast between trials was mainly on temperature range and distribution. In addition, we limited our dataset to trials which had not been exposed to water stress or lack of mineral elements. Therefore, the model validity is only ensured for similar environmental conditions. As shown by Blanco-Pastor *et al.* (2019), the genetic diversity exploited for the selection of new varieties is widely used in natural ecotypes originating from north-western Europe. This area of origin fully encompasses the extension of our studied area. Therefore, it would be interesting to check if the model also manages to simulate accurately the behavior of genotypes from geographic areas with very different climates and photoperiodic conditions such as northern Europe and the Mediterranean area.

Under the trial conditions, the heading date was always measured, meaning that the floral induction was always reached by enough tillers for the date of heading start to be measured. As no fail of the floral induction was observed, our dataset did not allow us to verify what would be the behavior of the model on the same varieties cultivated under environmental conditions, which would not allow the floral transition, for instance with winter temperature too high to complete primary induction. Tested

under conditions where the temperature regime did not complete primary induction requirements as well as in conditions where they completed very early, the model was able to produce a large range of reproductive behavior from no floral transition to very late heading (not shown). This constituted a major improvement in comparison of the simple empiric models used for the comparison, which are not valid in conditions where floral induction is not realized. To evaluate the whole potential of the model, it would be interesting to have trials in more contrasted sites, especially in geographical areas where winter temperatures are higher and could be potentially insufficiently low to allow full primary induction.

4.4. Conclusion

L-GrassF is a complex functional-structural model, which is able to simulate many variables about plant vegetative and reproductive morphogenesis such as the heading date, the final number of leaves per tillers, the number of spikelets per ear, the rate of appearance and the final length of the leaves. In this chapter, its evaluation was realized with a dataset of observed heading dates for seven cultivars grown in contrasted environments. Despite the uncertainties associated to the dataset, L-GrassF was performant in the prediction of the heading date with a similar or better accuracy than the empiric models currently used (mean heading date of GEVES network and sum of thermal time).

Further studies with more complete observation datasets would be required to evaluate the full potential of the model.

Résumé du chapitre 4

Le catalogue de variétés fourragères français rassemble des variétés de phénologie reproductive diversifiée. Le jeu de données fourni par le GEVES regroupe les dates d'épiaison mesurées pour 7 variétés cultivées dans 6 localités françaises de 2003 à 2017.

L'objectif de ce chapitre est de tester la capacité du modèle L-GrassF à simuler la diversité des phénotypes observée en tenant compte de l'interaction entre la diversité génétique (7 variétés) et la variabilité environnementale (6 sites – 15 années).

Afin d'étudier le comportant du modèle dans les conditions environnementales du jeu de données, une analyse de sensibilité a été conduite dans 3 environnements contrastés du jeu de données. Cette analyse de sensibilité a également révélé les paramètres les plus sensibles du modèle dans la gamme environnementale d'étude.

La calibration du modèle sur les trois paramètres les plus sensibles a été réalisée sur un sous-ensemble du jeu de données correspondant à 60% du jeu de données initial. Les jeux de paramètres ont ensuite été utilisés pour simuler les observations du jeu de validation (40% restants du jeu de données initial).

Enfin, la qualité de prédiction du modèle a été comparée à celle de méthodes simples actuellement utilisés pour prédire la date d'épiaison. Cette étude comparative a montré que la qualité de prédiction du modèle était comparable à celle des méthodes couramment employées mais n'a permis la comparaison que sur une partie du potentiel du modèle.

Discussion générale

1. Atteinte des objectifs de l'étude

1.1. Objectifs et hypothèse

Pour comprendre et prédire la réponse des prairies face aux nouvelles problématiques auxquelles est confrontée l'agriculture telles que l'adaptation au changement climatique et l'introduction de plus de diversité au sein des couverts végétaux, il est nécessaire de développer des modèles capables de rendre compte de la variabilité phénotypique des plantes en fonction de l'interaction entre la diversité génétique et la variabilité environnementale. L'objectif de cette thèse était d'élaborer un modèle pour répondre à cet enjeu au niveau de la phénologie reproductive des graminées pérennes.

Pour parvenir à cet objectif, nous soutenons la thèse que l'amélioration de la prise en compte de la diversité génétique et de la variabilité environnementale dans le cadre de la prédiction de la phénologie reproductive des graminées pérennes nécessite une représentation explicite des processus d'induction florale et de morphogénèse à l'échelle de la talle.

1.2. Déroulement de l'étude et principaux résultats

La première étape de cette thèse a été d'identifier les principaux processus contrôlant la phénologie des graminées pérennes et leurs conséquences sur la plante. Dans ce cadre, la revue de littérature présentée au Chapitre 1 a mis en évidence les nombreux changements de la morphogénèse des talles de graminées pérennes déclenchés par l'induction florale (modification du plastochrone, modification du type d'organes produits par l'apex, accélération de la croissance foliaire et allongement des entrenœuds). Elle a également souligné l'importance de l'état morphologique de la plante sur la réalisation de l'induction des talles (apex initié, feuilles émergées, relations entre les talles pour le transfert d'un signal inducteur). Il est enfin apparu que

la talle était l'échelle la plus appropriée pour étudier la phénologie des graminées pérennes car c'est à cette échelle que se déroulent l'ensemble des processus du développement reproducteur et que sont définis les principaux stades phénologiques (stade végétatif, transition florale, épiaison et anthèse). A celle échelle, la date d'épiaison ressort comme la résultante de processus d'induction et de processus de morphogénèse végétative (rythme de production des feuilles). Enfin, la revue a permis d'appréhender le fort empirisme des modèles existant sur les questions de phénologie et leur faible niveau d'intégration de la morphogénèse dans la représentation du développement reproducteur. Parallèlement, les modèles détaillés pour les céréales ne sont peu adaptés aux plantes prairiales du fait du caractère complexe de la démographie des talles d'une prairie. Ainsi, les modèles préexistants à cette thèse ne semblent pas en mesure de répondre aux enjeux présentés plus haut.

A partir de ce constat, il s'est avéré nécessaire de développer un modèle du développement reproducteur des graminées pérennes.

Dans un premier temps, une expérimentation, rapportée au Chapitre 2, a été conduite pour quantifier certains des changements provoqués par l'induction florale au niveau de la morphogénèse des talles au cours du développement reproducteur en fonction des conditions d'induction et de la diversité génétique. Elle a permis d'établir une corrélation entre le nombre final de feuilles des talles et la date d'épiaison. Elle a également montré que la durée séparant l'induction primaire de l'induction secondaire avait un effet non-linéaire sur le retard de la date d'épiaison, la production de feuilles et la production d'épillets.

Afin de rendre compte à la fois des processus d'induction et de morphogénèse, notre choix s'est porté sur les modèles structure-fonction individu-centrés (FSPM) et le modèle L-Grass (Verdenal *et al.*, 2008), qui permet de simuler la croissance foliaire de *Lolium perenne* à l'échelle de la talle et les dynamiques de tallage à l'échelle de la plante, a été utilisé comme point de départ. Outre l'ajout d'un module de phénologie complet, il a également été nécessaire d'appliquer des modifications à certains processus de croissance du modèle initial pour améliorer sa capacité à simuler des plantes sur de plus longues périodes de temps que celles considérées dans la version initiale du modèle ainsi que dans des conditions de température variables.

Le nouveau modèle appelé L-GrassF a fait l'objet d'une évaluation sur sa capacité à saisir la variabilité phénotypique grâce aux données issues de l'expérimentation présentée au Chapitre 2. En étudiant les principales variables de sortie du modèle (date d'épiaison, nombre de feuilles final par talle et nombre d'épillets par épi), nous avons pu identifier des paramètres associés au phénotype de chaque individu. Une analyse par composantes principales a également permis d'identifier les proximités entre les individus simulés et les corrélations entre paramètres.

Une seconde évaluation du modèle a été conduite pour étudier sa capacité à simuler la variabilité de la date d'épiaison de plusieurs variétés cultivées dans des environnements contrastés du point de vue du régime annuel des températures. Cette étape a dans un premier temps nécessité une analyse de sensibilité qui a permis d'identifier les paramètres les plus sensibles du modèle. De cette analyse, il est ressorti que dans les conditions environnementales étudiées (principalement le nord-ouest de la France), ou l'induction florale était toujours satisfaite, les paramètres les plus sensibles étaient des paramètres impliqués dans la croissance foliaire et la vitesse d'induction secondaire. Par la suite, la calibration du modèle s'est limitée aux paramètres les plus sensibles. La capacité du modèle à simuler la diversité phénotypique sur la date d'épiaison due à la variabilité environnementale a été étudiée pour sept variétés représentées par un unique jeu de paramètres. Les performances du modèle ont enfin été comparées à celles des modèles empiriques utilisés jusqu'à présent. La comparaison a révélé une qualité de prédiction du modèle L-GrassF similaire à celle des autres modèles. Cependant, à la différence des modèles empiriques L-GrassF propose une prédiction dynamique de la totalité de la morphogénèse des talles à partir de leur initiation ainsi que de nombreuses variables associées (longueur des feuilles, nombre de feuilles et nombre d'épillets). Une évaluation de la totalité du potentiel du modèle nécessiterait un jeu de données en conditions réelles ayant un niveau de précision similaire à celui obtenu par l'expérimentation du Chapitre 2. Il serait également intéressant d'élargir la gamme de conditions environnementales du jeu de données pour évaluer les améliorations apportées par l'implémentation fine des processus d'induction, notamment l'induction primaire, dont la sensibilité était réduite dans les conditions environnementales étudiées.

En conclusion, cette étude a atteint son objectif initial d'amélioration de la prise en compte de la diversité génétique et de la variabilité environnementale pour la prédiction de la phénologie. Elle a validé l'hypothèse de la nécessité de prendre en compte explicitement les interactions entre induction florale et morphogénèse pour simuler la phénologie reproductive. Elle a également abouti à un outil logiciel fonctionnel en libre accès (https://github.com/openalea-incubator/lgrass) et à une paramétrisation du modèle pour sept variétés représentatives de la diversité phénotypique du ray-grass anglais pour la phénologie reproductive.

2. Prendre en compte la diversité génétique dans les modèles

2.1. Caractériser la diversité génétique chez *Lolium perenne*

Chez *Lolium perenne*, la séparation géographique des populations a abouti à des populations aux caractéristiques phénologiques très contrastées, associée à une forte diversité génétique (Blanco-Pastor *et al.*, 2019). L'homme a également cherché à diversifier la précocité des variétés par la sélection variétale. Toutefois, la diversité génétique représentée dans les variétés commerciales est de moindre mesure (Blanco-Pastor *et al.*, 2019). En plus de la diversité intervariétale, il existe une importante diversité génétique au sein des populations et des variétés synthétiques (Bourdon and Noël, 2005). Celle-ci a pour origine la reproduction sexuée allogame de *Lolium perenne* responsable d'un brassage génétique important et d'une forte diversité génétique entre les différentes graines formées (Gillet, 1980; Durand and Lafarge, 2013).

Au cours de cette étude, nous avons tenté d'évaluer la capacité du modèle L-GrassF à rendre compte de ces deux niveaux de diversité.

Il nous a été possible de rendre compte de la diversité intervariétale grâce à la calibration du modèle sur les données du GEVES. Pour cette calibration, nous avons toutefois dû faire l'hypothèse que le phénotype de la phénologie des variétés pouvait être représenté par une unique date correspondant à la date de début d'épiaison.

Pour rendre compte de la diversité intravariétale, nous avons réalisé une calibration du modèle individu par individu. Cette méthode donne une bonne vision de la diversité de paramètres nécessaire pour simuler les différents phénotypes d'une variété mais elle n'est pas suffisamment synthétique pour permettre la comparaison de la diversité entre plusieurs variétés. Il serait dès lors intéressant de pouvoir associer chaque variété à un unique jeu de paramètres et à une variabilité aléatoire permettant de représenter la diversité intravariétale. Cet élément aléatoire, pourrait être porté par chaque paramètre mais aux vues des forte interactions entre les paramètres, il serait plus judicieux de la faire porter par des n-uplets de paramètres ayant un effet moyen de même sens. Une autre possibilité serait d'identifier des séquences génétiques liées aux paramètres du modèle et de reporter la diversité allélique sur la variabilité aléatoire des paramètres.

2.2. Simuler la diversité intraspécifique

Production de pollen et de graines

La diversité génétique au sein des populations de *Lolium perenne* résulte du brassage génétique obtenu par la reproduction sexuée. La représentation de la diversité des comportements reproducteurs dus à la génétique initiale des plantes d'une population peut donc être utilisée pour prédire les nouvelles combinaisons génétiques possibles. Ces études nécessiteraient toutefois l'intégration dans le modèle des phases tardives du développement reproducteur tel que l'anthèse et la formation des grains. Dans un premier temps, un modèle simple tel que celui proposé par Abel *et al.* (2018) pourrait être intégré à L-GrassF.

A un premier niveau, le modèle permet de déterminer les individus susceptibles de fleurir une année donnée, mais également la fenêtre temporelle durant laquelle un génotype donné va fleurir. A partir de là, il serait possible de déterminer les génotypes

dont la période de floraison est en partie commune, rendant le croisement possible. A un second niveau, L-GrassF est en mesure de déterminer le nombre d'épillets produit par talle, à partir duquel peut être calculé le nombre de fleurs par talle (Sartie *et al.*, 2018). De là, en utilisant la distribution spatiale des plantes, il serait possible d'étudier la pollinisation et les génotypes en découlant (Griffiths, 1950).

Evolution des populations

On a vu que le ray-grass anglais présente une grande plasticité dans sa morphogenèse et que chaque génotype est susceptible de prendre des formes très diverses selon son environnement. Cette forme végétative a des impacts sur les phases reproductives et donc sur le succès reproducteur de l'individu. Mais la diversité intra-population est également responsable de l'évolution d'une population en réponse aux changements environnementaux, du fait de la diversité et du succès reproducteur de ses différents individus.

3. Vers la simulation du développement reproducteur à l'échelle de la plante et des conséquences sur la pérennité

3.1. L'échelle plante chez les graminées pérennes

Chez les graminées pérennes, l'unité fonctionnelle de base de la plante est la talle. En effet, chaque talle d'une plante est capable individuellement d'assurer son autotrophie, le prélèvement d'eau et des ressources minérales et d'avoir un développement reproducteur complet. Ainsi, la totalité du cycle de vie annuel d'une graminée pérenne peut être expliqué en ne considérant que l'échelle talle. Pourtant, à une échelle de temps pluriannuelle, c'est à l'échelle de la plante qu'il faut considérer l'individu (Durand and Lafarge, 2013). En effet, le développement reproducteur d'une

talle étant fini, la survie de l'individu au sens génétique est assurée par les talles de la plante restées végétatives.

Les talles d'une plante sont issues du processus de tallage qui correspond au développement des bourgeons axillaires au niveau de chaque phytomère. Le tallage est responsable d'une forte hétérogénéité des âges des talles d'une plante, qui ont donc été exposées à des conditions environnementales différentes les unes des autres en fonction de leur date d'initiation. Simuler l'apparition des talles ainsi que leur développement reproducteur individuel est donc indispensable pour simuler les dates d'épiaison des différentes talles d'une plante ainsi que pour déterminer la proportion de talles reproductrices d'une plante.

3.2. Le développement reproducteur de la plante comme propriété émergente du modèle ?

De son héritage du modèle L-Grass, le modèle L-GrassF a conservé la possibilité de simuler les dynamiques de tallage au sein d'une plante mais aussi d'un couvert. Il est possible de simuler les phases de tallage croissante lorsque le couvert est ouvert et les phases de ralentissement et d'arrêt du tallage lorsque le couvert est fermé. Les nouveaux développements du modèle concernant les aspects reproducteurs à l'échelle de la talle individuelle permettent eux de prédire le devenir des talles en fonction de leur date d'initiation ainsi que leur morphogénèse. Ainsi, le modèle dans son ensemble est en mesure de simuler l'apparition de chaque talle de son initiation à sa floraison et/ou à sa mort, ce qui permet d'étudier l'évolution de la population de talles d'une plante au cours du temps en termes de nombre de talles ainsi que de leur stade phénologique.

3.3. Test d'hypothèses de transfert d'induction entre les talles d'une plante

Dans la littérature, l'indépendance des talles d'une plante pour l'induction florale est discutée. Pour certaines espèces comme *Lolium perenne*, il semble que la majorité des talles reproductrices ont émergé au plus tard au cours de l'exposition aux conditions inductrices (Havstad *et al.*, 2004). Ainsi, l'hypothèse d'une induction indépendante de chaque talle semble suffisante pour expliquer les proportions de talles reproductives en fonction de leur date d'initiation. En revanche, chez d'autres espèces, certaines talles émergées après la fin des conditions d'induction secondaire (longue photopériode) ont présenté un développement reproducteur (Havstad *et al.*, 2004). De plus, chez *Dactylis glomerata* et *Bromus inermis* lorsque seule une partie des talles sont exposées à des conditions d'induction secondaire (après une induction primaire), certaines talles non-exposées deviennent reproductrices (Havstad *et al.*, 2003). Pour ces espèces, l'explication de la proportion de talles reproductrices semble donc nécessiter l'hypothèse d'une transmission d'un signal inducteur entre les talles d'une plante. Une telle hypothèse nécessite également une rétroaction pour empêcher l'ensemble des talles de la plante de devenir reproductrices. Or, dans le modèle L-GrassF, chaque talle est identifiée individuellement et il est possible de connaître l'identité de l'ensemble des talles-mères successives dont elle est issue. Par la représentation du tallage et de l'induction florale à l'échelle de la talle, il est également possible de connaître la date d'initiation de la talle et les conditions environnementales, notamment les conditions inductrices, dans lesquelles elle s'est développée. Grace à ces deux possibilités, L-GrassF est à même d'être utilisé pour tester différentes hypothèses de transfert d'un signal inducteur entre les talles d'une plante.

3.4. Compréhension de la mortalité des talles et de la remontaison

Le développement reproducteur d'une talle a pour conséquence finale sa mort. Au cours du développement floral, on assiste donc à un important renouvellement de la population de talles d'une plante.

La remontaison est un phénomène encore mal expliqué. Elle est définie par le développement reproductif tardif de certaines talles au cours d'une seconde vague après la première vague d'épiaison. Il se produit après une coupe réalisée lorsque le nombre de talles épiées de la première vague d'épiaison a atteint son maximum. Compte tenu des connaissances sur l'induction florale, deux hypothèses peuvent être proposées pour expliquer le phénomène : (i) les talles reproductrices lors de la remontaison proviennent de bourgeons axillaires existant au moment de l'induction primaire, donc induit, dont le développement a été inhibé par la fermeture du couvert puis permis par la réouverture du couvert lors de la coupe. Les conditions de photopériode favorable de l'été permettant l'induction secondaire de ces talles. (ii) Ces talles nouvellement formées sont induites par un transfert de signal inducteur des talles de la première vague d'épiaison.

4. Vers une utilisation du modèle dans des conditions de croissance non-optimales

Au cours de cette thèse, le développement reproducteur n'a été étudié que dans des conditions qualifiées d'optimales pour la croissance (absence de stress hydrique et nutrition minérale optimale, photosynthèse optimale). Afin d'élargir la gamme environnementale de validité du modèle, il serait intéressant de le compléter par des modules de simulation de l'interception du rayonnement lumineux et de la photosynthèse développés dans L-Grass par Verdenal (Verdenal, 2009) ainsi que du développement racinaire et de l'assimilation des éléments minéraux (Migault, 2015). L'ajout de ces fonctionnalités au modèle permettrait de tester les différentes hypothèses proposées dans la littérature sur les réponses du développement reproducteur en conditions stressantes (Thomas and Evans, 1990; Bahmani *et al.*, 2002; Zeiter *et al.*, 2016).

5. Quels usages pour le modèle L-GrassF?

Le modèle L-GrassF a montré ses performances pour prédire la date d'épiaison. Toutefois, du fait de sa complexité (30 paramètres), c'est un modèle particulièrement lourd à calibrer. De plus, la réalisation de simulations nécessite un temps de calcul important (> 20min). Pour ces raisons, le modèle L-GrassF est inadapté à un usage généralisé par les agriculteurs ou les conseillers agricoles. Dans le contexte climatique actuel où les variations interannuelles de température sont limitées, l'utilisation de modèles simples de prédiction (fonction du temps thermique ou des dates indicatives fournies par le GEVES) apporte déjà une prédiction suffisamment précise de la date d'épiaison.

L-GrassF a plutôt vocation dans sa version actuelle à être un outil heuristique, permettant le test d'hypothèses écophysiologiques (synchronisation entre talles, établissements de lois de réponse…). Grâce à la représentation 3D, L-GrassF permet d'étudier l'interception de la lumière par les organes aériens en utilisant le couplage avec un modèle radiatif (Chelle *et al.*, 2004; Verdenal, 2009). Ceci présente un fort intérêt pour l'étude des interactions plante-plante, en permettant notamment d'expliquer et de quantifier certains traits morphologiques du feuillage conférant un avantage compétitif vis-à-vis des plantes voisines, tel que la hauteur des plantes ou la surface des feuilles pour la compétition lumineuse (Barillot *et al.*, 2012).

Dans le cadre du changement climatique, le soin apporté à la représentation de l'induction florale dans le modèle L-GrassF permettra son utilisation pour étudier les effets du changement climatique, ce que ne permettent pas les modèles empiriques (Kipling *et al.*, 2016).

Dans le modèle L-GrassF, chaque organe est représenté par un module auquel sont associées des propriétés et des fonctions. Grâce à leur interprétation en 3D, il est également possible de calculer l'interception de rayonnement par chaque organe (Verdenal, 2009). Le modèle pourrait, par exemple, permettre de relier les fonctionnement trophiques et morphogénétiques des graminées pendant les phases végétatives (Gauthier *et al.*, 2020) et post-florales (Barillot *et al.*, 2016).

6. Conclusion

Notre étude a permis l'élaboration d'un modèle intégrateur des connaissances écophysiologiques actuelles sur le développement reproducteur des graminées pérennes. Le modèle développé intègre (i) les processus d'induction florale en relation avec les conditions environnementales et la morphologie de la talle, (ii) les effets de la transition florale sur la morphogénèse des talles. Par ces processus, il permet de simuler la date d'épiaison, le nombre de feuille final par talle, le nombre d'épillets par épi ainsi que l'ensemble de la morphogénèse végétative et reproductive. Cette thèse a abouti à la proposition d'un outil informatique intégratif et fonctionnel du développement reproducteur chez les graminées pérennes. Un jeu de paramètre permettant de simuler la diversité phénotypique de la date d'épiaison existant chez les variétés commerciales de *Lolium perenne* a également été généré.

Par la suite, le modèle pourra servir de base pour étudier la floraison à des échelles supérieures à la talle. Dans il premier temps, il serait intéressant d'utiliser le modèle tel qu'implémenté actuellement en exploitant sa capacité à simuler le tallage. Cela permettrait d'étudier l'ensemble des conséquences du développement reproducteur sur l'évolution de la population de talles à l'échelle de la plante entière. Par la suite, il serait nécessaire d'intégrer des processus de modulation du développement pour des conditions de croissance non-optimales telle que les stress hydriques ou minéraux. De telles amélioration rendrait possible l'utilisation du modèle pour prédire les interactions entre plantes au sein d'un couvert. Afin de pleinement valider la généricité du modèle dans sa capacité à prédire la date d'épiaison, il serait enfin nécessaire de le confronter à des conditions environnementales plus contrastées que celles étudiées ici.

Références

Aamlid TS, Heide OM, Boelt B. **2000**. Primary and Secondary Induction Requirements for Flowering of Contrasting European Varieties of Lolium perenne. *Annals of Botany* **86**: 1087–1095.

Abel S, Byrne SL, Asp T, Boelt B. **2018**. Predicting anthesis date of perennial ryegrass (Lolium perenne L.) with growing degree-days at heading. *Grass and Forage Science* **73**: 233–238.

Allred KW. **1982**. Describing the grass inflorescence. *Rangeland Ecology & Management/Journal of Range Management Archives* **35**: 672–675.

Anslow RC. **1963**. Seed Formation in Perennial Ryegrass. *Grass and Forage Science* **18**: 90–96.

Arojju SK, Barth S, Milbourne D, Conaghan P, Velmurugan J, Hodkinson TR, Byrne SL. **2016**. Markers associated with heading and aftermath heading in perennial ryegrass full-sib families. *BMC Plant Biology* **16**.

Arumuganathan K, Dale PJ, Cooper JP. **1991**. Vernalization in Lolium temulentum L.: Responses of In Vitro Cultures of Mature and Immature Embryos, Shoot Apices and Callus. *Annals of Botany* **67**: 173–179.

Bahmani I. **2000**. *Influence des facteurs environnementaux sur la dynamique de tallage et la croissance des feuilles des cultivars de Raygrass pérenne (Lolium pérenne) "Ellet" et "Grasslands ruanui."* Vandoeuvre-les-Nancy, INPL.

Bahmani I, Thom ER, Matthew C, Lemaire G. **2002**. Flowering propensity of two New Zealand perennial ryegrass cultivars originating from different ecotypes. *New Zealand Journal of Agricultural Research* **45**: 129–137.

Barillot R, Chambon C, Andrieu B. **2016**. CN-Wheat, a functional–structural model of carbon and nitrogen metabolism in wheat culms after anthesis. II. Model evaluation. *Annals of Botany* **118**: 1015–1031.

Barillot R, Combes D, Chevalier V, Fournier C, Escobar-Gutiérrez AJ. **2012**. How does pea architecture influence light sharing in virtual wheat–pea mixtures? A simulation study based on pea genotypes with contrasting architectures. *AoB PLANTS* **2012**.

Barre P, Ruttink T, Muylle H, Lootens P, Sampoux J-P, Rohde A, Combes D, Roldán-Ruiz I. **2017**. Natural diversity in vegetative and reproductive investments of perennial ryegrass is shaped by the climate at the place of origin. *Grass and Forage Science*.

Barre P, Turner LB, Escobar Gutiérrez A. **2015**. Leaf length variation in perennial forage grasses. *Agriculture* **5**: 682–696.

Barrett PD, Laidlaw AS, Mayne CS. **2005**. GrazeGro: a European herbage growth model to predict pasture production in perennial ryegrass swards for decision support. *European Journal of Agronomy* **23**: 37–56.

Bean EW. **1970**. Short-day and Low-temperature Control of Floral Induction in Festuca. *Annals of Botany* **34**: 57–66.

Blanco-Pastor JL, Manel S, Barre P, Roschanski AM, Willner E, Dehmer KJ, Hegarty M, Muylle H, Ruttink T, Roldán-Ruiz I, Ledauphin T, Escobar-Gutiérrez A, Sampoux J-P. **2019**. Pleistocene climate changes, and not agricultural spread, accounts for range expansion and admixture in the dominant grassland species Lolium perenne L. *Journal of Biogeography* **46**: 1451–1465.

Bommer D. **1961**. SAMEN-VERNALISATION PERENNIERENDER GRASERARTEN. *ZEITSCHRIFT FUR PFLANZENZUCHTUNG-JOURNAL OF PLANT BREEDING* **46**: 105-+.

Bonesmo H, Bélanger G. **2002**. Timothy Yield and Nutritive Value by the CATIMO Model: I. Growth and Nitrogen. *Agronomy Journal* **94**: 337–345.

Borrill M. **1959**. Inflorescence Initiation and Leaf Size in Some Gramineae. *Annals of Botany* **23**: 217–227.

Bourdon P, Noël D. **2005**. Méthodes et objectifs de sélection des plantes fourragères. : 12.

Boval M, Edouard N, Sauvant D. **2015**. A meta-analysis of nutrient intake, feed efficiency and performance in cattle grazing on tropical grasslands. *animal* **9**: 973–982.

Brooking IR, Jamieson PD, Porter JR. **1995**. The influence of daylength on final leaf number in spring wheat. *Field Crops Research* **41**: 155–165.

Buxton DR, Marten GC. **1989**. Forage Quality of Plant Parts of Perennial Grasses and Relationship to Phenology. *Crop Science* **29**: 429–435.

Byrne SL, Guiney E, Donnison IS, Mur LAJ, Milbourne D, Barth S. **2009**. Identification of genes involved in the floral transition at the shoot apical meristem of Lolium perenne L. by use of suppression subtractive hybridisation. *Plant Growth Regulation* **59**: 215–225.

Carrère P, Pontes L, Andueza D, Louault F, Rosseel D, Taini E, Pons B, Toillon S, Soussana J-F. **2010**. Evolution de la valeur nutritive de graminées prairiales au cours de leur cycle de développement. *Fourrages*.

Casal JJ. **2013**. Photoreceptor Signaling Networks in Plant Responses to Shade. *Annual Review of Plant Biology* **64**: 403–427.

Casal JJ, Deregibus VA, Sanchez RA. **1985**. Variations in tiller dynamics and morphology in Lolium multiflorum Lam. vegetative and reproductive plants as affected by differences in red/far-red irradiation. *Annals of Botany* **56**: 553–559.

Casal JJ, Sáchez RA, Deregibus VA. **1987**. Tillering Responses of Lolium multiflorum Plants to Changes of Red/Far-Red Ratio Typical of Sparse Canopies. *Journal of Experimental Botany* **38**: 1432–1439.

Casal JJ, Sanchez RA, Deregibus VA. **1986**. The effect of plant density on tillering: The involvement of R/FR ratio and the proportion of radiation intercepted per plant. *Environmental and Experimental Botany* **26**: 365–371.

Chapman DF, Lee JM, Waghorn GC. **2014**. Interaction between plant physiology and pasture feeding value: a review. *Crop and Pasture Science* **65**: 721–734.

Chelle M, Hanan J, Autret H. **2004**. Lighting virtual crops: the CARIBU solution for open L-systems. *Proceedings of the 4th international workshop on functional-structural plant models*. C. Godin et al. UMR AMAP, Montpellier, France, 194.

Chen A, Li C, Hu W, Lau MY, Lin H, Rockwell NC, Martin SS, Jernstedt JA, Lagarias JC, Dubcovsky J. **2014**. PHYTOCHROME C plays a major role in the acceleration of wheat flowering under long-day photoperiod. *Proceedings of the National Academy of Sciences* **111**: 10037–10044.

Chuine I. **2010**. Why does phenology drive species distribution? *Philosophical Transactions of the Royal Society B: Biological Sciences* **365**: 3149–3160.

Cleland EE, Chuine I, Menzel A, Mooney HA, Schwartz MD. **2007**. Shifting plant phenology in response to global change. *Trends in Ecology & Evolution* **22**: 357–365.

Clemence TGA, Hebblethwaite PD. **1984**. An appraisal of ear, leaf and stem 14CO2 assimilation, 14C-assimilate distribution and growth in a reproductive seed crop of amenity Lolium perenne. *Annals of Applied Biology* **105**: 319–327.

Colasanti J, Coneva V. **2009**. Mechanisms of Floral Induction in Grasses: Something Borrowed, Something New. *PLANT PHYSIOLOGY* **149**: 56–62.

Colvill KE, Marshall C. **1984**. Tiller dynamics and assimilate partitioning in Lolium perenne with particular reference to flowering. *Annals of Applied Biology* **104**: 543–557.

Cooper JP. **1950**. Day-Length and Head Formation in the Ryegrasses*. *Grass and Forage Science* **5**: 105–112.

Cooper JP. **1958**. The Effect of Temperature and Photoperiod on Inflorescence Development in Strains of Timothy (phleum Spp.). *Grass and Forage Science* **13**: 81–91.

Cooper JP. **1960**. Short-day and low-temperature induction in Lolium. *Annals of Botany* **24**: 232–246.

Corrall AJ, Fenlon JS. **1978**. A comparative method for describing the seasonal distribution of production from grasses. *The Journal of Agricultural Science* **91**: 61.

Darwinkel A. **1978**. Patterns of tillering and grain production of winter wheat at a wide range of plant densities. *NJAS Wageningen Journal of Life Sciences* **26**: 383–398.

Davies A. **1971**. Growth rates and crop morphology in vernalized and non-vernalized swards of perennial ryegrass in spring. *The Journal of Agricultural Science* **77**: 273–282.

Davies I. **1978**. Developmental characteristics of grass varieties in relation to their herbage production: 3. Tiller development in Dactylis glomerata and Lolium perenne in relation to head emergence. *The Journal of Agricultural Science* **94**: 125–136.

Davies A, Thomas H. **1983**. Rates of Leaf and Tiller Production in Young Spaced Perennial Ryegrass Plants in Relation to Soil Temperature and Solar Radiation. *Annals of Botany* **51**: 591–597.

DeJong TM, Da Silva D, Vos J, Escobar-Gutiérrez AJ. **2011**. Using functional–structural plant models to study, understand and integrate plant development and ecophysiology. *Annals of Botany* **108**: 987–989.

Donmez E, Sears RG, Shroyer JP, Paulsen GM. **2001**. Genetic Gain in Yield Attributes of Winter Wheat in the Great Plains. *Crop Science* **41**: 1412–1419.

Doole GJ, Romera AJ. **2015**. Trade-offs between profit, production, and environmental footprint on pasture-based dairy farms in the Waikato region of New Zealand. *Agricultural Systems* **141**: 14–23.

Durand J-L, Andrieu B, Barillot R, Barre P, Combes D, Enjalbert J, Escobar Gutiérrez A, Faverjon L, LeCarpentier C, Litrico I, Louarn G, Migault V, Sanchez Rodriguez L. **2016**. Progresser dans la simulation mathématique des performances des mélanges de variétés fourragères pour composer et améliorer les prairies. *Fourrages*: 21–28.

Durand J-L, Lafarge M. **2013**. *Comment l'herbe pousse: Développement végétatif, structures clonales et spatiales des graminées*. Quae.

Ergon Å, Hamland H, Rognli OA. **2013**. Differential expression of VRN1 and other MADS-box genes in Festuca pratensis selections with different vernalization requirements. *Biologia Plantarum* **57**: 245–254.

Evans LT. **1958**. Lolium temulentum L., a Long-day Plant requiring only One Inductive Photocycle. *Nature* **182**: 197.

Evans LT. **1960a**. The influence of temperature on flowering in species of Lolium and in Poa pratensis. *The Journal of Agricultural Science* **54**: 410–416.

Evans LT. **1960b**. The Influence of Environmental Conditions on Inflorescence Development in Some Long-Day Grasses. *New Phytologist* **59**: 163–174.

Fiorelli CF, Woodward SJR, Wastney ME, Thom ER, Bahmani I. **2001**. Modelling factors affecting reproductive development of perennial ryegrass in Waikato dairy pastures. *PROCEEDINGS OF THE CONFERENCE-NEW ZEALAND GRASSLAND ASSOCIATION*.165–170.

Fournier C, Andrieu B. **2000**. Dynamics of the Elongation of Internodes in Maize (Zea mays L.): Analysis of Phases of Elongation and their Relationships to Phytomer Development. *Annals of Botany* **86**: 551–563.

Gauthier M, Barillot R, Schneider A, Chambon C, Fournier C, Pradal C, Robert C, Andrieu B. **2020**. A functional structural model of grass development based on

metabolic regulation and coordination rules (R Hancock, Ed.). *Journal of Experimental Botany*: eraa276.

GEVES. **2006**. *Classement des variétés de plantes fourragères inscrites en liste A sur le Catalogue Officiel français*. CTPS - Comité technique permanent de la sélection.

Gillet M. **1980**. *Les graminées fourragères: description, fonctionnement, applications à la culture de l'herbe*. Gauthier-Villars.

Gillet M, Breisch H. **1982**. Crise du tallage et remontaison chez les graminées fourragères : données complémentaires. *Agronomie* **2**: 187–192.

Gonthier R, Francis D. **1989**. Changes in the pattern of cell division in the shoot and root meristems of Lolium perenne during the transition from vegetative to floral growth. *Journal of Experimental Botany* **40**: 285–292.

Griffiths DJ. **1950**. The liability of seed crops of perennial ryegrass to contamination by wind-borne pollen. *The Journal of Agricultural Science* **40**: 19–38.

Groot JCJ, Lantinga EA. **2004**. An object-oriented model of the morphological development and digestibility of perennial ryegrass. *Ecological Modelling* **177**: 297–312.

Havstad LT, Aamlid TS, Heide OM, Junttila O. **2003**. Transfer of florigenic stimuli between tillers in photoperiodically split plants of Dactylis glomerata and Bromus inermis. *Physiologia Plantarum* **118**: 270–277.

Havstad LT, Aamlid TS, Heide OM, Junttila O. **2004**. Transfer of flower induction stimuli to non-exposed tillers in a selection of temperate grasses. *Acta Agriculturae Scandinavica, Section B - Soil & Plant Science* **54**: 23–30.

Hay RKM. **1990**. The influence of photoperiod on the dry matter production of grasses and cereals. *New Phytologist* **116**: 233–254.

Hazard L, Betin M, Molinari N. **2006**. Correlated Response in Plant Height and Heading Date to Selection in Perennial Ryegrass Populations. *Agronomy Journal* **98**: 1384–1391.

Hazard L, Ghesquière M, Barraux C. **1996**. Genetic variability for leaf development in perennial ryegrass populations. *Canadian Journal of Plant Science* **76**: 113–118.

He J, Le Gouis J, Stratonovitch P, Allard V, Gaju O, Heumez E, Orford S, Griffiths S, Snape JW, Foulkes MJ, Semenov MA, Martre P. **2012**. Simulation of environmental and genotypic variations of final leaf number and anthesis date for wheat. *European Journal of Agronomy* **42**: 22–33.

Heide OM. **1987**. Photoperiodic control of flowering in Dactylis glomerata, a true short-long-day plant. *Physiologia Plantarum* **70**: 523–529.

Heide OM. **1988**. Flowering requirements of Scandinavian Festuca pratensis. *Physiologia Plantarum* **74**: 487–492.

Heide OM. **1994**. Control of flowering and reproduction in temperate grasses. *New Phytologist* **128**: 347–362.

Heide OM, Bush MG, Evans LT. **1985**. Interaction of photoperiod and gibberellin on growth and photosynthesis of high-latitude Poa pratensis. *Physiologia Plantarum* **65**: 135–145.

Herrmann A, Schachtel GA. **2001**. OSYAQ, an organ-specific growth model for forage grasses. *Grass and Forage Science* **56**: 268–284.

Höglind M, Van Oijen M, Cameron D, Persson T. **2016**. Process-based simulation of growth and overwintering of grassland using the BASGRA model. *Ecological Modelling* **335**: 1–15.

Huyghe C, Litrico I, Surault F. **2012**. Agronomic value and provisioning services of multi-species swards

Jamieson PD, Semenov MA, Brooking IR, Francis GS. **1998**. Sirius: a mechanistic model of wheat response to environmental variation. *European Journal of Agronomy* **8**: 161–179.

Jégo G, Bélanger G, Tremblay GF, Jing Q, Baron VS. **2013**. Calibration and performance evaluation of the STICS crop model for simulating timothy growth and nutritive value. *Field Crops Research* **151**: 65–77.

Jewiss OR. **1972**. Tillering in grasses—its significance and control. *Grass and Forage Science* **27**: 65–82.

Johnston MJ, Waite R. **1965**. Studies in the lignification of grasses. I. Perennial rye-grass (S 24) and cocksfoot (S 37). *The Journal of Agricultural Science* **64**: 211–219.

Jouven M, Carrère P, Baumont R. **2006**. Model predicting dynamics of biomass, structure and digestibility of herbage in managed permanent pastures. 1. Model description. *Grass and Forage Science* **61**: 112–124.

Kemp DR, Eagles CF, Humphreys MO. **1989**. Leaf growth and apex development of perennial ryegrass during winter and spring. *Annals of botany* **63**: 349–355.

King RW, Evans LT. **1991**. Shoot Apex Sugars in Relation to Long-Day Induction of Flowering in Lolium temulentum L. *Functional Plant Biology* **18**: 121–135.

King RW, Heide OM. **2009**. Seasonal flowering and evolution: the heritage from Charles Darwin. *Functional Plant Biology* **36**: 1027–1036.

Kipling RP, Virkajärvi P, Breitsameter L, Curnel Y, De Swaef T, Gustavsson A-M, Hennart S, Höglind M, Järvenranta K, Minet J, Nendel C, Persson T, Picon-Cochard C, Rolinski S, Sandars DL, Scollan ND, Sebek L, Seddaiu G, Topp CFE, Twardy S, Van Middelkoop J, Wu L, Bellocchi G. **2016**. Key challenges and priorities for modelling European grasslands under climate change. *Science of The Total Environment* **566–567**: 851–864.

Kleinendorst A. **1974**. Some effects of vernalization on the reproductive capacity of Lolium perenne L. *Netherlands journal of agricultural science*.

Lang A. **1965**. Physiology of flower initiation. In: Lang Anton, ed. *Differenzierung und Entwicklung / Differentiation and Development*. Berlin, Heidelberg: Springer Berlin Heidelberg, 1380–1536.

Langer RHM. **1956**. Growth and Nutrition of Timothy (phleum Pratense). *Annals of Applied Biology* **44**: 166–187.

Langer RHM, Ryle SM, Jewiss OR. **1964**. The Changing Plant and Tiller Populations of Timothy and Meadow Fescue Swards. I. Plant Survival and the Pattern of Tillering. *Journal of Applied Ecology* **1**: 197–208.

Le Treut H. **2018**. *AcclimaTerra - Anticiper les changements climatiques en Nouvelle-Aquitaine. Pour agir dans les territoires.*

Lecarpentier C, Barillot R, Blanc E, Abichou M, Goldringer I, Barbillon P, Enjalbert J, Andrieu B. **2019**. WALTer: a three-dimensional wheat model to study competition for light through the prediction of tillering dynamics. *Annals of Botany* **123**: 961–975.

Lindsey KE, Peterson ML. **1964**. Floral Induction and Development in Poa pratensis L.1. *Crop Science* **4**: cropsci1964.0011183X000400050033x.

Litrico I, Barkaoui K, Barradas A, Barre P, Béguier V, Birouste M, Bristiel P, Crespo D, Deléglise C, Ghesquiere M, Godinho B, Hernandez P, Julier B, Louarn G, Meisser M, Mosimann E, Picon-Cochard C, Roumet C, Volaire F. **2016**. Utiliser les mélanges fourragers pour s'adapter au changement climatique : opportunités et défis. : 12.

Malvoisin P. **1984**. Organogenèse et croissance du maître-brin du blé tendre (Triticum aestivum) du semis à la floraison. I.–Relations observées entre la croissance foliaire et la différenciation des ébauches foliaires ou florales. *Agronomie* **4**: 557–564.

Martin G, Durand J-L, Duru M, Gastal F, Julier B, Litrico I, Louarn G, Médiène S, Moreau D, Valentin-Morison M, Novak S, Parnaudeau V, Paschalidou F, Vertès F, Voisin A-S, Cellier P, Jeuffroy M-H. **2020**. Role of ley pastures in tomorrow's cropping systems. A review. *Agronomy for Sustainable Development* **40**: 17.

Matthew C. **1992**. A study of seasonal root and tiller dynamics in swards of perennial ryegrass (Lolium perenne L.) : a thesis presented in partial fulfilment of the requirements for the degree of Ph D in Agronomy at Massey University.

Matthew C. **2002**. Translocation from flowering to daughter tillers in perennial ryegrass (Lolium perenne L.). *Australian Journal of Agricultural Research* **53**: 21–28.

Matthew C, Assuero SG, Black CK, Sackville Hamilton NR. **2000**. Tiller dynamics of grazed swards. *LEMAIRE, G.; HODGSON, J.; MORAES, A*.127–150.

Mazel C, Lafarge M, Hill DRC. **2005**. An individual-based, stochastic and spatial model to simulate the ramification of grass tillers and their distribution in swards. *Simulation Modelling Practice and Theory* **13**: 308–334.

McGrath S, Hodkinson TR, Charles TM, Zen DG, Barth S. **2010**. Variation in inflorescence characters and inflorescence development in ecotypes and cultivars of Lolium perenne L. *Grass and Forage Science* **65**: 398–409.

Meilhac J, Deschamps L, Maire V, Flajoulot S, Litrico I. **2020**. Both selection and plasticity drive niche differentiation in experimental grasslands. *Nature Plants* **6**: 28–33.

Meilhac J, Durand J-L, Beguier V, Litrico I. **2019**. Increasing the benefits of species diversity in multispecies temporary grasslands by increasing within-species diversity. *Annals of Botany* **123**: 891–900.

Migault V. **2015**. *Insertion de la morphogenèse racinaire dans L grass, un modèle structure-fonction de graminées fourragères*. Poitiers.

Moore KJ, Moser LE. **1995**. Quantifying developmental morphology of perennial grasses. *Crop Science* **35**: 37–43.

Morris MD. **1991**. Factorial Sampling Plans for Preliminary Computational Experiments. *Technometrics* **33**: 161–174.

Ong CK. **1978**. The physiology of tiller death in grasses. *Grass and Forage Science* **33**: 197–203.

Ong CK, Marshall C, Saoar GR. **1978**. The physiology of tiller death in grasses. 2. Causes of tiller death in a grass sward. *Grass and Forage Science* **33**: 205–211.

Paina C, Byrne SL, Domnisoru C, Asp T. **2014**. Vernalization Mediated Changes in the Lolium perenne Transcriptome. *PLOS ONE* **9**: e107365.

Parsons AJ, Robson MJ. **1980**. Seasonal changes in the physiology of S24 perennial ryegrass (Lolium perenne L.). 1. Response of leaf extension to temperature during the transition from vegetative to reproductive growth. *Annals of Botany* **46**: 435–444.

Parsons AJ, Robson MJ. **1981**. Seasonal changes in the physiology of S24 perennial ryegrass (Lolium perenne L.) 3. Partition of assimilates between root and shoot during the transition from vegetative to reproductive growth. *Annals of Botany* **48**: 733–744.

Perreta MG, Ramos JC, Vegetti AC. **2009**. Development and Structure of the Grass Inflorescence. *The Botanical Review* **75**: 377–396.

Poirier M, Durand J-L, Volaire F. **2012**. Persistence and production of perennial grasses under water deficits and extreme temperatures: importance of intraspecific vs. interspecific variability. *Global Change Biology* **18**: 3632–3646.

Prieto I, Violle C, Barre P, Durand J-L, Ghesquiere M, Litrico I. **2015**. Complementary effects of species and genetic diversity on productivity and stability of sown grasslands. *Nature Plants* **1**: 15033.

Ryle GJA. **1965**. Effects of daylength and temperature on ear size in S. 24 perennial ryegrass. *Annals of Applied Biology* **55**: 107–114.

Ryle GJA. **1966**. Effects of photoperiod in the glasshouse on the growth of leaves and tillers in three perennial grasses. *Annals of Applied Biology* **57**: 257–268.

Ryle GJA, Langer RHM. **1963**. Studies on the Physiology of Flowering of Timothy (Phleum pratense L.) II. Influence of Daylength and Temperature on Size of the inflorescence. *Annals of Botany* **27**: 233–244.

Sachs T, Novoplansky A, Cohen D. **1993**. Plants as competing populations of redundant organs. *Plant, Cell & Environment* **16**: 765–770.

Sampoux J-P, Baudouin P, Bayle B, Béguier V, Bourdon P, Chosson J-F, Deneufbourg F, Galbrun C, Ghesquière M, Noël D, Pietraszek W, Tharel B, Viguié A. **2011**. Breeding perennial grasses for forage usage: An experimental assessment of trait changes in diploid perennial ryegrass (Lolium perenne L.) cultivars released in the last four decades. *Field Crops Research* **123**: 117–129.

Sanderson MA, Goslee SC, Soder KJ, Skinner RH, Tracy BF, Deak A. **2011**. Plant species diversity, ecosystem function, and pasture Management—A perspective. *Canadian Journal of Plant Science*.

Sartie AM, Easton HS, Matthew C, Rolston MP, Faville MJ. **2018**. Seed yield in perennial ryegrass (Lolium perenne L.): comparative importance of component traits and detection of seed-yield-related QTL. *Euphytica* **214**: 226.

Schwartz MD. **2013**. Introduction. In: Schwartz MD, ed. *Phenology: An Integrative Environmental Science*. Dordrecht: Springer Netherlands, 1–5.

Scotton M. **2018**. Seed production in grassland species: Morpho-biological determinants in a species-rich semi-natural grassland. *Grass and Forage Science* **73**: 764–776.

Seppänen MM, Pakarinen K, Jokela V, Andersen JR, Fiil A, Santanen A, Virkajärvi P. **2010**. Vernalization response of Phleum pratense and its relationships to stem lignification and floral transition. *Annals of Botany* **106**: 697–707.

Simon JC, Lemaire G. **1987**. Tillering and leaf area index in grasses in the vegetative phase. *Grass and Forage Science* **42**: 373–380.

Song YH, Shim JS, Kinmonth-Schultz HA, Imaizumi T. **2015**. Photoperiodic Flowering: Time Measurement Mechanisms in Leaves. *Annual Review of Plant Biology* **66**: 441–464.

Stocker TF, D. Qin G-K, Plattner. **2013**. *Climate Change 2013: The Physical Science Basis. Contribution of Working Group I to the Fifth Assessment Report of the Intergovern- mental Panel on Climate Change*. IPCC.

Thomas H. **1980**. Terminology and definitions in studies of grassland plants. *Grass and Forage Science* **35**: 13–23.

Thomas H, Evans C. **1990**. Influence of drought and flowering on growth and water relations of perennial ryegrass populations. *Annals of Applied Biology* **116**: 371–382.

Van Esbroeck GA, Hussey MA, Sanderson MA. **1997**. Leaf Appearance Rate and Final Leaf Number of Switchgrass Cultivars. *Crop Science* **37**: 864.

Verdenal A. **2009**. De la simulation de la morphogénèse de l'appareil aérien du ray-grass anglais (Lolium perenne L.) : exploration d'un schéma cybernétique inspiré du concept d'auto-organisation et applications.

Verdenal A, Combes D, Escobar-Gutiérrez AJ. **2008**. A study of ryegrass architecture as a self-regulated system, using functional–structural plant modelling. *Functional Plant Biology* **35**: 911–924.

Vuffray Z, Deléglise C, Amaudruz M, Jeangros B, Mosimann E, Meisser M. **2016**. Phenological development of meadows - 21 years of observations. *Agrarforschung Schweiz* **7**: 322–329.

Wang J, Forster JW. **2017**. Flowering time regulation in perennial ryegrass. *Euphytica* **213**.

Williamson ML. **2008**. Differential responses of tillers to floral induction in perennial ryegrass (Lolium perenne L.) : implications for perenniality : a thesis presented in partial fulfilment of the requirements for the degree of Master of Science in Plant Biology at Massey University, Palmerston North, New Zealand.

Woods DP, Ream TS, Amasino RM. **2014**. Memory of the vernalized state in plants including the model grass Brachypodium distachyon. *Frontiers in Plant Science* **5**.

Woodward SJR, Oijen MV, Griffiths WM, Beukes PC, Chapman DF. **2020**. Identifying causes of low persistence of perennial ryegrass (Lolium perenne) dairy pasture using the Basic Grassland model (BASGRA). *Grass and Forage Science* **75**: 45–63.

Wu Z, Skjelvåg AO, Baadshaug OH. **2004**. Quantification of Photoperiodic Effects on Growth of Phleum pratense. *Annals of Botany* **94**: 535–543.

Yin X, Goudriaan J, Lantinga E, Vos J, Spiertz H. **2003**. A Flexible Sigmoid Function of Determinate Growth. *Annals of botany* **91**: 361–371.

Zeiter M, Schärrer S, Zweifel R, Newbery DM, Stampfli A. **2016**. Timing of extreme drought modifies reproductive output in semi-natural grassland. *Journal of Vegetation Science* **27**: 238–248.

Zhu Y, Tang L, Tan Z-H, Chen G-Q, Cao W-X. **2009**. Modeling leaf sheath and internode growth dynamics in wheat. *Crop Modeling and Decision Support*. Springer, 86–91.

Simon Rouet, 2021. **Modélisation de la phénologie reproductive du ray-grass anglais (Lolium perenne L.) : intégration des effets de l'environnement et de la diversité génétique sur les interactions entre morphogénèse végétative et induction florale.**

Résumé

Chez les graminées pérennes, le développement reproducteur est un évènement phénologique majeur qui affecte le fonctionnement écologique et agronomique des prairies. L'influence des facteurs environnementaux et génétiques, ainsi que de leurs interactions, conduisent à une forte diversité phénotypique du développement reproducteur qui rend particulièrement complexe de prédire la phénologie du développement reproducteur des graminées pérennes pour une large gamme de conditions, génotypes et usages. Les modèles informatiques permettent potentiellement d'intégrer ces interactions et ainsi améliorer notre connaissance du développement reproducteur et notre capacité de prédiction. L'objectif de cette thèse est de créer un modèle informatique capable de simuler les effets des facteurs de l'environnement et de la diversité génétique sur des stades critiques de la phénologie reproductive du ray-grass anglais : induction florale et épiaison.

Le modèle L-GrassF établit explicitement une continuité entre le développement végétatif de la plante et son développement reproducteur. La croissance foliaire et le tallage sont décrits à l'échelle de la talle individuelle. L'induction florale est modélisée pour chaque talle en fonction des températures et des photopériodes perçues depuis leur initiation. Le modèle rend également compte de l'impact de l'induction florale sur la vitesse de croissance des feuilles et l'allongement des entrenœuds. Enfin, la date d'épiaison est une propriété émergente du modèle résultant de l'interaction entre la date d'induction florale et la morphogénèse.

Une expérimentation en conditions contrôlées sur trois variétés de ray-grass anglais a d'abord permis de tester des hypothèses de modélisation liées aux interactions entre morphogénèse végétative et date d'épiaison. Elle a également servi à l'identification de paramètres rendant compte de la diversité génétique interne aux variétés. Finalement, le modèle a été évalué sur sa capacité à simuler la variabilité de la date d'épiaison observée pour sept variétés de ray-grass anglais cultivées dans des environnements contrastés entre 2001 et 2017. Cette thèse a permis i) d'établir un état des lieux des connaissances existant sur le développement reproducteur des graminées pérennes ii) de valider la nécessité de prendre en compte les processus de morphogénèse pour prédire la date d'épiaison iii) de construire un outil de modélisation opérationnel pour prédire la phénologie reproductive des graminées pérennes.

Mots-clés : phénologie, modélisation structure-fonction, épiaison, graminées fourragères pérennes, morphogénèse, induction florale

Simon Rouet, 2021. **Modeling the reproductive phenology of perennial ryegrass (*Lolium perenne* L.): integrating the effects of environment and genetic diversity on the interactions between vegetative morphogenesis and floral induction.**

Abstract

In perennial grasses, the reproductive development is a major phenological event that affects the ecological and agronomic functioning of grasslands. The influence of environmental and genetic factors, as well as their interactions, lead to a high phenotypic diversity of the reproductive development, which makes it particularly complex to predict the phenology of the reproductive development in perennial grasses for a wide range of conditions, genotypes and uses. Computer models have the potential to integrate these interactions and thus improve our knowledge of the reproductive development and our predictive ability. The objective of this thesis was to create a computer model able to simulate the effects of environmental factors and genetic diversity on critical stages of perennial ryegrass reproductive phenology: floral induction and heading.

The L-GrassF model explicitly establishes a continuity between the vegetative and reproductive development of the plant. Leaf growth and tillering are described at individual tiller scale. Floral induction is modeled for each tiller according to the temperatures and photoperiods perceived since their initiation. The model also accounts for the impact of floral induction on leaf growth rate and internode elongation. Finally, the heading date is an emergent property of the model resulting from the interaction between the date of floral induction and morphogenesis.

An experiment under controlled conditions on three perennial ryegrass varieties was first used to test modeling hypotheses related to the interactions between vegetative morphogenesis and heading date. Then, the results were used to identify parameters reflecting the genetic diversity within the varieties. Finally, the model was evaluated on its ability to simulate the variability of the heading date observed for seven perennial ryegrass varieties cultivated under contrasting environmental conditions between 2001 and 2017. This thesis allowed i) to establish an inventory of the existing knowledge on the reproductive development in perennial grasses ii) to validate the need of considering morphogenetic processes to predict the heading date iii) to build a modeling tool that can be used to predict the reproductive phenology of perennial grasses.

Keywords: phenology, functional-structural modeling, heading, perennial forage grasses, morphogenesis, floral induction